UNIVERSITY OF CÓRDOBA

DEPARTMENT OF PHYSICAL CHEMISTRY AND

APPLIED THERMODYNAMICS

Potential of energy demand reduction in buildings with green roofs under climatic conditions of southern Europe

Thesis submitted in partial fulfillment of the requirements for the

Degree of Doctor of Advanced Computing, Energy and Plasmas

MANUELA PORCARO

supervised by

Dr. Manuel Ruiz de Adana Santiago

Cordoba, May 2021

TITULO: *Potential of energy demand reduction in buildings with green roofs under climatic conditions of southern Europe*

AUTOR: *Manuela Porcaro*

Campus de Rabanales
Ctra. Nacional IV, Km. 396 A
14071 Córdoba

https://www.uco.es/ucopress/index.php/es/
ucopress@uco.es

TÍTULO DE LA TESIS: Potential of energy demand reduction in buildings with green roofs under climatic conditions of southern Europe

DOCTORANDA: MANUELA PORCARO

INFORME RAZONADO DEL DIRECTOR DE LA TESIS

(se hará mención a la evolución y desarrollo de la tesis, así como a trabajos y publicaciones derivados de la misma).

La doctoranda Manuela Porcaro ha realizado bajo mi dirección la tesis doctoral titulada "*Potential of energy demand reduction in buildings with green roofs under climatic conditions of southern Europe*".

Manuela Porcaro comenzó su relación con el grupo de investigación TEP 974 RATE Research in Applied Thermal Engineering en distintas estancias Erasmus Plus en la Universidad de Córdoba. Una primera estancia de Manuela desde septiembre de 2014 a enero de 2015 y una segunda estancia de marzo a julio de 2016. En estas estancias Manuela Porcaro desarrolló un programa de formación denominado "Training in modeling tools Green Roofs and energy saving in buildings".

Manuela Porcaro inició su etapa de Doctoranda inscribiéndose en el Programa de Doctorado en Computación Avanzada, Energía y Plasmas de la Universidad de Córdoba en diciembre de 2017. Realizó su formación con distintos cursos de formación y obtuvo la certificación C1 CAE en inglés, entre otras actividades formativas e inició su Plan de Investigación en junio 2018.

Los datos experimentales de esta tesis fueron obtenidos en la campaña experimental de ensayos en el periodo 2015 a 2017 dentro del proyecto GGI3003IDIB "*Optimizing the potential of green roofs for building retrofit: interaction between recycled substrates, water properties and energy efficiency*", financiado por la Agencia de Obra Pública de la Junta de Andalucía.

Los trabajos de simulación numérica realizados por la Doctoranda han sido muy detallados y exigentes hasta conseguir calibrar el modelo matemático empleado en la simulación con los datos experimentales obtenidos.

El trabajo de investigación de Manuela Porcaro ha dado lugar a distintas publicaciones entre las que cabe destacar: tres comunicaciones en congresos de carácter internacional, en 2014, 2018 y 2019 así como un articulo publicado en 2019 en revista internacional de impacto y otro articulo en proceso de revisión enviado en Diciembre 2020 a revista internacional de impacto.

De la doctoranda, aparte de su excelente calidad humana, me gustaría destacar, entre otras muchas cualidades, su extraordinaria capacidad de trabajo, que ha permitido realizar la tesis doctoral en el periodo 2017-2021 a pesar de encontrarse trabajando a tiempo completo en la empresa privada. Un ejemplo meritorio de constancia, tesón y disciplina que han soportado todo el trabajo de investigación desarrollado y que ha contribuido de forma notable a resolver las numerosas dificultades que se presentan a lo largo de un trabajo de esta naturaleza. Considero que este periodo ha permitido que Manuela Porcaro desarrolle las cualidades propias de una excelente investigadora.

Concluyendo, la metodología empleada, la calidad científica y los resultados de la investigación desarrollada en esta tesis doctoral se valoran de forma MUY FAVORABLE.

Por todo ello, SE AUTORIZA LA PRESENTACIÓN DE LA TESIS DOCTORAL.

Córdoba, 1 de Mayo de 2021

Firma del director

Fdo.: Manuel Ruiz de Adana Santiago

A mia madre

«…Chi tene 'a mamma
è ricche e nun 'o sape;
chi tene 'o bbene
è felice e nun ll'apprezza.
Pecchè ll'ammore 'e mamma
è 'na ricchezza
è comme 'o mare
ca nun fernesce maje.
Pure ll'omme cchiù triste e malamente
è ancora bbuon si vò bbene 'a mamma.
'A mamma tutto te dà,
niente te cerca.
E si te vede e' chiagnere
senza sapè 'o pecché,
t'abbraccia e te dice:
"Figlio!!!"
E chiagne nsieme a te…»

(Totò)

Me gustaría agradecer todas aquellas personas que de una forma u otra me han apoyado durante todo el desarrollo de mi tesis.

Gracias…

A Milagros Montijano, por el maravilloso dibujo de la portada. Ha sido emocionante contarte mis ideas y verlas reflejada tan bien en papel.

A los grupos de investigación que han participado en el proyecto "*Optimizing the potential of green roofs for building retrofit: interaction between recycled substrates, water properties and energy efficiency*", por la financiación y el apoyo técnico recibidos. Al Prof. Dr. Tom Vanwalleghem por su contribución en este trabajo.

A mi director de tesis, Manuel, por seguir creyendo en mi y darme una posibilidad tras otra. Tus consejos han sido fundamentales para crecer personal y profesionalmente.

A mi jefe, Raul, por devolverme la ilusión y recordarme que nunca es tarde para un nuevo comienzo. Gracias por confiar en mi y enseñarme a confiar en ti.

A Francesca, per aver condiviso con me anche questo percorso. A Domenico, per esserci stato sempre, indipendentemente dallo spazio e dal tempo. Vi voglio bene.

A mis compañeras y amigas Rosa, Marta, Nati y Maria del Campo. Gracias por las charlas, los consejos, el animo y por escucharme siempre. Vuestra amistad ha sido un regalo precioso.

A mis suegros, Luciano y Carmen, y mis cuñadas, Isabel y Carmen. Saber de tener en España otra familia tan hermosa me ha ayudado a superar momentos muy

difíciles. Gracias por suportarme tanto y no dejarme nunca sola. Vuestro cariño ha sido fundamental en todos estos años.

A nonno Giovanni, il mio tesoro prezioso. Grazie per aver mantenuto la promessa di esserci in ogni momento importante della mia vita. A nonna Ersilia, nonna Filomena e nonno Fortunato. Ovunque voi siate sono certa mi stiate guardando, spero di avervi resi orgogliosi di me.

A Francisco, por apoyarme siempre. Tu amor, ayuda y consejos han sido los más importantes para llevar a cabo todo esto. Nunca te estaré suficientemente agradecida y me siento muy afortunada por tenerte en mi vida.

Alla mia famiglia, mamma, papà e Daniela. Siete stati e sarete sempre il mio centro di gravità. Senza di voi nulla di tutto questo e nulla di tutto ciò che sono riuscita a fare nella vita sarebbe stato possibile. Vi amo infinitamente.

Infine, vorrei ringraziare me stessa. Per tutte le volte che ho saputo rialzarmi dopo una caduta. Per aver trovato non so dove la forza e il coraggio di prendere decisioni che mi hanno cambiato la vita, compreso questa di realizzare un dottorato nel momento più intenso della mia carriera professionale. Per avere ancora voglia di sorprendermi ed imparare. Per la resilienza che ho saputo dimostrare in tante situazioni difficili. Per avere fiducia nelle mie capacità e dimostrarlo a tutti con orgoglio. Per credere sempre in un ideale e provare a migliorarmi sempre.

Por todo esto y a todos vosotros…muchas gracias de corazón.

Manuela Porcaro

Córdoba, 1 de Mayo 2021

Preface

The thesis ***"Potential of energy demand reduction in buildings with green roofs under climatic conditions of southern Europe"*** was written as a part of a PhD study during the past four years in the Department of Physical Chemistry and Applied Thermodynamics at University of Córdoba, Spain. The thesis is presented as a collection of the following research papers: two international papers and three national and international conferences.

Paper I	Long term experimental analysis of thermal performance of extensive green roofs with different substrates in Mediterranean climate.
Paper II	Exploring the reduction of energy demand of a building with an eco-roof under different irrigation strategies.
Congress I	Capacidad de reducción de la temperatura del forjado de un edificio con una cubierta verde.
Congress II	Cooling potential of green roofs under South European continental climate.
Congress III	Energy saving potential of green roofs in South European climates.

Summary

In Europe, after the Kyoto Protocol in 1997, lots of efforts focused on controlling the global warming and reducing emissions into the atmosphere. All European Directives concerning the energy efficiency of buildings promoted the rehabilitation of old buildings and the use of renewable energy to cover the energy needs of cooling and heating of buildings. The rehabilitation of a building consists in improving its energy performance, reducing the thermal flux that is exchanged between the building and the external environment. This may be achieved by active strategies, such as implementing efficient HVAC systems, or passive strategies such as green roofs or ventilated façades, that encompassed both opaque and transparent elements of the building envelope, to insulate it during the winter months and protect it from heat gains during the summer months.

Green roofs are passive construction systems of low environmental impact that have a lot of environmental advantages, such as the absorption of CO_2, the thermal insulation capacity and the retention of meteoric water. The objective of this thesis was to study experimentally and numerically the potential of energy demand reduction in buildings with green roofs and eco-roofs, green roofs without plants, under climatic conditions of Southern Europe.

Firstly, two numerical models of an eco-roof and a traditional gravel ballasted roof were calibrated with experimental data of heat flux, in order to simulate their energy behaviour. Then, the effects of climatic variables and the volumetric water content of the substrate on the evapotranspiration and on the heat flux of the eco-roof were evaluated. Finally, 20 different irrigation strategies were studied in order to investigate the reduction of heat flux through the roof assembly and to identify the strategy that allowed the greatest reduction of energy demand with the lowest water consumption.

Secondly, it was analysed experimentally the energy behaviour of different substrates of green roofs through a dynamic analysis based on several parameters such as time lag, TL, decrement factor, DF, soil-air temperature, Tsa, and cooling potential, CP. Then it was evaluated the reduction of energy demand of the building with green roofs respect to a traditional gravel ballasted roof.

High reductions of annual energy demand were obtained with the eco-roof, 40% without irrigation strategy and 95.8% with 80 min of irrigation every day in the morning, respect to a traditional gravel ballasted roof. The irrigation strategy that allowed to achieve the highest reduction of annual energy demand with the lowest waste of water was irrigating 10 min in the morning in alternate days, 46.7% with 380 l/m^2 year.

The experimental analysis of the green roofs with different substrates showed that the substrate with 100% commercial growing medium, managed to retain more water than the rest of the plots and obtained the highest reduction of annual energy demand, up to 80.7%, respect to the traditional roof. Furthermore, the dynamic variables used for the analysis of the green roofs showed that this type of installation is able to achieve significant reductions of slab temperature and heat flux between the indoor and outdoor of the building, the reduction of the maximum peak of the internal temperature and the reduction of the maximum daily temperature excursions, compared to the traditional roof.

These results showed that both eco-roof and green roof are passive systems that allow to achieve high reduction of energy demand for the rehabilitation of old buildings. A proper irrigation strategy and the presence of plants can help further to improve the energy performance of the roof.

Resumen

En Europa, después del Protocolo de Kyoto en 1997, muchos esfuerzos se centraron en controlar el calentamiento global y reducir las emisiones a la atmósfera. Todas las Directivas europeas relativas a la eficiencia energética de los edificios promovieron la rehabilitación de edificios antiguos y el uso de energías renovables para cubrir las necesidades energéticas de refrigeración y calefacción de edificios. La rehabilitación de un edificio consiste en mejorar su rendimiento energético, reduciendo el flujo térmico que se intercambia entre el edificio y el ambiente exterior. Esto se puede lograr mediante estrategias activas, como la implementación de un sistema eficiente de climatización, o estrategias pasivas como cubiertas verdes o fachadas ventiladas, que engloban elementos opacos y transparentes de la envolvente del edificio para aislarlo durante los meses de invierno y protegerlo del calor durante los meses de verano.

Las cubiertas verdes son sistemas constructivos pasivos de bajo impacto ambiental que tienen muchas ventajas ambientales, como la absorción de CO_2, la capacidad de aislamiento térmico y la retención de agua meteórica. El objetivo de esta tesis fue estudiar experimental y numéricamente el potencial de reducción de la demanda energética en edificios con cubiertas verdes y cubiertas ecológicas, cubiertas verdes sin plantas, en las condiciones climáticas del sur de Europa.

En primer lugar, se calibraron dos modelos numéricos de una cubierta ecológica y un techo de grava tradicional con datos experimentales de flujo de calor, con el fin de simular sus comportamientos energéticos. A continuación, se evaluaron los efectos de las variables climáticas y el contenido de agua del sustrato sobre la evapotranspiración y sobre el flujo de calor de la cubierta ecológica. Finalmente, se estudiaron 20 estrategias de riego con el fin de investigar la reducción del flujo de calor a través del techo e identificar la estrategia que permitiera la mayor reducción de la demanda energética con el mayor aprovechamiento de agua.

En segundo lugar, se analizó experimentalmente el comportamiento energético de diferentes sustratos de cubiertas verdes a través de un análisis dinámico basado en varios parámetros como el time lag, TL, decrement factor, DF,

temperatura sol-aire, Tsa y potencial de enfriamiento, CP. Finalmente, se evaluó la reducción de la demanda energética del edificio con cubiertas verdes respecto a un techo de grava tradicional.

Elevadas reducciones de la demanda energética anual se obtuvieron con el techo ecológico, un 40% sin estrategia de riego y un 95,8% con 80 min de riego todos los días por la mañana, respecto a un techo tradicional. La estrategia de riego que permitió lograr la mayor reducción de la demanda energética anual con el menor desperdicio de agua fue regando de 10 min por la mañana en días alternos, 46,7% con 380 l / m^2 año.

El análisis experimental de las cubiertas verdes con diferentes sustratos mostró que el sustrato 100% comercial, logró retener más agua que el resto de las parcelas y obtuvo la mayor reducción de demanda anual de energía, hasta un 80,7%, respecto al techo tradicional. Además, las variables dinámicas utilizadas para el análisis de las cubiertas verdes mostraron que este tipo de instalación es capaz de lograr reducciones significativas de la temperatura del forjado y del flujo de calor entre el interior y el exterior del edificio, la reducción del pico máximo de la temperatura interior y la reducción de las excursiones de temperatura máxima diaria, en comparación con el techo tradicional.

Estos resultados mostraron que tanto el eco-roof como el green-roof son sistemas pasivos que permiten lograr una alta reducción de la demanda energética para la rehabilitación de edificios antiguos. Una estrategia de riego adecuada y la presencia de plantas pueden ayudar a mejorar aún más el rendimiento energético del techo.

Riassunto

In Europa, dopo il Protocollo di Kyoto del 1997, molti sforzi si sono concentrati sul controllo del riscaldamento globale e sulla riduzione delle emissioni nell'atmosfera. Tutte le Direttive Europee riguardanti l'efficienza energetica degli edifici hanno promosso la riabilitazione di vecchi edifici e l'uso di energie rinnovabili per coprire il fabbisogno energetico di raffreddamento e riscaldamento. La riabilitazione di un edificio consiste nel migliorare le sue prestazioni energetiche, riducendo il flusso termico che viene scambiato tra l'edificio e l'ambiente esterno. Ciò può essere ottenuto mediante strategie attive, come l'implementazione di un sistema HVAC efficiente, o strategie passive come tetti verdi e facciate ventilate, che comprendono elementi sia opachi che trasparenti dell'involucro dell'edificio, per isolarlo durante i mesi invernali e proteggerlo dal calore durante i mesi estivi.

I tetti verdi sono sistemi costruttivi passivi a basso impatto ambientale che presentano molti vantaggi ambientali, come l'assorbimento di CO_2, la capacità di isolamento termico e la ritenzione dell'acqua meteorica. L'obiettivo di questa tesi è stato quello di studiare sperimentalmente e numericamente il potenziale di riduzione del fabbisogno energetico in edifici con tetti verdi e tetti ecologici, tetti verdi senza piante, nelle condizioni climatiche del sud Europa.

In primo luogo, sono stati calibrati due modelli numerici di un tetto ecologico e di un tetto tradizionale in ghiaia con dati sperimentali del flusso di calore, al fine di simulare il loro comportamento energetico. Successivamente, sono stati valutati gli effetti delle variabili climatiche e del contenuto d'acqua del substrato sull'evapotraspirazione e sul flusso termico del tetto ecologico. Infine, sono state studiate 20 strategie di irrigazione al fine di indagare la riduzione del flusso di calore attraverso il tetto e identificare la strategia che consentirebbe la massima riduzione della domanda di energia con il minor consumo di acqua.

In secondo luogo, il comportamento energetico dei diversi substrati del tetto verde è stato analizzato sperimentalmente attraverso un'analisi dinamica basata su vari parametri come il time lag, TL, decrement factor, DF, temperatura sol-aria, Tsa e potenziale di raffreddamento, CP. Infine, è stata valutata la riduzione del

fabbisogno energetico dell'edificio con tetto verde rispetto ad un tradizionale tetto in ghiaia.

Elevate riduzioni del fabbisogno energetico annuo sono state ottenute con il tetto ecologico, 40% senza strategia di irrigazione e 95,8% con 80 min di irrigazione tutti i giorni al mattino, rispetto a un tetto tradizionale. La strategia di irrigazione che ha permesso di ottenere la massima riduzione del fabbisogno energetico annuo con il minor spreco di acqua è stata irrigando10 min al mattino in giorni alterni, 46,7% con 380 l / m^2 anno.

L'analisi sperimentale dei tetti verdi con diversi substrati ha mostrato che il substrato 100% organico riusciva trattenere più acqua rispetto agli altri substrati ottenendo la maggior riduzione di fabbisogno energetico annuo, fino all'80,7%, rispetto al tetto tradizionale. Inoltre, le variabili dinamiche utilizzate per l'analisi dei tetti verdi hanno evidenziato che questo tipo di installazione è in grado di ottenere riduzioni significative della temperatura del solaio e del flusso termico tra interno ed esterno dell'edificio, la riduzione del picco massimo della temperatura interna e la riduzione delle massime escursioni termiche giornaliere, rispetto al tetto tradizionale.

Questi risultati hanno dimostrato che sia il tetto ecologico che il tetto verde sono sistemi passivi che consentono di ottenere un'elevata riduzione del fabbisogno energetico per la riabilitazione di vecchi edifici. Una corretta strategia di irrigazione e la presenza di piante possono aiutare ulteriormente a migliorare le prestazioni energetiche del tetto.

NOMENCLATURE

A	area [m^2]
C	case study
C_{cover}	cloudiness factor of the sky
C_e^g	bulk transfer coefficient [-]
C_h^g	bulk transfer coefficient [-]
CP	cooling potential [ºC]
c_p	specific heat [J kg^{-1} K^{-1}]
D	drainage [l m^{-2}]
DF	decrement factor [-]
e	thickness [m]
ED	energy demand [%]
ET	evapotranspiration [l m^{-2}]
F_g	net heat flux to ground surface [W m^{-2}]
F_{gnd}	view factor from surface to ground [-]
F_{sky}	view factor from surface to sky [-]
h_c	convective heat transfer coefficient [W m^{-2} K^{-1}]
$h_{c,f}$	foliage convective heat transfer coefficient [W m^{-2} K^{-1}]
$h_{c,s}$	soil convective heat transfer coefficient [W m^{-2} K^{-1}]
h_o	heat transfer coefficient by radiation and convection at the outer surface [W m^{-2} K^{-1}]
hr	mean radiative heat transfer coefficient [W m^{-2} K^{-1}]
$I_{ir}^{\downarrow}$	total incoming long-wave radiation [W m^{-2}]
$I_s^{\downarrow}$	total incoming short-wave radiation [W m^{-2}]
LAI	leaf area index [-]
l_g	latent heat of vaporization at the ground surface temperature [J kg^{-1}]
K	hydraulic conductivity [m s^{-1}]
P	performance of the eco-roof [W h l^{-1}]
q_a	mixing ratio of the air [-]
q_g	mixing ratio at the ground surface [-]
Q	cumulative energy gains [W h m^{-2}]
$\dot{Q}$	heat flux [W m^{-2}]
$\dot{Q}_S$	sensible heat flux [W m^{-2}]
$\dot{Q}_L$	latent heat flux [W m^{-2}]
R	rainfall [l m^{-2}]
RH	relative humidity [%]
SR	solar radiation [W m^{-2}]

T_a	air temperature near the soil [K]
T_{amb}	ambient air [K]
T_f	foliage temperature [K]
T_g	ground surface temperature [K]
T_{hs}^3	average temperature between the plot surface temperature and the sky temperature [K]
TL	time lag [h]
T_o	outdoor temperature [K]
T_{sky}	sky temperature [K]
U	transmittance [W m^{-2} K^{-1}]
VWC	volumetric water content [m^3 m^{-3}]
W	quantity of irrigation water [l m^{-2}]
WD	wind direction [º]
WS	wind speed [m s^{-1}]
z	depth [m]
Greek letters	
α	product of the solar absorptance of the exterior surface and the rate of total solar radiation incident per unit area upon surface [W m^{-2}]
α_o	solar absorptance of exterior surface
α_g	albedo of ground surface [-]
ΔR	infrared radiation difference between surface and sky and surroundings [W m^{-2}]
ε	infrared emittance of surface [-]
ε_0	emittance of the clear sky [-]
ε_f	emissivity of the foliage [-]
ε_g	emissivity of the ground surface [-]
λ	thermal conductivity [W m^{-1} K^{-1}]
ρ_{ag}	density of air at ground surface temperature [kg m^{-3}]
σ	Stefan-Boltzmann constant [W m^{-2} K^{-4}]
σ_f	fractional vegetation coverage [-]
Subscripts	
a	air
eco	eco-roof
exp	experimental
f	foliage
g	ground
Glob,H	global on the horizontal axis
num	numerical

o	outdoor
ref	reference
sa	sol-air
w	week
y	year

Contents

List of figures

List of tables

Chapter 1

Introduction and state of the art

Nowadays the topic of energy saving is one of the most discussed in the world. In the last forty years, the use of fossil fuels to generate energy has increased exponentially and this has caused serious damage in terms of greenhouse gas production. A high concentration of greenhouse gases allows the solar radiation to pass through the atmosphere, causing an increase in the value of the earth's temperature, glaciers melting and extreme weather events.

In Europe, residential buildings represent the 40% of the final energy consumption [1]. The fossil fuels, such as hydrocarbons, coal and natural gas, used until now for the building's installations to maintain internal building temperatures have been one of the major causes of CO_2 emissions in the atmosphere.

1.1 EU legislation on energy saving

The first international agreement for the control of global warming was the Kyoto Protocol in 1997, signed by 180 nations [2]. The main objective was the reduction of emissions into the atmosphere. The overall reduction obligation was 5.2% and in Europe 8%. Despite being a global political program, the Kyoto protocol was incomplete because it was not signed by the USA, China and India, which were among the countries that produced the highest CO_2 emissions.

The European Union introduced new measures to prevent the climate change after the Kyoto Protocol, such as the "20-20-20 Plan" [3], which started in June 2009. This plan envisaged the reduction of greenhouse gases by 20%, the increase to 20% of energy produced from renewable sources and the 20% increase in overall

energy savings by 2020. The main actions implemented to achieve these objectives were:

- Revision and improvement of the EU-ETS system (European Union Emission Trading Scheme), an environmental policy tool that sets a maximum threshold for emissions produced by companies;
- Increase by 5.5% the quantity of energy produced through renewable sources in each member State and add a share for each country, based on the GDP;
- Reduction of CO_2 emissions produced by cars, with a limit of 130 gCO_2/km from 2012 for new cars and of 95 gCO_2/km by 2020;

The next objective of the European Union was the "40-27-30 Plan" [4], in order to reduce the CO_2 emissions by 40% by 2030 and between 80% and 95% by 2040 respect to 1990 and to increase the energy demand covered by renewable sources to 27% by 2030.

With regard to the energy efficiency in buildings, the Directive 2002/91/EC [5] introduced new methodologies to calculate the energy performance in buildings and to draft the energy certificate. This Directive was amended and supplemented by the Directive 2010/31/EU [6], which strengthened the goal of reducing the energy consumption and introduced the nearly zero energy buildings, nZEB, a building that has a very high energy performance. Furthermore, the very low amount of energy required in an nZEB is covered by renewable sources.

Another European Directive was the Directive 2012/27/EU [7], which introduced new measures to achieve the goal of reducing energy consumption by 20% by 2020. To do it, each Member State had to ensure that 3% of public areas was rehabilitate every year, starting from 1 January 2014 and that from 2020 all new buildings had to be nZEB. Directives 2010/31/EU and 2012/27/EU were amended with directive 2018/844/EU that required to the Member States to plan long-term renovation strategies for residential and no-residential buildings and update them every three years as part of the National Energy Efficiency Action Plan [8].

In December 2018, Renewable Energy Directive 2018/2001/EU [9] entered into force, helping the EU to meet its emissions reduction commitments under the Paris Agreement of 2015 [10] and strengthening the use of energy from renewable sources. In the frame of the *Renovation Wave Strategy* [11], published in 2020, the Directive 2018/2001/EU will be reviewed in June 2021, reinforcing the renewable

heating and cooling target and setting minimum energy performance standards for existing buildings. Moreover, it could be decided to use the EU Emissions Trading System (EU ETS) to fund new energy efficiency projects for lower income populations.

Among the priorities of the European Commission in the period between 2019 and 2024, there are several studies and strategic plans:

- The *European Green Deal Plan*, that promotes the stop of greenhouse emissions by 2050, the efficient use of resources for a clean and circular economy and restore biodiversity. To achieve it, several actions will be required such as invest in environmentally friendly technologies, decarbonise the energy sector, ensure energy efficient buildings and cooperate with international partners to better improve global environmental standards.
- The Energy Poverty plans, such as *STEP (Solutions to Tackle Energy Poverty), EmpowerMed* and *SocialWatt*. All of these plans aim to support EU countries in their efforts to promote public engagement on the issue of energy poverty, through the (EU) 2020/1563 [12]. Energy poverty means low incomes and poor energy efficiency of buildings. The 6.9% of the EU population cannot heat their home adequatly [13] and deficient indoor temperatures and the exposure to harmful chemicals contribute to health problems and mortality.
- The *Comprehensive study of building energy renovation activities and the uptake of nearly zero-energy buildings in the EU* [14], that aims to carry out an exhaustive analysis of all the renovation activities to achieve nearly zero-energy buildings (NZEB) implemented in the EU from 2012 to 2016.
- The *New European Bauhaus*, an interdisciplinary project to plan future ways of living and to translate the *Green Deal Plan* into daily actions to build a sustainable future. The main focus of the interdisciplinary groups will be the research and promotion of new sustainable materials and recovery projects of old buildings.

1.2 Retrofitting of existing buildings

Generally, the insulating capacity of the construction systems and their impact on the thermal performance of buildings is measured with the thermal transmittance value (U), which is defined as the rate of heat flow across one sq. meter of a surface when there is a temperature difference of one Kelvin between the inside and outside surfaces [15]. The U value is measured in W/m^2 K and is calculated with Eq. (1).

$$U = \frac{1}{\frac{1}{h_{c,in}} + \sum_{i=1}^{n} \frac{e_n}{\lambda_n} + \frac{1}{h_{c,out}}} \quad (1)$$

Where $h_{c,in}$ is the indoor convective heat transfer coefficient [W/m^2 K]; $h_{c,out}$ is the outdoor convective heat transfer coefficient [W/m^2 K]; e is the thickness of the material [m]; λ is the thermal conductivity of the material [W/mK].

In Europe, the average U value of envelope in residential buildings built before 1945 and between 1945–1969 are 1.45 W/m^2 K and 1.39 W/m^2 K, respectively [16,17]. In Spain, the U value for the envelope of the new buildings has to be less than 0.5 W/m^2 K, depending on the climatic zone [18]. This means that the thermal transmittance of the old buildings is significantly higher than the value established in the regulations. Moreover, traditional flat roofs have high thermal conductivity and absorb external heat in summer [19]. To achieve the objective of reducing energy consumption by 2030, retrofit strategies are necessary to address the ageing buildings and to reduce the global energy consumption for heating and cooling demands.

The retrofitting of a building consists in improving its energy performance, reducing the thermal flux that is exchanged between the building and the external environment. The result is an improvement of the internal thermal comfort, the reduction of the pollutant emissions and energy consumption [20]. The retrofitting interventions must be carefully studied based on the type of construction, the materials used and the climatic zone.

The thermal performance of a building can be improved by active strategies, such as implementing energy efficient HVAC systems [21–23], or passive strategies encompassing both opaque and transparent elements of the building envelope, to insulate the building during the winter months and protect it from heat gains during the summer months [24].

The present thesis focused on the study of green roofs for the energy rehabilitation of buildings, as one of the passive construction systems of low environmental impact.

1.3 Green roofs

Green roofs have a lot of environmental advantages and are very popular in the North of Europe, where this technology has been implemented in more than the 10% of all new buildings [25].

A green roof has a good thermal insulation capacity, retains meteoric water, absorbs CO_2 and local noise pollution and minimises the heat island effects in cities [26–28]. Green roofs ensure less energy losses in winter and the maintenance of the internal temperature in summer [29]. Furthermore, green roofs contribute to a delay in the storm peak runoff to the drainage system and also enrich biodiversity in cities [30,31]. One of the major energy benefits of the green roofs is the cooling effect due to the evapotranspiration [32], ET, that helps to maintain internal conditions of comfort. ET is the combination of water evaporation from the soil and transpiration from the plants.[33].

There are three types of green roof: intensive, semi-intensive and extensive. An intensive green roof, commonly called “roof garden”, has a higher thickness, between 150 and 400 mm, and the plant species used require a lot of maintenance and irrigation. A semi-intensive green roof needs periodically maintenance and irrigation and has a thickness of 120-250 mm, while an extensive green roof is used mainly to cover large non-walkable roofs, has a thickness of 60-200 mm and the plant species require low maintenance, see Figure 1. The present thesis focused on extensive green roofs.



	Extensive green roof	Semi intensive green roof	Intensive green roof
Maintenance	Low	Periodically	High
Irrigation	No	Periodically	Regularly
Plant communities	Moss-Sedum-Herbs and Grasses	Grass- Herbs and Shrubs	Lawn or Perennials, Shrubs and Trees
Cost	Low	Middle	High
Weight	60–150 kg/m^2	120–200 kg/m^2	180–500 kg/m^2
Use	Ecological protection layer	Designed green roof	Park like garden
System build- up height	60–200 mm	120–250 mm	150–400 mm underground garages ≥ 1000 mm

Figure 1. Classification of green roofs according to type of usage, construction factors and maintenance requirements [34].

The layout of a green roof from top to bottom consists in vegetation, substrate, filter, drainage layer, root barrier, waterproofing membrane and roof slab [34], as shown in Figure 2.

Figure 2. Layout of a green roof.

1.3.1 Extensive green roofs under different climatic conditions

Climatic conditions significantly influence the energetic behaviour of green roofs. Previous research studies on extensive green roofs analysed experimentally and numerically their behaviour under different climatic conditions. An extensive green roof was studied in the cool wet climate of the Pacific Northwest [35], showing the necessity of plants that retain a great quantity of water to counter the environmental constraints imposed by regional climate.

Other research focused on subtropical climate, showing the importance to choose droughts tolerant plants and a high deep of the substrate [36], to obtain good thermal benefits. Some authors achieved a reduction of the surface temperature of a bare rooftop for subtropical climatic conditions [37], although the relative humidity affected negatively the reduction of surface temperature. Long term studies about thermal performances of green roofs in subtropical climates showed that the best cooling effects were obtained in summer. However, an improve of the thickness of substrate layer helped to reach better insulation, both in summer and winter [38].

In tropical climates, green roofs showed good thermal benefits [39,40] and high reduction of daily peak indoor temperature, compared to a traditional roof [41]. Moreover, green roofs proved to be very suitable as efficient systems to reduce the urban heat island in tropical megacities, up to 2°C [42].

A recent study in temperate monsoon climate analysed the effects of the substrate depth in an extensive green roof without irrigation [43]. The results showed that for this climate a substrate depth of 15 cm was the optimal to guarantee the survival of the plants.

Other works focused on weekly studies of green roofs in Mediterranean climate [44] achieving suitable reduction of the total transferred energy. A long term study in Mediterranean climate showed the hydrological efficiency of green roofs as effective systems to control the volume of rainfall [45].

1.3.2 Types of substrates in extensive green roofs

Different types of substrates in extensive green roofs were studied by some authors. Commercial substrates showed to be very suitable for these type of installations [46]. Other studies analysed the performance of extensive green roofs with

substrates composed of low-cost and waste materials, such as materials from the construction sector, to reduce their economic costs, achieving acceptable performances [47–49]. Furthermore, it was seen that the amount of water in the substrate helped to minimise the cooling demand in summer [50,51].

Some researches indicated that the type and characteristics of the substrate play an important role in the insulation of buildings [52,53]. A numerical simulation of different soil thickness showed that the ET of the substrate had a significant effect on the thermal performance of the green roof, expecially in summer [54]. Several energy simulations were performed in EnergyPlus software to investigate the thermal performance of five types of green roofs substrates [55]. It was found that the thermal performance of green roofs strongly depended on the thermophysical properties of the substrate used.

An experimental study was carried out to evaluate the impact of the substrate and irrigation on the thermal performance of green roofs [56]. This study suggested that the substrate and the soil moisture reduced the roof temperature and improved the thermal performance of the building. The characteristics of the most commonly substrates used are shown in Table 1.

Table 1. Characteristic of the most commonly substrates.

Reference	Thickness (m)	Composition	Conductivity (W/mK)	Density (kg/m3)	Specific heat (J/kgK)
[53]	0.25	-	0.25	-	-
[54]	0.04	Peat soil, powdered perlite and vermiculite aggregate	0.37	-	-
[56]	0.35	Natural soil and organic matter	-	1000	-
[56]	0.35	Perlite and organic matter	-	600	-
[57]	0.2	-	0.25	1600	890
[58]	0.2	Pumice, compost and sand	0.15	1020	1093
[59]	0.08	-	0.4	641	1000
[60]	0.1	-	0.35	1100	1200
[61]	0.15	Heavyweight	0.85	1639	1800
[61]	0.15	Lightweight	0.28	730	1100
[62]	0.1	-	0.4	-	-
[63]	0.3	-	0.9	1850	850
[64]	0.08	-	0.31	750	1348

1.3.3 Plants in extensive green roofs

Some of the benefits and thermal performance of the green roofs depend on the plant species used. Plants of a green roof, with their biological functions such as evapotranspiration and photosynthesis, can absorb and decrease the solar radiation transmitted to the soil [65]. Consequentially, the heat conducted to the indoor of the building is reduced and the roof insulation capacity is increased [66,67]. Plants are able to reduce the air temperature surrounding the roof [68] and function as a wind barrier so the energy losses due to the wind convection are minimized [69]. Furthermore, plants increase the rainfall retention capacity of the green roof [70].

The characteristics of the plants, such as leaf area index, LAI, stomatal resistance, stomatal conductance, fractional vegetation coverage, albedo and height affect green roof heat transfer [71,72]. LAI is the ratio of the entire one-sided area of the leaf divided by one unit of ground soil surface area and strongly influence the evaporation rate of the plant [73]. The stomatal resistance and stomatal conductance determine the aptitude of the plant to transfer moist to the roots and canopy [74]. The albedo indicates the fraction of shortwave radiation reflected by the leafs surface [75] and the fractional vegetation coverage is defined as the ratio between the soil surface shaded by leaves and the total soil surface and it is directly related to the cooling effect due to the plants [76].

Normally, the vegetation is chosen considering the geographic location, the climatic conditions, the type of green roof and the substrates characteristics [77]. Some studies were carried out on the finding of plant species based on the soil depth [78]. Plant species often used in extensive green roofs are *Sedums* for their ability to adapt well to different climatic conditions and for the low amount of water required [79]. An experimental study showed that *Sedums* also increase performance of neighbouring plants during summer water lack [79].

In recent studies *Sedums* growth and characteristics were analysed in different climates. An experimental research analysed *Sedums* tolerance and surface coverage in humid subtropical climate [80], showing a long-term survival with low amount of irrigation water. In tropical climate, where green roofs endure periodic drought stress, *Sedums* are able to regulate the foliage temperature and maintain the soil moisture [81]. *Sedums* are also especially indicated for green roof installation under Mediterranean and semi-arid climate, for the low maintenance cost and low water consumption [82].

1.3.4 Key performance indicators of green roofs

The overall performance of green roofs has been studied from several parameters. Many authors studied the heat flux through the layers of the roof as a performance parameter [83,84], where they obtained significant reductions compared to the traditional roofs. The cooling potential, CP, of the surface temperature of the green roof was another dynamic parameter analysed. This parameter was related to the mitigation of the urban heat islands [85,86].

Two dynamic parameters used also to study other passive construction systems, such as green façades, were time lag ,TL, and decrement factor, DF, [87,88]. Both parameters were used to study the reduction of energy demand [88]. Recently, these parameters were studied for a green roof with different plants during a summer week for the climatic conditions in the south of Italy [89], achieving an increase of TL and a reduction of DF with respect to a roof with only substrate.

Several studies analysed the influence of ET on the energy behaviour of green roofs [90–92]. While the different variables affecting ET are well known [33], the relative importance of each of these variables differs depending on the environmental conditions. An experimental study in subtropical Hong Kong native-woodland intensive green roof found that solar radiation had the strongest correlation with ET [93]. Another experimental study in a tropical extensive green roof showed that ET was largely dependent on solar radiation, relative humidity and wind speed, but found little influence of substrate moisture [94]. A numerical model of a green roof was developed to determine the ET effects on the heat transfer of a building [95]. The model suggested that a green roof installation is able to decrease the heat flux of the building envelope and the ET reduces further the temperature of the roof surface, providing a greater cooling effect. Other authors evaluated numerically the behaviour of green roofs focusing on the correlation between ET and the volumetric water content, VWC, of the growing media [96,97]. These results showed that the irrigation of a green roof increased ET values and mitigated the urban heat island effect, especially during the warmer periods. An experimental study also evaluated the effect of ET on VWC of both a green roof and a bare substrate for four summer days in Melbourne [98], suggesting that during the summer period the lack of water in the substrates halted the ET and the cooling effect of the roofs was reduced.

1.3.5 Irrigation of green roofs

The irrigation of green roofs helps to reduce the heat transfer between the exterior and the interior of a building, during the warmer months, and increases its thermal insulation capacity [99]. Some researchers demonstrated that in the coming 30 years many areas in the world will be water stressed, so the goal of irrigation installations of green roofs will be to achieve the maximum energy savings with minimum water consumption [100]. In recent literature some numerical studies proposed an irrigation controlling method based on the predicted ET and daily weather variables, in order to maximize the efficient use of water [101]. Other types of irrigation strategies were analysed in experimental research studies to identify the optimal irrigation frequency [102]. The results indicated that a substrate which is irrigated twice a week is able to reduce the heat amplitude under the roof slab surface up to 91.6%. A numerical model of a green roof was developed to study the irrigation management [103], showing that irrigation every 3 days to the field capacity and irrigation every 7 days to the saturation moisture content are two efficient watering schemes for the climatic condition of Shenzhen, China. A green roof model was simulated in EnergyPlus software to analyse the sensible heat flux reduction potential of several irrigation scenarios under different climatic conditions [104]. For cities with low excess heat and high annual precipitations, such as London and New York, a sensible heat reduction up to 75% was obtained. However, the irrigation strategies of these models were carried out with equal amount of water in all case studies.

1.4 The importance of green roofs as passive system for reducing the energy demand of buildings

The increasing of greenhouse gas production and the earth's temperature forced the European Union to introduce new measures to prevent the climate change and the reduction of emissions into the atmosphere. Retrofit strategies are necessary to address the ageing buildings and to reduce the global energy consumption for heating and cooling demands. Green roofs have a lot of energetic and environmental advantages. The good thermal insulation capacity and the cooling effect due to evapotranspiration make this installation a possible passive system for the rehabilitation of old buildings. Moreover, another advantage of a green roof is that it can be directly implemented on a traditional flat roof, that usually has high thermal conductivity and absorb external heat in summer.

Some researchers studied green roofs under different climatic conditions and the energy performance of green roofs with different substrates. Others focused on the types of plants more suitable for this kind of installation and the reduction of the heat transfer between the exterior and the interior of a building using an irrigation system.

Based on the few studies on eco-roofs, that are commonly considered as green roofs without plants, the lack in investigation on different irrigation schedule and amount of water and the influence of volumetric water content on the energy behaviour of different substrates, the present thesis focused on the reduction of energy demand of a building with eco-roof under different irrigation strategies and green roof installation with different substrates. Accordingly, research questions arise as the starting point of this thesis:

1) How does the volumetric water content of the substrate influence the energy behaviour of an eco-roof?
2) Which is the irrigation strategy that allows to obtain the highest reduction of energy demand of the roof with the less amount of water?
3) How does the volumetric water content of the substrate influence the energy behaviour of green roofs with different substrates?
4) Which are the most influential parameters in the energy behaviour of green roofs with different substrates?

Trying to solve these questions, this thesis presents an experimental and numerical analysis of eco-roofs and green roofs with different substrates under climatic conditions of Southern Europe, to study their potential of energy demand reduction for the rehabilitation of old buildings.

1.5 Hypothesis

The considerations to the results obtained in the thesis were based on the following hypothesis:

- The work focused on a study of reduction of energy demand of the building envelope through the roof. The walls and inter-floor slabs were not considered for this study.
- The results obtained were valid for the Mediterranean climatic conditions considered, defined as subtype Csa dry-summer subtropical with mild

winters and very warm summers, according to Köppen-Geiger climate classification.

- The study was carried out considering the thickness of the substrates equal to 10 cm.

1.6 Layout

The thesis has been written using the following chapter structure:

Chapter 1. The overview on the problem of the rehabilitation of old buildings in Europe and an excursus of the European legislation on energy saving are given in this chapter. It is also presented an overview on the different types of substrates and plants used for the green roof installations.

Chapter 2. Describes the main objective of the work carried out. It also outlines all the specific objectives that allowed to achieve the main objective.

Chapter 3. Describes the experimental and numerical methodology followed for the eco-roof and green roofs study.

Chapter 4. Includes the whole description of the calibration of the numerical models and the energy simulations performed of the eco-roof. It also includes the effect of climatic variables, volumetric water content of the substrate and evapotranspiration on heat flux.

Chapter 5. Expounds the dynamic parameters studied for the green roofs with different substrates, for the summer and winter period.

Chapter 6. The energy analysis of the eco-roof under different irrigation strategies and the green roofs with different substrates is analysed in this chapter.

Chapter 7. Provides the conclusions achieved in this thesis.

Appendix A. Shows an experimental campaign of 2 years to determine the thermal performance of 3 green roofs with different substrate.

Appendix B. Addresses the numerical analysis of two models of eco-roof and traditional gravel ballasted roof to study the reduction of energy demand of a building with eco-roof under different irrigation strategies.

Appendix C. Shows the decrease in temperature of a slab with green roof respect to a traditional gravel ballasted roof.

Appendix D. Discusses the cooling potential of 3 green roofs with different substrates**.**

Appendix E. Discusses the energy saving potential of 3 green roofs with different substrates, compared to a traditional gravel ballasted roof.

Chapter 2

Objectives

The OVERALL OBJECTIVE of this thesis was to study experimentally and numerically the potential of energy demand reduction in buildings with green roofs and eco-roofs under climatic conditions of Southern Europe.

The overall objective indicated in this thesis was linked to the following SPECIFIC OBJECTIVES:

1) Evaluate the influence of climatic variables and volumetric water content of the substrate on heat flux of eco-roofs.
2) Investigate the irrigation strategies for eco-roofs that allow the greatest reduction of energy demand with the lowest water consumption.
3) Analyse the influence of volumetric water content of different substrates on layers temperature of the green roofs.
4) Identify the most influential parameters in the energy behaviour of green roofs with different substrates.

The results derived from these objectives could be interesting for the energy renovation of both public and private buildings to drive energy efficiency in the framework of *European Green Deal*.

Chapter 3

Materials and method

The results of this thesis are based on experimental campaigns on an eco-roof and three green roofs with different substrates carried out in the University of Cordoba, from 2015 to 2017, during the project GGI3003IDIB "Optimizing the potential of green roofs for building retrofit: interaction between recycled substrates, water properties and energy efficiency", by the Agency of Public Works of Andalucía, Junta de Andalucía, Spain. Financial support of the European Regional Development Fund (ERDF). Furthermore, numerical simulations of an eco-roof and a traditional gravel ballasted roof were performed using energy simulation tools. The experimental and numerical methodology used in this thesis are presented in this chapter.

3.1 Overview of the methodology

Three main steps were followed in order to achieve the objectives of this thesis, as shown in Figure 3:

- Experimental and numerical study to evaluate the energy behaviour of an eco-roof, under different irrigation strategies, during the year 2015, compared to a traditional gravel ballasted roof.
- Experimental study of three green roofs with different substrates, during the years 2016-2017, compared to a traditional gravel ballasted roof.
- Experimental and numerical study of a traditional gravel ballasted roof, during the years 2015-2016-2017.

First, the thesis focused on the experimental study of the heat flux, $\dot{Q}$, exchanged between the indoor and the outdoor of a building through a traditional gravel ballasted roof and an eco-roof, a green roof without plants, in order to evaluate the $\dot{Q}$ reduction when using an eco-roof, with the contribution only of the commercial substrate. Moreover, the effects of the climatic variables and the volumetric water content of the substrate, VWC, on evapotranspiration, ET, were analysed. Finally, experimental $\dot{Q}$ values were used to calibrate two numerical models, one of the traditional roof and another one of the eco-roof in order to study different irrigation strategies. The objective was to evaluate the one that had the highest reduction of energy demand with respect to the lowest amount of irrigation water. This study was carried out with the experimental data of 2015, when the plants had not yet grown.

The second part of the study was carried out with the experimental data of 2016-2017, when the whole surface of roof plots was covered by plants. The thesis focuses on the experimental study of 3 green roofs with different substrates, compared to the traditional gravel ballasted roof. A dynamic energy analysis based on different parameters such as, time lag, TL, decrement factor, DF, sol-air temperature, Tsa, cooling potential, CP, and heat flux, $\dot{Q}$, was carried out. Finally, the reduction of energy demand of the three green roofs respect to the traditional gravel ballasted roof were analysed.

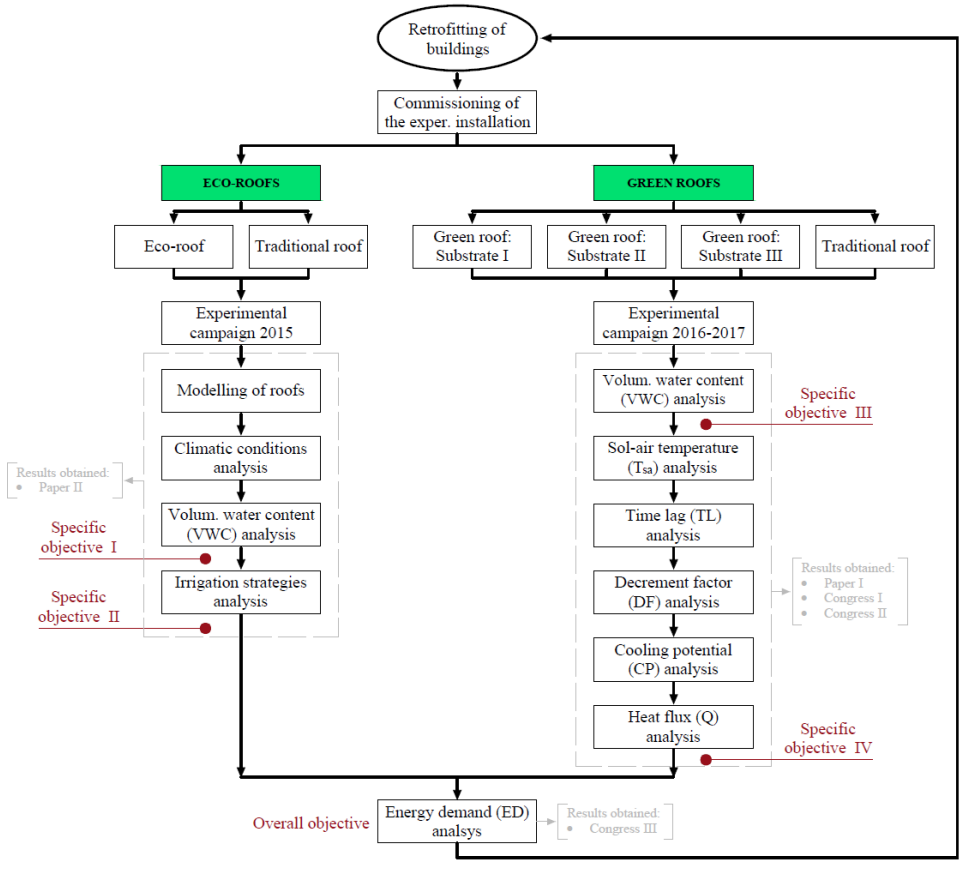

Figure 3. Overview of the methodology.

3.2 Experimental materials and facilities

3.2.1 Building

The experimental installation was installed in 2015 on the roof of an office building located in the University of Córdoba, see Figure 4. Córdoba is located in Southern Spain, where the climatic conditions are typically Mediterranean, defined as subtype Csa dry-summer subtropical, according to Köppen-Geiger climate classification [105], with mild winters and very warm summers. The building was constructed in 1956 and its dimensions were 27.7 m length, 9.5 m width and 7 m hight. No shadows of trees or other buildings fell on the roof. The indoor air

conditions of the building were in free evolution, without any climate control program.

Figure 4. Areal view of the building before the green roofs were installed.

3.2.2 Experimental installation

The experimental installation consisted in 6 plots of green roofs, P1 to P6, and one plot of traditional gravel ballasted roof, Pref, installed on the roof of the office building, see Figure 5, where E and W refer to East and West. Images of a plot with green roof and the plot with traditional roof of the experimental installation are shown in Figure 6.

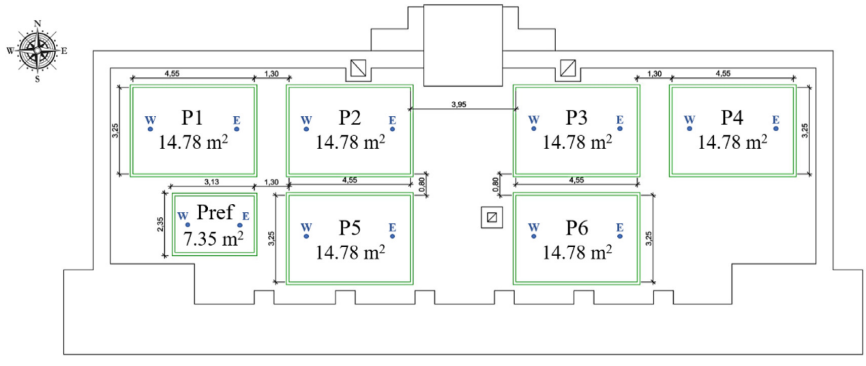

Figure 5. Roof plan with green roof plots.

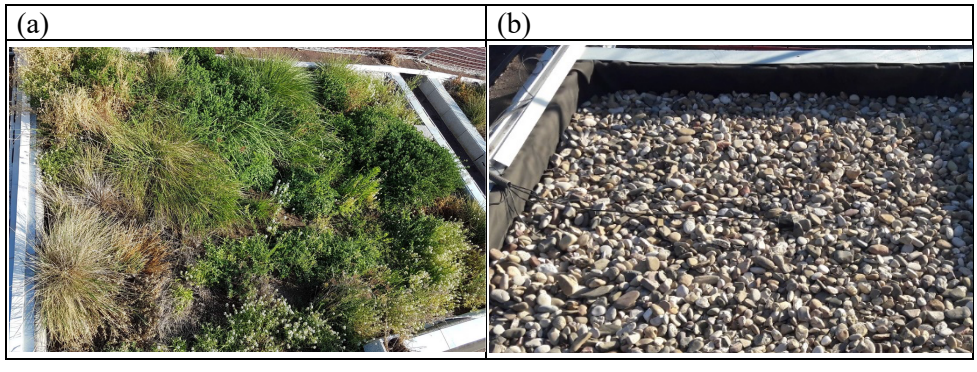

Figure 6. Images of (a) a plot with green roof and (b) the plot with traditional roof.

Twelve autochthonous Mediterranean plant species were planted in the plots. These were selected by their adaptation to tolerate drought stress, intense lighting, extreme heat and shallow substrates, which are exactly the biological and ecological characteristics needed for green roofs in urban Mediterranean ecosystems. The species used were: Acinos alpinus, Bellis perennis, Brachypodium retusum, Cerastium tomentosum, Dianthus arenarius, Lobularia maritima, Lotus corniculatus, Paronychia argentea, Phagnalon saxatile, Sanguisorba minor, Sedum sediforme and Trifolium repens.

The area of each plot was divided into 18 experimental micro-plots of 0.75 m^2. 12 plants were planted in each micro-plot, 1 unit of each selected species, see Figure 7. The placement of the different species was not carried out randomly. It

was based on the premise that all the species interacted with each other, in order to evaluate these interactions. The number of units planted in the available area of the plot resulted in a planting density of 15.34 plants/m^2.

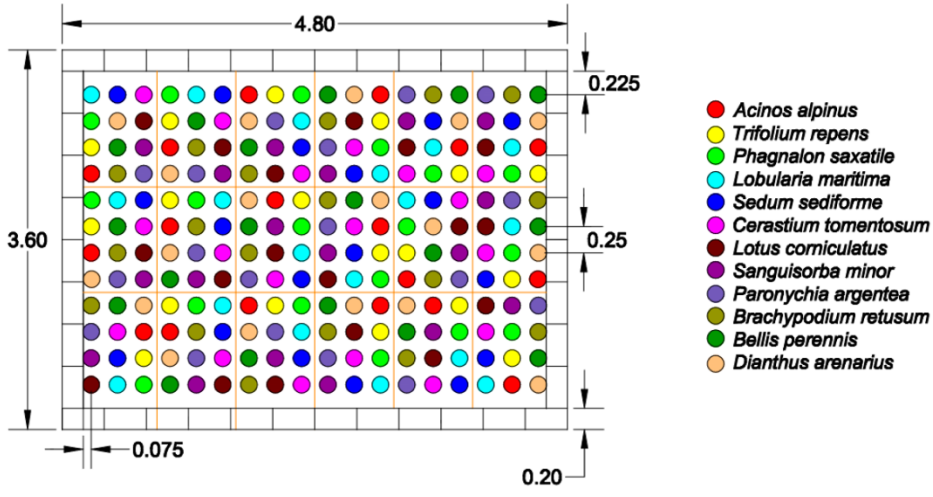

Figure 7. Placement of the different species in the plots with green roofs

This study only focused on plots P1, P2, P5 and Pref, the other were used for other agronomic studies. Each plot presented a different substrate with different percentages by volume of commercial growing medium, composed of organic material and volcanic gravel, and recycled construction materials, as shown in Table 2.

Table 2. Growing media composition of the three plots with green roof.

Plot	P1	P2	P5
Commercial growing medium	100%	75%	50%
Recycled aggregates construction materials	0%	25%	50%

The layers of the plots with green roof, ordered from bottom to top, were: roof slab (λ= 2.3 W/m K; c_p= 1000 J/kg K), waterproof membrane, root-barrier, water storage layer (λ= 0.17 W/m K; c_p= 900 J/kg K), filter sheet and commercial

growing medium, see Figure 8a. The layers of the gravel ballasted roof, from bottom to top, were roof slab, waterproof membrane and a layer of gravel ballasted (λ= 0.55 W/m K; c_p= 1000 J/kg K), see Figure 8b.

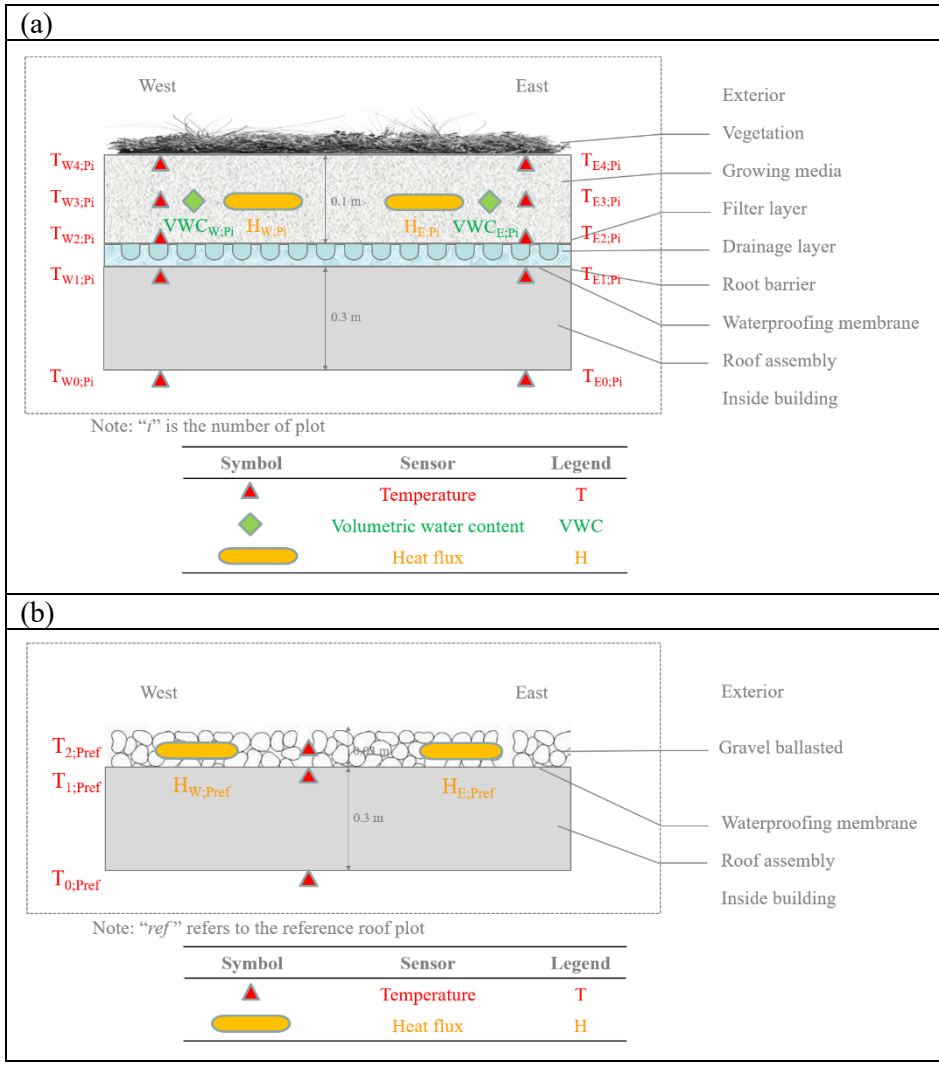

Figure 8. Layers of the plots.

3.2.3 Experimental facilities

All the plots with eco-roof and green roof were equipped with 10 probes along the vertical profile to measure the temperature, T, two probes for the volumetric water content, VWC, and two probes for the heat flux $\dot{Q}$, see Figure 8a. The plot with the traditional gravel ballasted roof also was equipped with 3 temperature probes along the vertical profile and 2 probes to measure the $\dot{Q}$, see Figure 8b. All the data were recorded every 15 min from 1/07/2015 to 31/12/2017 by a specific acquisition system. All the technical specifications are summarized in Table 3. The measures of these variables were used to analyse the energy performance of the plots.

Table 3. Technical specification of the devices used in the experimental campaign.

Equipment	Accuracy	Variable	Unit
Thermistors	±0,25ºC (-10 to 70^{0}C)	Temperature	[ºC]
Heat flux plate	±5%	Heat flux	[W/m^{2}K]
Water content reflectometer	±2.5% (0 to 50%)	Volumetric water content	[%]
Capacitive relative humidity	2% (0 to 100%)	Air relative humidity	[%]
Platinum resistance temperature	0.2ºC (-40 to 70ºC)	Air temperature	[ºC]
Silicon photocell solar radiation	5% (350 nm to 1100 nm)	Solar radiation	[W/m^2]
Wind speed and direction sensor	1% (0 to 100 m/s) 3º (0 to 360º)	Wind speed and direction	[m/s] [º]

The green roofs were equipped with a drip irrigation system managed by a time schedule module. The irrigation was provided during the warmest months in summer to prevent water stress in plants. The irrigation system operated twice a day in P1, P2 and P5, for 10 minutes and fed by 27 l each time.

During the experimental campaign, the meteorological data also were recordered by a weather station placed near the installation. The climatic variables recordered were ambient air temperature, T_o, relative humidity, RH_o, rainfall, R, wind speed, WS, direction of the wind, WD, and solar radiation, SR. The technical specifications of the devices used to record these data are also shown in Table 3. During the experimental campaign only 0.3% of failure occurred in the monitoring system and to fill the gaps in the data appropriate interpolation methods were used.

3.3 Eco-roof methodology

An eco-roof was studied throughout the year 2015, for the climatic conditions of Córdoba. In this study, the eco-roof is defined as a green roof without plants. Firstly, numerical models were calibrated with the experimental data of heat flux exchanged between the interior and the external environment of the building through the roof, then different irrigation strategies were evaluated. Finally, energetic parameters were studied.

3.3.1 Building models

Two building models were designed in order to simulate the energy behaviour of the traditional gravel ballasted roof and the eco-roof. These models were developed using DesignBuilder software [106], which is the graphical interface of EnergyPlus [107]. A 3D model of the building is shown in Figure 9.

First of all, all the geometric and thermal characteristics of the building and the two roofs were considered, see Table 4.

Table 4. Geometrical and thermal characteristics of the study building.

Geometrical characteristics	Height	9.0 [m]
	Floors	3
	Area	264.0 [m^2]
Thermal characteristics	U external walls	3.0 [W/m^2K]
	U ground	2.0 [W/m^2K]
	U traditional roof	2.9 [W/m^2K]
	U eco-roof	1.3 [W/m^2K]
	U windows	5.7 [W/m^2K]

Then a climatic database with the climatic conditions of Córdoba, collected every 30 min by the weather station in 2015, was set in the simulation software program. In this way, the software simulated with the same conditions of the days of the experimental campaigns.

The models were calibrated for the months of August, which represented the typical summer month for the climatic conditions of Córdoba, with high values of outdoor

air temperature and solar radiation and December, which represented the typical winter month with low values of outdoor air temperature and solar radiation. Data of heat flux collected every 15 min during the experimental campaign were used to calibrate the models.

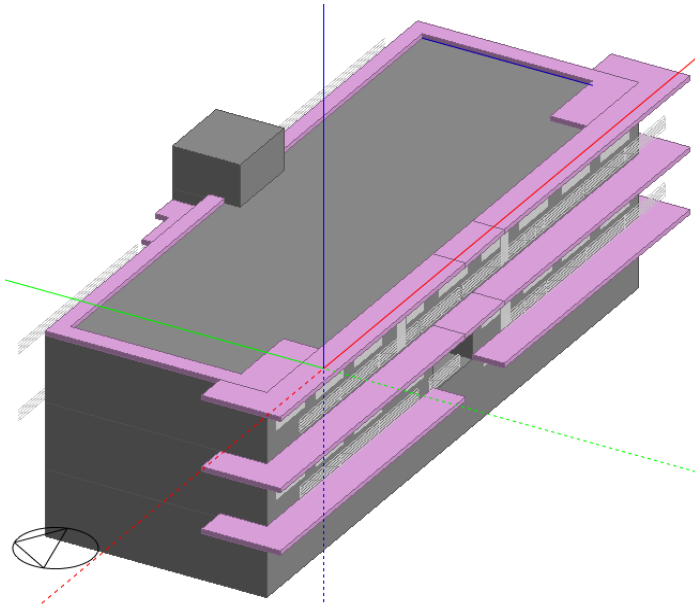

Figure 9. 3D model of the building developed with DesignBuilder.

The eco-roof energy analysis of the DesignBuilder software was based on the Army Corps of Engineers' FASST vegetation models [108,109]. In this model the energetic contribution was divided into a budget for the foliage layer, F_f, and a budget for the ground surface, F_g, [110]. The overall energy balance at the soil surface was given by Eq. (1), where the final term is the conduction of heat into the soil. The present work focused on an eco-roof only with substrate, so the energy balance of the roof was calculated without the contributions of the plants.

$$F_g = \left(1 - \sigma_f\right)\left[I_s^{\downarrow}\left(1 - \alpha_g\right) + \varepsilon_g I_{ir}^{\downarrow} - \varepsilon_g \sigma T_g^4\right] - \frac{\sigma_f \varepsilon_g \varepsilon_f \sigma}{\varepsilon_g + \varepsilon_f - \varepsilon_g \varepsilon_f}\left(T_g^4 - T_f^4\right) + \dot{Q}_s + \dot{Q}_L + K \times \frac{\partial T_g}{\partial z} \quad (1)$$

Where σ_f is the fractional vegetation coverage (zero in the eco-roof); $I_s^{\downarrow}$ is the total incoming short-wave radiation; α_g is the albedo of ground surface; $I_{ir}^{\downarrow}$ is the total incoming long-wave radiation; ε_g is the emissivity of the ground surface; T_g is the ground surface temperature; ε_f is the emissivity of the foliage; σ is the Stefan-Boltzmann constant; T_f is the foliage temperature; $\dot{Q}_s$ is the sensible heat flux; $\dot{Q}_L$ is the latent heat flux; K is the hydraulic conductivity and z is the depth.

Sensible heat flux, $\dot{Q}_s$, in an eco-roof depended on the temperature difference between the soil and the external air and the wind speed, as expressed by Eq. (2).

$$\dot{Q}_s = \rho_{ag} C_{p,a} C_h^g WS \left(T_a - T_g\right) \quad (2)$$

Where ρ_{ag} is the density of air at ground surface temperature; $C_{p,a}$ is the specific heat of air at constant pressure; C_h^g is the bulk transfer coefficient; WS is the wind speed; T_a is the air temperature near the soil and T_g is the ground surface temperature.

Latent heat flux, $\dot{Q}_L$, in an eco-roof depended on the difference between the mixing ratio of the soil surface and air and the wind speed, as expressed by Eq. (3).

$$\dot{Q}_L = C_e^g \cdot l_g \cdot WS \cdot \rho_{ag} \cdot (q_a - q_g) \quad (3)$$

Where C_e^g is the bulk transfer coefficient; l_g is the latent heat of vaporization at the ground surface; q_a is the mixing ratio of the air near to the soil and q_g is the mixing ratio at the ground surface.

3.3.2 Irrigation strategies

To investigate the reduction of heat flux through the roof assembly from the exterior to the interior of the building with eco-roof respect to the traditional gravel ballasted roof, 20 irrigation strategies were evaluated.

The irrigation strategies consisted of watering at five specific moments of the day with four different quantities of water. The daily irrigation schedules were: (i) once a day in the morning, (ii) once a day during the night, (iii) twice a day with the irrigation quantity divided between morning and evening, (iv) once a day in the

afternoon and finally (v) once a day in the morning in alternate days, i.e. it was irrigated on Monday, Wednesday, Friday and Sunday. The quantities of irrigation water were: (i) 3.7 l/m^2·day, (ii) 7.3 l/m^2·day, (iii) 11.0 l/m^2·day, (iv) 14.6 l/m^2·day, considering that 10 minutes of irrigation corresponded to 1.83 l/m^2. The combination of the five schedules and four irrigation quantities resulted in 20 irrigation strategies, $C1_{20}$ to $C5_{80}$, as summarized in Table 5. The numbers 1-5 indicated the daily irrigation schedule and the subscripts 20-80 indicated the daily minutes of irrigation. A case C0 without irrigation strategy also was studied.

The experimental eco-roof installation was provided with the irrigation strategy $C3_{20}$.

Table 5. Irrigation schedule.

Case studies	Irrigation period [min/day]	Quantity of water [l/m^2 day]	Irrigation schedule	Schedule
C0	0	0	-	-
$C1_{20}$	20	3.7	8:30 am	Every day
$C2_{20}$	20	3.7	8:30 pm	Every day
$C3_{20}$	20	3.7	8:30 am/8:30 pm	Every day
$C4_{20}$	20	3.7	1:00 pm	Every day
$C5_{20}$	20	3.7	8:30 am	Alternate days
$C1_{40}$	40	7.3	8:30 am	Every day
$C2_{40}$	40	7.3	8:30 pm	Every day
$C3_{40}$	40	7.3	8:30 am/8:30 pm	Every day
$C4_{40}$	40	7.3	1:00 pm	Every day
$C5_{40}$	40	7.3	8:30 am	Alternate days
$C1_{60}$	60	11.0	8:30 am	Every day
$C2_{60}$	60	11.0	8:30 pm	Every day
$C3_{60}$	60	11.0	8:30 am/8:30 pm	Every day
$C4_{60}$	60	11.0	1:00 pm	Every day
$C5_{60}$	60	11.0	8:30 am	Alternate days
$C1_{80}$	80	14.6	8:30 am	Every day
$C2_{80}$	80	14.6	8:30 pm	Every day
$C3_{80}$	80	14.6	8:30 am/8:30 pm	Every day
$C4_{80}$	80	14.6	1:00 pm	Every day
$C5_{80}$	80	14.6	8:30 am	Alternate days

The irrigation strategies of the eco-roof were based on a mass balance expressed by Eq. (4).

$$\Delta VWC = W + R - ET - D \quad (4)$$

Where ΔVWC is the variation of the volumetric water content stored in the substrate, W is the quantity of irrigation water, R is rainfall quantity, ET is the evapotranspiration and D is the drainage.

3.3.3 Parameters evaluated

The eco-roof under different irrigation strategies was studied according to the following parameters:

- Evapotranspiration, ET, of the substrate that was calculated directly from the latent heat flux calculations for the substrate, see Eq. (3), and the corresponding values of latent heat of water vaporization [110]. Although the term ET is used throughout this document, it should be noted that for the eco-roof the transpiration term was zero, as it was studied without vegetation. Therefore, all transformation of liquid water from the eco-roof to the atmosphere was through evaporation from the bare soil surface only.

- Heat flux, $\dot{Q}$, obtained in the eco-roof and the traditional gravel ballasted roof. Heat flux of the eco-roof, $\dot{Q}_{eco}$, was calculated with the sum of sensible heat flux and latent heat flux, expressed by Eqs. (2) and (3), respectively. The heat flux of the traditional gravel ballasted roof, $\dot{Q}_{trad}$, was calculated with the transfer model based on the conduction transfer functions, CTFs, [111,112]. In addition, experimental $\dot{Q}$ was used as calibration parameter of the roof models. The probes used to measure $\dot{Q}$ are shown in Figure 8. The positive and negative $\dot{Q}$ values indicated heat entering and leaving, respectively.

- Energy demand, ED, of the building with the eco-roof under different irrigation strategies, compared to the traditional gravel ballasted roof. ED was calculated by Eq. (5), where Q_{Pref} is the sum of the positive gains of the traditional roof and Q_{eco} is the sum of the positive gains of the eco-roof.

$$ED = \frac{Q_{Pref} - Q_{eco}}{Q_{trad}} \cdot 100 \quad (5)$$

- The energy performance of the eco-roof, P_{eco}, was analysed with a ratio, in order to evaluate the irrigation strategies that led the highest reduction of energy demand with respect to the lowest amount of irrigation water, expressed by Eq. (6), where Q_{ref} is the sum of the positive gains of the traditional roof and Q_{eco} is the sum of the positive gains of the eco-roof.

$$P_{eco} = \frac{Q_{ref} - Q_{eco}}{W} \quad (6)$$

3.4 Green roofs methodology

Three green roofs with different substrates were studied throughout the years 2016 and 2017, for the climatic conditions of Córdoba. Different experimental parameters were evaluated in order to study the energy performance of the green roofs.

3.4.1 Parameters evaluated

The three plots with green roof were evaluated according to several dynamic parameters:

- Sol-air temperature, T_{sa}, which is defined as the outside air temperature which, in the absence of solar radiation, would give the same temperature distribution and rate of heat transfer through a roof as exists due to the combined effects of the actual outdoor temperature distribution plus the incident solar radiation [113]. T_{sa} was calculated with Eq. (7) for a traditional roof [114]. This equation was characterized to calculate T_{sa} for plots with green roofs, Eq. (8), taking into account evapotranspiration contribution, according to [89,110].

$$T_{sa} = T_{amb} + \frac{\Delta R}{h_o} + \frac{\alpha}{h_o} \quad (7)$$

$$T_{sa} = \frac{h_c}{h_c + h_r} T_a + \frac{h_r}{h_c + h_r} T_{sky} + \frac{\alpha}{h_c + h_r} \quad (8)$$

Where T_{amb} is the external air temperature; ΔR is the infrared radiation difference between surface and sky and surroundings, expressed by Eq. (9); h_o is the heat transfer coefficient by radiation and convection at the outer surface, expressed by Eq. (10); h_c is the mean convective heat transfer coefficient, expressed by Eq. (11); h_r is the mean radiative heat transfer coefficient, expressed by Eq. (12); T_a is the air temperature near the soil; α is the product of the solar absorptance of the exterior surface and the rate of total solar radiation incident per unit area upon surface expressed by Eq. (13); T_{sky} is the sky temperature, which was calculated considering the sky as a black body [115], expressed by Eq. (14).

$$\Delta R = \varepsilon \cdot \sigma \cdot (F_{sky} \cdot \left(T_{sky}^4 - T_{amb}^4\right) + F_{gnd} \cdot \left(T_g^4 - T_{amb}^4\right) \quad (9)$$

$$h_o = 10.08 + 10.8 \cdot WS \quad (10)$$

$$h_c = \sigma_f \cdot h_{c_f} + \left(1 - \sigma_f\right) \cdot h_{c,s} \quad (11)$$

$$h_r = \frac{\varepsilon_f \cdot \varepsilon_g}{\varepsilon_g + \varepsilon_f - \varepsilon_g \cdot \varepsilon_f} \cdot \left(4 \cdot \sigma \cdot T_{hs}^3\right) \quad (12)$$

$$\alpha = \alpha_o \cdot SR_{Glob,H} \quad (13)$$

$$T_{sky} = T_{amb} \cdot (\varepsilon_0 + 0.8 \cdot (1 - \varepsilon_0) \cdot C_{cover})^{0.25} \quad (14)$$

- Decrement factor, DF, defined as the ratio between the maximum daily excursions of the internal and external temperature fluctuations [87], expressed by Eq. (15).

$$DF = \frac{T_{i,max} - T_{i,min}}{T_{e,max} - T_{e,min}} \quad (15)$$

- Time lag, TL, defined as the time difference between the maximum peak of the internal temperature and the maximum peak of the external

temperature for summer climatic conditions, expressed by Eq. (16), and the time difference between the minimum peak of the internal temperature and the minimum peak of the external temperature for winter climatic conditions, expressed by Eq. (17), [87].

$$TL_{summer} = t_{Ti,max} - t_{Te,max} \quad (16)$$

$$TL_{winter} = t_{Ti,min} - t_{Te,min} \quad (17)$$

DF and TL were evaluated considering $T_{sa,Pi}$ as the external boundary temperature for all the plots and $T_{1,Pi}$ as the internal boundary temperature for P1, P2 and P5, see Figure 8a. $T_{1,Pref}$ was considered the internal boundary temperature for the reference plot, see Figure 8b.

- Cooling potential, CP, is defined as the difference between the maximum internal boundary temperature of the reference plot and the maximum internal boundary temperature of the green roofs, according to Eq. (18).

$$CP = T_{1,Pref,max} - T_{1,Pi,max} \quad (18)$$

Where $T_{1,Pref,max}$ is the maximum slab temperature value for Pref and $T_{1,Pi,max}$ is the maximum slab temperature value for P1, P2 and P5. CP was only calculated for the considered summer period.

- Heat flux, measured in the growing medium in the plots with green roofs and in the gravel ballasted layer in the reference plot, see Figure 8. The heat flux sensors were placed such that a positive and negative reading signifies heat entering and leaving the building, respectively.
- Energy demand, ED, of the building with green roofs, compared to the traditional gravel ballasted roof. ED was calculated by Eq. (19), where $\mathrm{Q_{Pref}}$ is the sum of the positive gains of the traditional roof and $\mathrm{Q_{Pi}}$ is the sum of the positive gains of the green roof.

$$ED = \frac{\mathrm{Q}_{Pref} - \mathrm{Q}_{Pi}}{\mathrm{Q}_{Pref}} \cdot 100 \quad (19)$$

Chapter 4

Eco-roof analysis

In this chapter, two numerical models of eco-roof and traditional gravel ballasted roof were carried out. The impact of climatic variables and volumetric water content of the substrate on evapotranspiration were evaluated. Then, the effect of the volumetric water content of the substrate due to different irrigation strategies on the heat flux through the eco-roof, was obtained. Paper II shown in appendix B addressed the results of this chapter.

4.1 Calibration of the numerical models

The calibration of two numerical models, one of a traditional gravel ballasted roof and one of an eco-roof, that corresponded to P1 without plants, was carried out with the DesignBuilder software, as defined in 3.3.1.

The climatic variables recordered in 2015 to analyse the eco-roof were ambient air temperature, T_o, relative humidity, RH_o, rainfall, R, wind speed, WS, direction of the wind, WD, and solar radiation, SR. The average values of monthly climatic data are shown in Table 6.

Table 6. Average values of monthly climatic data of Córdoba, 2015.

2015	T_o [°C]	RH_o [%]	SR [Wh/m²]	WD [°]	WS [m/s]	R [mm]
January	10.6	89.9	90	171.5	1.6	0.9
February	10.9	81.9	116.5	184.4	2.2	0.84
March	11.4	71.9	200.6	201.6	1.5	0.5
April	15.8	66.4	227.1	199.1	1.7	1.7
May	18.6	61.3	257.5	192.6	1.9	1.3
June	24.9	43.5	323.7	206.7	2.0	0
July	29.1	40.5	318.3	206.9	1.9	0
August	27.6	45	265.6	207.8	2.0	0
September	22.5	53.5	221.7	201.2	1.8	0.2
October	18.5	73.8	146.2	155.9	1.3	1.4
November	12.8	77.5	137.1	135.8	1.1	1.0
December	10.2	77.6	95.9	110	1.0	0.2

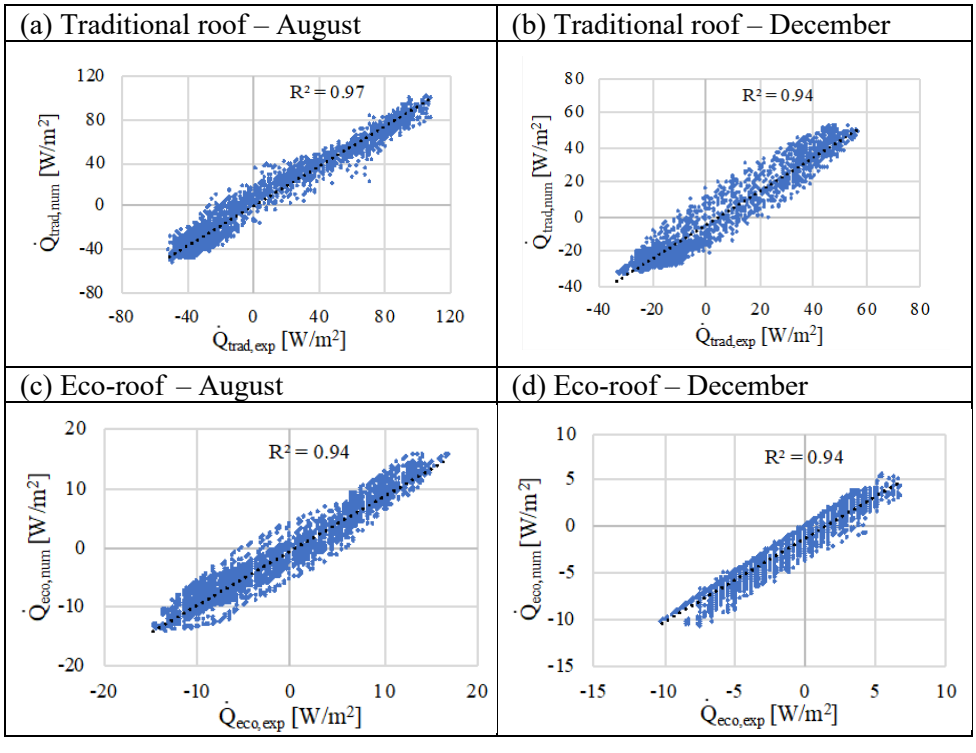

Figure 10. Calibration of models of the traditional gravel ballasted roof in (a) August and (b) December, and the eco-roof in (c) August and (d) December.

Data of heat flux collected every 15 min during the experimental campaign were used to calibrate the models. The R^2 values of $\dot{Q}$ experimental respect to $\dot{Q}$ numerical obtained were always equal or higher than 0.94, see Figure 10.

The calibrated numerical models were used to analyse the behaviour of the eco-roof under different irrigation strategies. Firstly, the effects of climatic variables and volumetric water content of the substrate on evapotranspiration were studied. Then, the influence of evapotranspiration on heat flux was evaluated. Finally, a study on the effect of volumetric water content of the substrate on weekly energy was performed. All the results of the analysis are described below.

4.2 Effect of climatic variables on evapotranspiration

A weekly analysis of the effects of climatic variables on the ET of the eco-roof was carried out. Two typical weeks for the climatic conditions of Córdoba were selected for this study: a summer week from 15/08/2015 to 21/08/2015, where the eco-roof was provided with the experimental irrigation strategy $C3_{20}$ and a winter week from 02/01/2015 to 08/01/2015 with no irrigation schedule, C0, see Table 5.

The climatic variables used were outdoor air temperature, T_o, solar radiation, SR, wind speed, WS, and outdoor relative humidity, RH_o. The results of this analysis are shown in Figure 11. It can be observed that the trends obtained of the climatic variables on ET were similar for both weeks, although different slopes were obtained. The ET values increased when the values of T_o, WS and SR rose, see Figure 11a, Figure 11c and Figure 11d, respectively. However, the ET values increased when the RH_o values decreased, see Figure 11b. In previous studies of the effects of climatic conditions on ET, similar trends were obtained [33,91].

For the summer week, the ET values were usually higher than those during the winter week, see Figure 11, mainly due to the high values of T_o and SR and low values of RH_o achieved with respect to those during the winter week. For the winter week, almost all the ET values were lower than 0.05 mm/h.

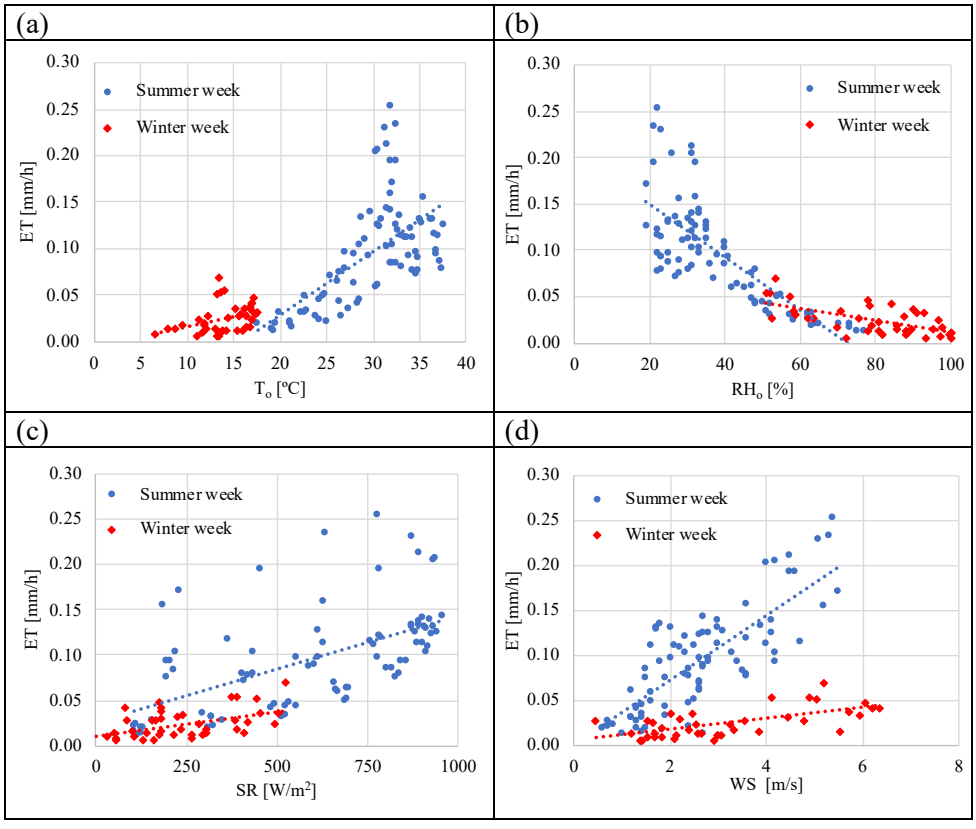

Figure 11. Effect of climatic conditions (a) outdoor air temperature; (b) outdoor relative humidity; (c) solar radiation; (d) wind speed, on evapotranspiration.

4.3 Effect of volumetric water content of the substrate on evapotranspiration

An analysis of the effects of VWC on ET for all the irrigation strategies was carried out for the two weeks studied, a summer week from 15/08/2015 to 21/08/2015, where the eco-roof was provided with the experimental irrigation strategy $C3_{20}$ and a winter week from 02/01/2015 to 08/01/2015 with no irrigation schedule, C0, see Table 5.

The average weekly results of VWC with respect to ET are represented in Figure 12. For the summer week, it can be observed that ET values increased when the weekly average of VWC increased. The highest average ET values were

obtained for the irrigation strategies $C1_{60}$ and $C1_{80}$, 0.379 mm/h and 0.390 mm/h, with an average VWC value of 36.6% for both cases, see Figure 12. The lowest average ET values were obtained for the irrigation strategies C0 and $C3_{20}$, 0.008 mm/h and 0.04 mm/h, with average VWC values of 4.0% and 10.0%, respectively. Thus, it can be said that the weekly average VWC value of the substrate had a significant impact on ET during the summer week.

For the winter week, the highest average ET values were achieved for the irrigation strategies $C1_{40}$ to $C5_{80}$, see Figure 12. The case C0, which had no irrigation schedule, achieved the lowest value of ET, 0.008 mm/h, with an average VWC value of 15.7%. The average VWC value for C0 depended on the rain during this winter week. The results obtained for the winter week showed that average ET values did not have a significant variation when average VWC values and irrigation strategies were modified.

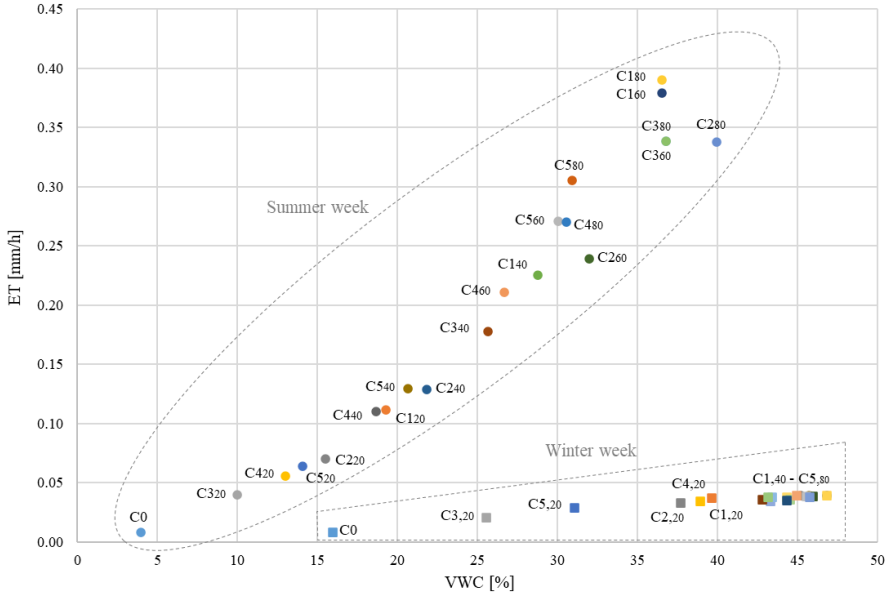

Figure 12. Average weekly results of evapotranspiration and volumetric water content of the substrate.

4.4 Effect of evapotranspiration on heat flux

A weekly study of the average heat fluxes, $\dot{Q}$, average evapotranspiration, ET, and irrigation strategies of the eco-roof was performed for the typical summer week selected, from 15/08/2015 to 21/08/2015. However, this analysis was not carried out for the winter week selected, because the ET values did not vary significantly with respect to the different irrigation strategies, as shown in section 4.3.

The results of the relationship between average heat fluxes, $\dot{Q}$, and average evapotranspiration, ET, under the irrigation strategies are shown in Figure 13. The $\dot{Q}$ values represented were the average positive heat flux values, energy flux gains. It can be observed that the average $\dot{Q}$ values were reduced when average ET values increased. This trend was opposite to the relationship between VWC on ET, as shown in Figure 12. The lowest average $\dot{Q}$ values were achieved for $C1_{60}$ and $C1_{80}$, 6.5 W/m^2 and 6.4 W/m^2, coinciding with the highest ET values, 0.379 mm/h and 0.39 mm/h, respectively, see Figure 13. The highest average $\dot{Q}$ values for the cases with an irrigation strategy, were achieved by $C3_{20}$ and $C4_{20}$, 29.7 W/m^2 and 29.3 W/m^2, respectively. For C0, an average $\dot{Q}$ value of 31.4 W/m^2 and an ET value close to zero were obtained, due to the absence of irrigation. The results showed that if a significant reduction of $\dot{Q}$ is required, high ET values are needed, i.e. irrigation strategies with a high quantity and frequency of water application should be used.

For the selected summer week, the $\dot{Q}$ value of the traditional gravel ballasted roof was 52.3 W/m^2, 40% more than the $\dot{Q}$ value of the eco-roof rate with no irrigation strategy, C0. The use of an irrigation strategy for the eco-roof allowed a significant reduction of the average $\dot{Q}$ value, up to 87.7% for the strategy $C1_{80}$ with respect to the traditional gravel ballasted roof. Therefore, an eco-roof provided with an optimized irrigation strategy could be used to reduce the heat transfer through the roof assembly of a building.

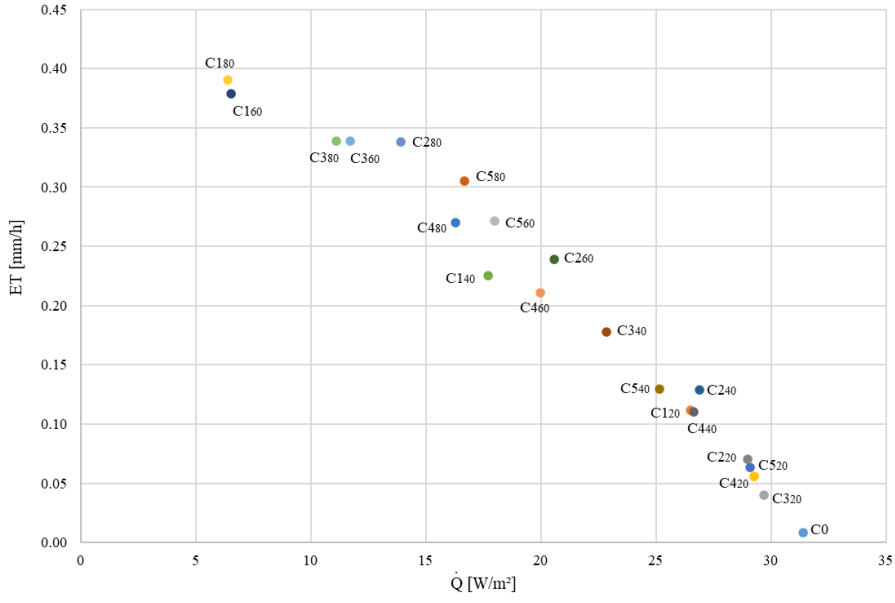

Figure 13. Average weekly results of evapotranspiration and heat flux for a typical summer week.

4.5 Effect of volumetric water content on weekly energy

The relationship between irrigation and cumulative energy gains, Q, for the different case studies is shown in Figure 14. Comparing the irrigation strategies with the same quantity of water and different watering schedule, the results showed that for the case studies $C1_{20}$ to $C5_{20}$, the Q values obtained, from the lowest to the highest, were: $C1_{20}$, 1829.1 W·h/m^2; $C2_{20}$, 2151.9 W·h/m^2; $C5_{20}$, 2153.9 W·h/m^2; $C4_{20}$, 2195.9 W·h/m^2, and $C3_{20}$, 2230.5 W·h/m^2, see Figure 14. Therefore, for these case studies, the irrigation during the morning allowed the greatest reduction of Q to be obtained, as the highest values of ET and VWC were achieved during the morning, see Figure 12 and Figure 13. However, the lowest reduction of Q was obtained watering twice a day with the irrigation quantity divided between morning and evening, $C3_{20}$.

For the irrigation strategies $C1_{40}$ to $C5_{40}$, the Q values from lowest to highest were: $C1_{40}$, 1043.8 W·h/m^2; $C3_{40}$, 1440.0 W·h/m^2; $C5_{40}$, 1711.3 W·h/m^2; $C2_{40}$, 1828.2 W·h/m^2, and $C4_{40}$, 1838.1 W·h/m^2, see Figure 14. Hence, the lowest value

of Q was obtained by irrigating during the morning, while the highest was by irrigating at 1pm. These results agreed with the previous ET analysis, see Figure 13. Among the cases $C1_{60}$ to $C5_{60}$, the irrigation strategies with Q values from the lowest to the highest were: $C1_{60}$, 189.1 W·h/m^2; $C3_{60}$, 504.1 W·h/m^2; $C5_{60}$, 882.0 W·h/m^2; $C4_{60}$, 1198.0 W·h/m^2; $C2_{60}$, 1235.1 W·h/m^2, see Figure 14. Therefore, the highest and lowest values of $\dot{Q}$ were achieved by watering during the morning, at 8:30 am, and during the afternoon, at 1:00 pm, respectively. Finally, for the cases $C1_{80}$ to $C5_{80}$, the irrigation strategies with Q values from the lowest to the highest were: $C1_{80}$, 168.5 W·h/m^2; $C3_{80}$, 454.7 W·h/m^2; $C2_{80}$, 695.1 W·h/m^2; $C5_{80}$, 750.9 W·h/m^2; $C4_{80}$, 878.8 W·h/m^2, see Figure 14.

Comparing the irrigation strategies with the same watering schedule and different quantities of water, the results showed that Q reduced as the quantity of water increased. For the cases C1, with irrigation at 8:30 am, $C1_{40}$ achieved a Q value 42.9% lower than $C1_{20}$, while $C1_{60}$ achieved a Q value 81.8% lower than $C1_{40}$. However, $C1_{80}$ presented a slight reduction in Q compared to $C1_{60}$, 10.8%. Therefore, the cases C1 followed an asymptotic trend. Regarding the cases C2, with irrigation at 8:30 pm, $C2_{40}$ achieved a Q value 15.0% lower than $C2_{20}$, while $C2_{60}$ achieved a Q value 32.4% lower than $C2_{40}$. Finally, $C2_{80}$ reduced the Q value 56.2% with respect to $C2_{60}$. It can be observed that the Q results for the cases C2 presented a decreasing linear trend. For the cases C3, strategies with irrigation twice a day, $C3_{40}$ obtained a Q value 32.4% lower than $C3_{20}$, $C3_{60}$ obtained a Q value 65.0% lower than $C3_{40}$ and $C3_{80}$ achieve a slight reduction in Q compared to $C3_{60}$, 9.8%. Therefore, the cases C3 also followed an asymptotic trend, as in cases C1. For the cases C4, with the irrigation schedule at 1:00 pm, the Q value of $C4_{40}$ was 16.3% lower than $C4_{20}$, the Q value of $C4_{60}$ was 34.8% lower than $C4_{40}$, and finally, the Q value of $C4_{80}$ was 26.7% lower than $C4_{60}$. Regarding cases C5, the strategies with irrigation on alternate days, it can be observed that $C5_{40}$ achieved 20.5% of Q values lower than $C5_{20}$, $C5_{60}$ achieved 48.4% of Q values lower than $C5_{40}$ and, finally, $C5_{80}$ obtained 14.8% of Q values lower than $C5_{60}$. Therefore, the results of the cases C5 presented a decreasing linear trend, with low reduction of Q values when the watering increased.

These results showed that the greatest reduction in Q was obtained for the strategies with irrigation once a day in the morning, at 8:30 am. In addition, the greater the irrigation of water, the greater the reduction of Q. In any case, it is important to stress that even with the same overall quantity of water, important differences in Q can be obtained, simply by changing the irrigation management.

This implies that even under the same water quantity, it is important to optimize irrigation scheduling.

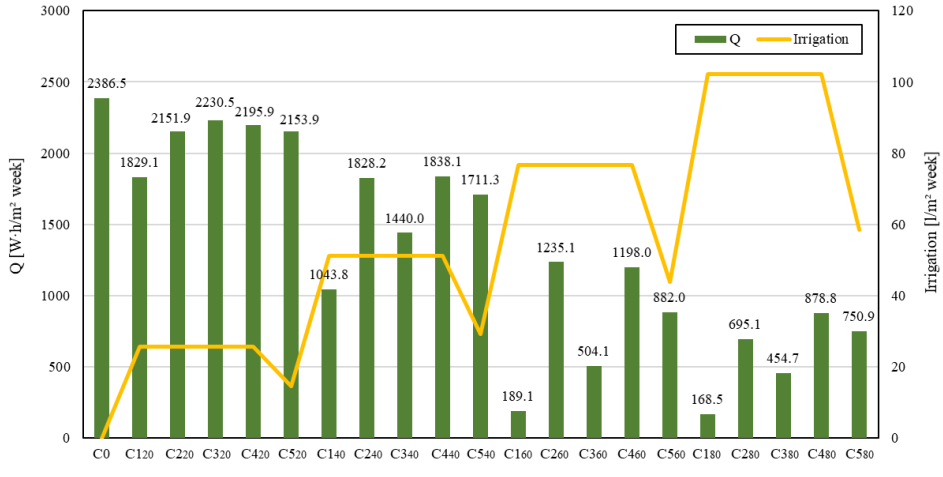

Figure 14. Relationship between cumulative energy gains and irrigation for a typical summer week.

4.6 Conclusion of the chapter

In this chapter, an analysis of the thermal performance of an eco-roof under 20 different irrigation strategies, compared to a traditional gravel ballasted roof, was carried out. Hence, a building model with two different roofs, an eco-roof and a traditional gravel ballasted roof, was calibrated with experimental data of heat flux. The study was performed during the year 2015 for the climatic conditions of Córdoba (Spain). An analysis based on evapotranspiration, ET, volumetric water content of the substrate, VWC, and heat flux, $\dot{Q}$,was performed.

The weekly results showed that the ET values increased when the values of outdoor air temperature, wind speed and solar radiation rose, and outdoor air relative humidity values decreased. The VWC value of the substrate also had a significant impact on ET during the summer, such that the higher the VWC, the higher the ET. The highest average ET values in summer were obtained for the strategies with irrigation once a day at 8:30 am for 60 min and 80 min. The results

obtained in winter showed that average ET values did not have a significant variation when the VWC and irrigation strategy were modified.

ET had a great impact on the reduction of $\dot{Q}$ of the eco-roof, since the weekly $\dot{Q}$ values were reduced when weekly ET values increased. The lowest weekly $\dot{Q}$ values were achieved for the strategies with irrigation once a day at 8:30 am for 60 min and 80 min, coinciding with the highest weekly ET. The greatest reduction of weekly $\dot{Q}$ were always achieved by watering every day during the morning.

Finally, the weekly energy analysis showed that the volumetric water content strongly influenced the cumulative energy gains of the eco-roof, achieving high reduction of Q when the eco-roof was under the proposed irrigation strategies.

These results showed that ET was directly linked with the atmospheric conditions and the water content in the substrate of the eco-roof and contributed to the $\dot{Q}$ reduction of the eco-roof. Therefore, a proper irrigation strategy could help further to reduce the $\dot{Q}$ exchanged between the interior and the external environment of the building through the roof installation.

Chapter 5

Green-roof analysis

In this chapter an experimental study of green roofs with different substrates was performed. A dynamic analysis based on several parameters such as time lag, TL, decrement factor, DF, soil-air temperature, Tsa, and cooling potential, CP, in order to evaluate the reduction of energy demand of the building with green roof respect to a traditional gravel ballasted roof was carried out. The green roof plots were studied throughout the years 2016 and 2017. The analysis of the experimental results for 2016 is presented in weekly, monthly and annual analysis to correctly understand the behaviour of the extensive green roof plots for the climatic conditions of Córdoba. Nevertheless, the analysis of the experimental results for 2017 is presented in annual analysis, because the monthly average temperature values were similar for both years, see Table 7.

5.1 Previous analysis

Before the analysis of the three green roofs with different substrates, the characteristics of the plants were evaluated. The values of fractional vegetation coverage, σ_f , and the leaf area index, LAI, for each plot were $\sigma_f = 0.59$ and LAI = 2 for P1, $\sigma_f = 0.56$ and LAI = 1.7 for P2, and $\sigma_f = 0.53$ and LAI = 1.5 for P5.

Then, the same climatic variables of the eco-roof analysis were recorded, T_o, RH_o, R, WS, WD and SR. The average values of monthly climatic data from 2016 to 2017 are shown in Table 7.

Table 7. Average values of monthly climatic data of Córdoba, 2016-2017.

2016	T_o [°C]	RH_o [%]	SR [Wh/m²]	WD [°]	WS [m/s]	R [mm]
January	10.6	89.8	88.9	156.8	1.6	1.9
February	10.9	81.6	119.2	177.8	2.1	1.5
March	11.4	71.8	199.2	194.3	1.5	0.9
April	15.7	66.5	226.2	223.0	1.7	3.8
May	18.6	61.3	257.4	203.6	1.9	2.9
June	24.9	43.5	324.8	223.6	2.0	0
July	29.1	40.5	318.1	215.5	1.9	0
August	28.5	41.6	297.9	229.9	1.6	0
September	24.9	44.1	243.0	184.9	1.7	0.1
October	19.6	65.1	160.6	165.6	1.2	2.7
November	12.5	77.9	110.1	132.7	1.4	4.7
December	10.4	81.1	100.4	66.3	1.2	1.4
2017	T_o [°C]	RH_o [%]	SR [Wh/m²]	WD [°]	WS [m/s]	R [mm]
January	7.6	74.3	122.9	135.7	1.2	0.6
February	11.7	78.8	118.3	153.3	1.6	1.7
March	13.1	74.3	197.2	151.9	1.6	2.4
April	17.4	60.1	260.5	166.2	1.6	2.3
May	20.7	58.9	298.5	216.4	1.7	1.5
June	27.4	40.2	340.1	199.8	1.9	0.3
July	28.0	40.6	319.2	239.5	2.0	0
August	27.9	42.1	282.5	224.5	1.4	0.2
September	23.9	47.0	239.7	226.9	1.3	0
October	20.8	58.1	180.3	105.1	1.1	0.9
November	12.1	71.0	126.5	79.8	1.2	1.7
December	8.1	83.7	97.3	121.2	1.4	1.2

5.2 Summer behaviour of extensive green roofs

A typical summer week was selected for the study of the summer behaviour of the green roof plots, analysing in depth the climatic conditions, the substrate temperature profile and the TL, DF and CP parameters.

The climatic conditions for the selected summer period, from 23/07/2016 to 29/07/2016, are shown in Figure 15. The values of total horizontal solar radiation and external air temperature were similar for each day of the week, reaching peaks of 994 W/m^2 and 39.4 ºC, respectively, see Figure 15a. It can also be observed a

weekly oscillation of relative humidity between 14.5% and 73.7%, a weekly variation of wind speed between 0 m/s and 4.8 m/s and absence of rainfall, see Figure 15b.

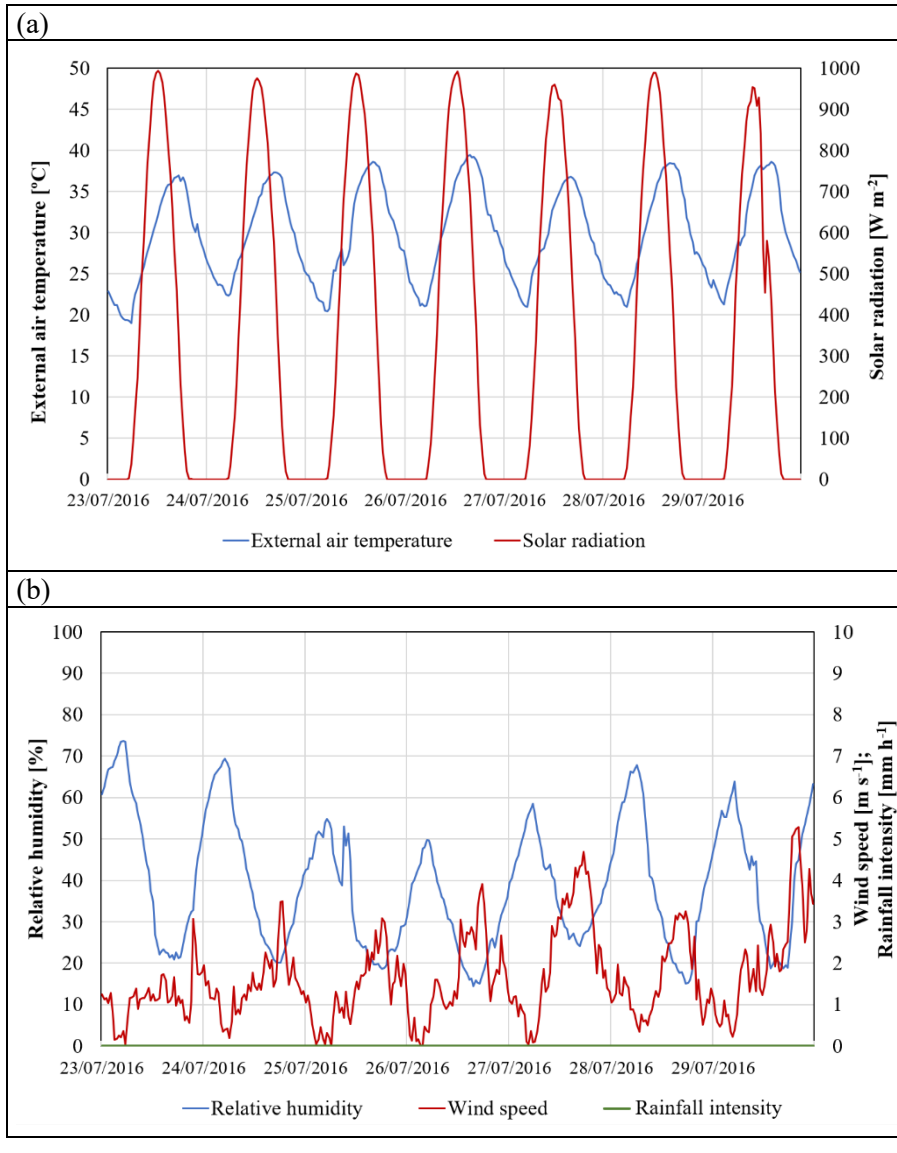

Figure 15. Climatic conditions of the selected summer period. (a) Solar radiation and external air temperature. (b) Rainfall, windspeed and relative humidity

5.2.1 Weekly analysis of sol-air temperature, temperature profile and volumetric water content

The temperature values measured and sol-air temperature calculated, T_{sa}, for the three plots with green roof and for the reference plot, Pref, and VWC in the substrates of P1, P2 and P5, for the selected summer period are shown in Figure 16. The T and VWC values were obtained from the average value measured by the two probes located in the same horizontal profile.

Regarding the water content in the substrate, it can be observed an increase in its value in the three green roofs when the irrigation was operating. For P1, VWC values oscillated between 18.3% and 26.4% during the week, with a weekly average value of 22.8%, see Figure 16a. For P2, the variation was less than for P1, between 9.7% and 12.8%, with a weekly average value of 11.1%, see Figure 16b, and finally, for P5, the oscillation obtained was between 14.1% and 17.9%, with a weekly average value of 15.9%, see Figure 16c. These results showed that the substrate of P1, with 100% commercial growing medium, managed to retain more water in summer than the rest of the plots, using the same amount of watering. The substrate of P2, with 75% commercial growing medium and 25% recycled construction materials, was the one that retained the least water, with values lower than the substrate of P5, with 50% commercial growing medium and 50% recycled construction materials, see Figure 16b and 13c. It can also be seen that the maximum temperatures in the green roofs were achieved for T_4, measured in the upper part of the substrate, with values of 48.5 ºC, 55.7 ºC and 48.2 ºC for P1, P2 and P5, respectively. For the last days of the week, the highest T_4 values of the green roofs decreased as the water content in the substrate increased, especially in P1, see Figure 16a, 13b and 13c. Therefore, these results show the relation between the substrate used and VWC. However, the highest $T_{2,Pref}$ values were stable throughout the week, because there was no irrigation and the highest external temperatures was also constant, see Figure 15a.

The temperature values measured decreased according to the depth of the four plots. The minimum temperature values for the three plots with green roofs were obtained for T_1, measured below the drainage layer, oscillating between 27.6 ºC and 34.8 ºC for P1, see Figure 16a, between 27.2 ºC and 35.9 ºC for P2, see Figure 16b, and between 27.3 ºC and 33.6 ºC for P5, see Figure 16c. For Pref, $T_{1,Pref}$ values variated between 30.1 ºC and 50.1 ºC.

Regarding T_{sa}, similar values were obtained for the three plots with green roofs, with maximum and minimum values of 60.0 ºC and 18.5 ºC, respectively. However, T_{sa} values for Pref increased significantly during the morning, up to 80.5 ºC, and decreased during the night, up to 16.0 ºC.

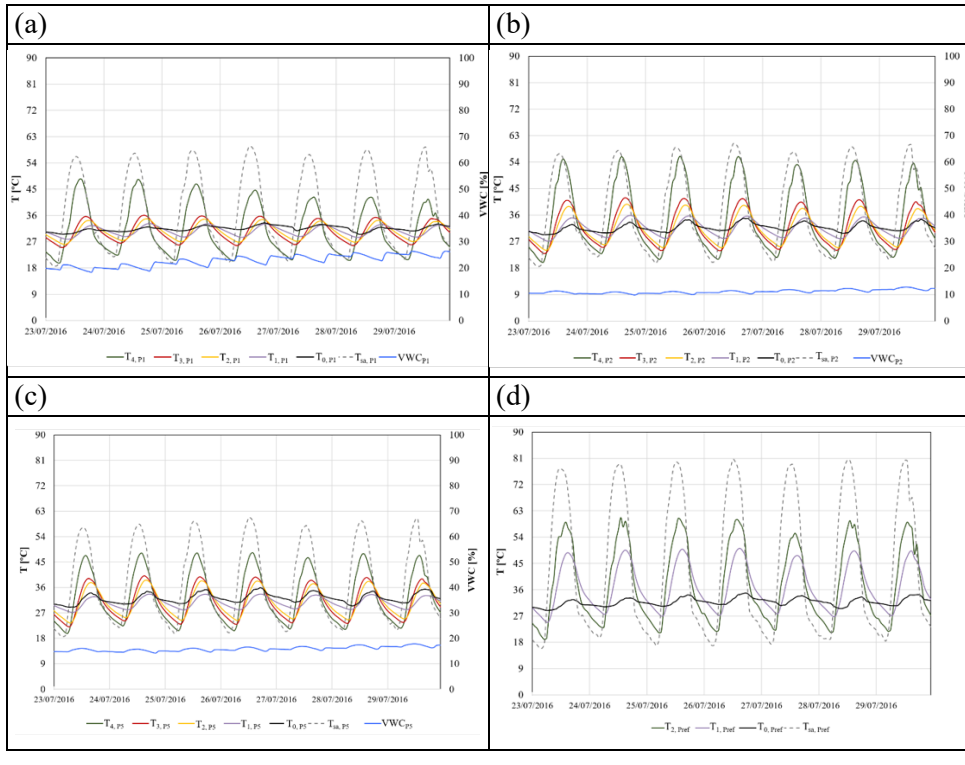

Figure 16. Temperature profile measured, sol-air temperature and water content measured in the substrate for (a) P1; (b) P2; (c) P5; (d) Pref, in the summer period.

5.2.2 Weekly analysis of time lag and decrement factor

The values of decrement factor, DF, and time lag, TL, for the three plots with green roof and the reference plot, Pref, were calculated using Eqs. (15) and (16), respectively. The daily results of DF and TL for the summer week are shown in Figure 17.

The parameter DF showed the oscillations of $T_{1,Pi}$ (ΔT_i), temperature values between the roof slab and the root barrier, respect to the oscillations of $T_{sa,Pi}$ (ΔT_e), see Eq. (15). The higher ΔT_e or the lower ΔT_i, the lower DF is. In Figure 16, it can be observed that ΔT_e values were similar for the three green roofs, because the T_{sa}

values were similar. The ΔT_i values varied in each plot with green roofs, mainly due to the capacity of the substrate to retain water during the daily irrigation. Therefore, the higher capacity to retain water, the lower values of ΔT_i and DF were obtained, see Figure 16. The lowest DF values were always achieved in P1, with an average weekly value of 0.12, see Figure 17a, in agreement with the lowest values of $T_{1,P1}$, as shown in Figure 16a, mainly due to the high capacity of the substrate to retain water. Comparing the three plots with green roofs, the highest DF values were obtained in P2, with an average weekly value of 0.19, see Figure 17a, mainly due to the low capacity of retaining water in its substrate, so the oscillations of $T_{1,P2}$ were higher, see Figure 16b. The DF values increased significantly in Pref. It can be observed that Pref presented the highest DF values throughout the selected period, with an average weekly value of 0.36, see Figure 17a, mainly due to the fluctuation of the slab temperature, $T_{1;Pref}$, see Figure 16d. These results indicated that, for very warm and dry climatic conditions, the higher the capacity to retain water in the substrate, the higher the reduction in the oscillation of the slab temperature, $T_{1,Pi}$, and DF is.

The TL parameter measured the difference in time between the maximum daily $T_{sa,Pi}$ values and the maximum daily $T_{1,Pi}$ values for the summer climatic conditions, see Eq. (16). The TL results were mainly related to the fractional vegetation coverage, the leaf area index, the composition of the substrates and their capacity to retain water and the water accumulated in the drainage layer. The TL values shown in Figure 17b could be divided into several part of TL according to the layers of the plots. There was a TL from the maximum daily $T_{sa,Pi}$ value to the maximum daily $T_{4,Pi}$ value (vegetation layer), see Figure 16, another TL of maximum daily temperatures from $T_{4,Pi}$ to $T_{2,Pi}$ (substrate layer), see Figure 16, and finally, another TL of maximum daily temperatures from $T_{2,Pi}$ to $T_{1,Pi}$ (water accumulation layer), see Figure 16. The TL values due to the vegetation layer were similar for the three plots, between 1 h and 2 h. The TL values due to the substrate layer were higher for P1 than P2 and P5, due to volumetric water content of the substrates. Finally, the highest TL values due to the water accumulation layer were for P2, see Figure 16. In this case, the substrate drained more water than the other substrates and consequently there was more water accumulated in this layer. As a result, the order of the plots that presented from the highest to the lowest values of TL were P1, P2, P5 and Pref, with average weekly values of 6:08h, 5:17h, 4:17h and 2:42h, respectively, see Figure 17b, mainly due the cross-effects of the different layer of the plots. Previous studies also showed the importance of vegetation and composition of the substrate in the dynamic characterization of a green roof [89],

with maximum weekly average TL values of 4:20h. Nevertheless, in the present work higher TL values were found, up to 6.08 h, as shown in Figure 17b. The TL values confirm the green roof benefits for the retrofit of buildings without insulation by delaying the peak in the maximum surface temperature.

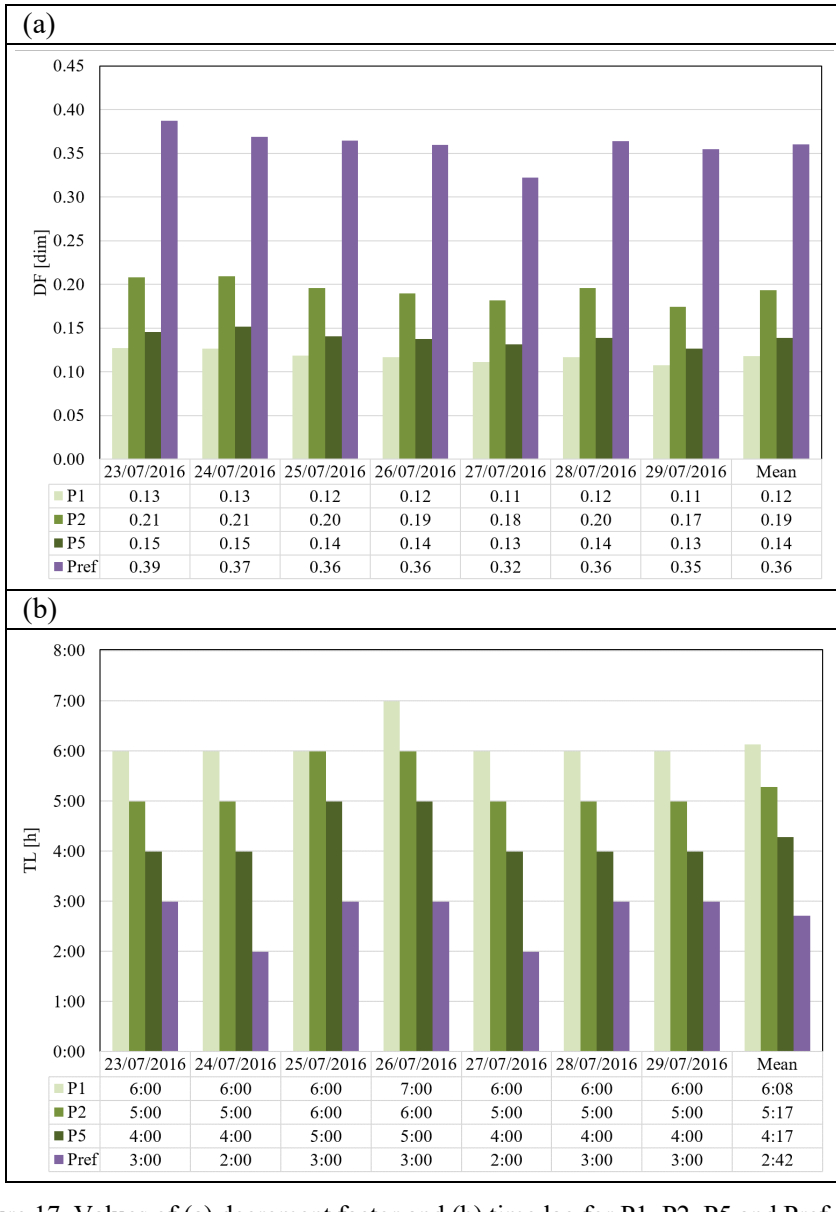

	23/07/2016	24/07/2016	25/07/2016	26/07/2016	27/07/2016	28/07/2016	29/07/2016	Mean
P1	0.13	0.13	0.12	0.12	0.11	0.12	0.11	0.12
P2	0.21	0.21	0.20	0.19	0.18	0.20	0.17	0.19
P5	0.15	0.15	0.14	0.14	0.13	0.14	0.13	0.14
Pref	0.39	0.37	0.36	0.36	0.32	0.36	0.35	0.36

	23/07/2016	24/07/2016	25/07/2016	26/07/2016	27/07/2016	28/07/2016	29/07/2016	Mean
P1	6:00	6:00	6:00	7:00	6:00	6:00	6:00	6:08
P2	5:00	5:00	6:00	6:00	5:00	5:00	5:00	5:17
P5	4:00	4:00	5:00	5:00	4:00	4:00	4:00	4:17
Pref	3:00	2:00	3:00	3:00	2:00	3:00	3:00	2:42

Figure 17. Values of (a) decrement factor and (b) time lag for P1, P2, P5 and Pref in the selected summer period.

5.2.3 Weekly analysis of cooling potential

The cooling potential, CP, of the three plots with green roofs was evaluated for the selected summer period, according to Eq. (18). The results of daily CP and a weekly average value for each plot are shown in Figure 18. It can be seen that the highest CP values were obtained in P1, with a weekly average value of 16.3 ºC. The second plot with the highest CP was P5, with a weekly average of 15.8 ºC, 3% less than P1. Finally, P2 had the lowest CP values compared to the rest of the plots with green roofs, a 15% less than P1. This study showed that the plots with green roofs always allowed the slab temperature to reduce by more than 12.7 ºC, compared to Pref. These results were inversely proportional to the DF values, Figure 17a, where the green roof that had the greatest capacity to retain water in the substrate, P1, achieved the best results. Therefore, the higher the capacity to retain water in substrate, the higher CP is.

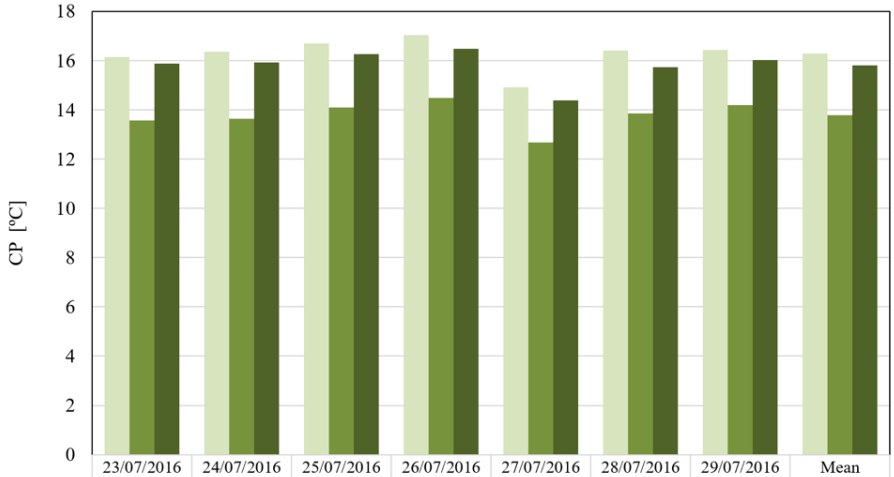

	23/07/2016	24/07/2016	25/07/2016	26/07/2016	27/07/2016	28/07/2016	29/07/2016	Mean
P1	16.1	16.4	16.7	17.0	14.9	16.4	16.4	16.3
P2	13.6	13.6	14.1	14.5	12.7	13.8	14.2	13.8
P5	15.9	15.9	16.3	16.5	14.4	15.7	16.0	15.8

Figure 18. Cooling potential values for P1, P2 and P5 in the selected summer period.

5.3 Winter behaviour of extensive green roofs

A weekly analysis for a typical winter week, similar to that performed in section 5.2, was carried out. The winter week selected was from 12/12/2016 to 18/12/2016. The climatic conditions, the substrate temperature profile and the TL and DF

parameters were also analysed for this week. The climatic conditions for the selected winter period are shown in Figure 19.

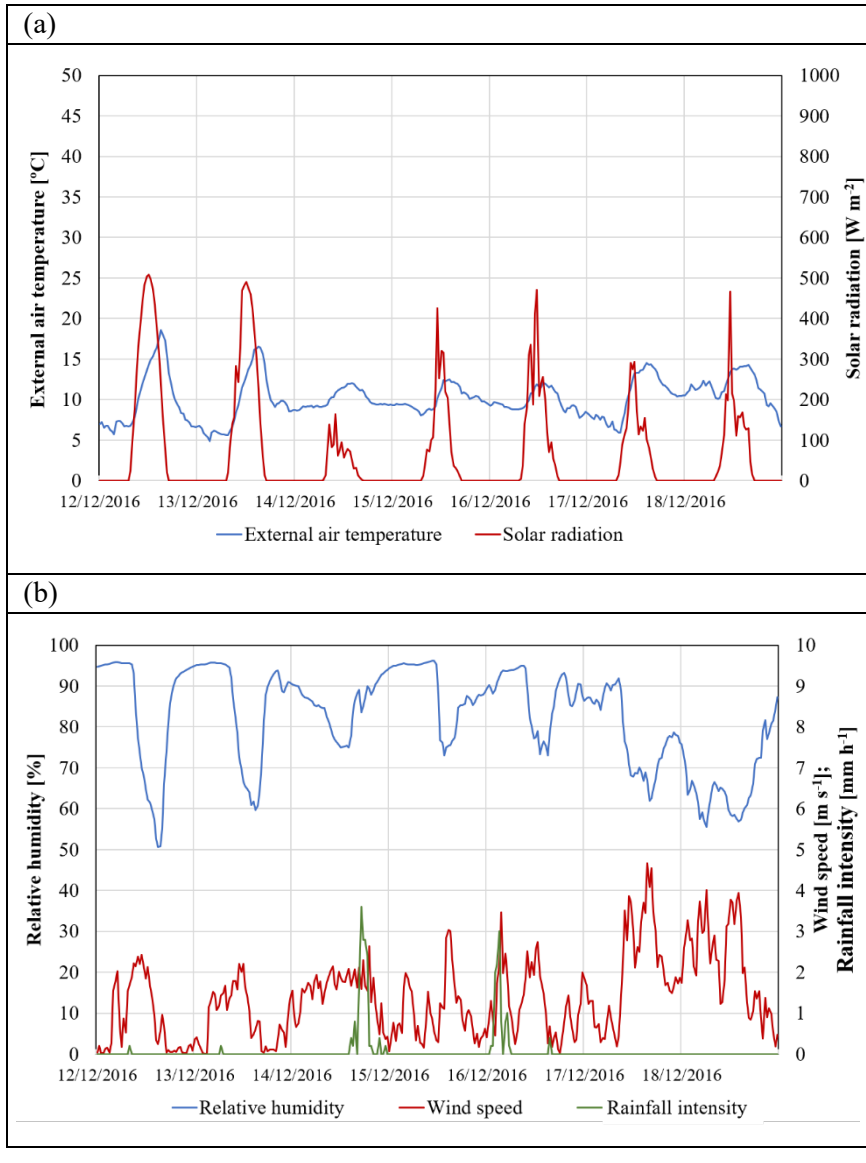

Figure 19. Climatic conditions of the selected winter period. (a) Solar radiation and external air temperature. (b) Rainfall, windspeed and relative humidity.

The peak values of total horizontal solar radiation and external air temperature varied each day, with maximum values of 507.7 W/m^2 and 18.6 ºC during the first day, respectively, see Figure 19a. The selected week also had some rainy days, with a total weekly rainfall of 26.8 mm/h, see Figure 19b. The minimum values of total horizontal solar radiation and external air temperature were obtained for day 14/12/2016, see Figure 19a, coinciding with the day with the highest rainfall, see Figure 19b. It can also be observed an oscillation of relative humidity between 50.7% and 96.1% and wind speed between 0 m/s and 4.7 m/s.

5.3.1 Weekly analysis of sol-air temperature, temperature profile and volumetric water content

Temperature profile, sol-air temperature and volumetric water content in the substrate of the three plots with green roof and the reference plot for the selected winter week are shown in Figure 20. The irrigation during this week wasn't planned, so the percentage of water present in the substrate depended on the air humidity and the amount of rainfall, see Figure 19b. It can be observed that the weekly average VWC values for the three plots with green roof were similar, 47.6%, 48.2% and 47.7% for P1, P2 and P5, respectively. For the first two days, that had low rainfall, the VWC values oscillated between 39.5 % and 43.6%. However, these values increased in the following days, that had high rainfall, up to 56.8%, 56.7% and 51.2% for P1, P2 and P5, respectively. Regarding the temperatures measured, the T_4 values for green roofs and the T_2 values for Pref oscillated each day, more than the rest of the temperature values measured, due to the fact that the climatic conditions had more influence on their reading. The maximum T_4 values obtained were 17.8 ºC, 19.8 ºC and 17.1 ºC for P1, P2 and P5, respectively, and the maximum T_2 values obtained for Pref was 27.2ºC. These temperature peaks decreased as a function of the depth measured for the four plots, as well as for the summer period studied, obtaining the lowest oscillations for T_1 for all plots. The maximum values of T_1 for P1, P2, P5 and Pref were 11.6 ºC, 12.6 ºC, 12.2 ºC and 16.5 ºC, respectively.

In Figure 20, it can also be seen that the T_{sa} values for the plots with green roof were similar, with maximum and minimum values of 28.2 ºC and 4.8 ºC, respectively. However, T_{sa} values for Pref increased significantly during the morning, up to 41.2 ºC, and decreased during the night, up to 3.2 ºC.

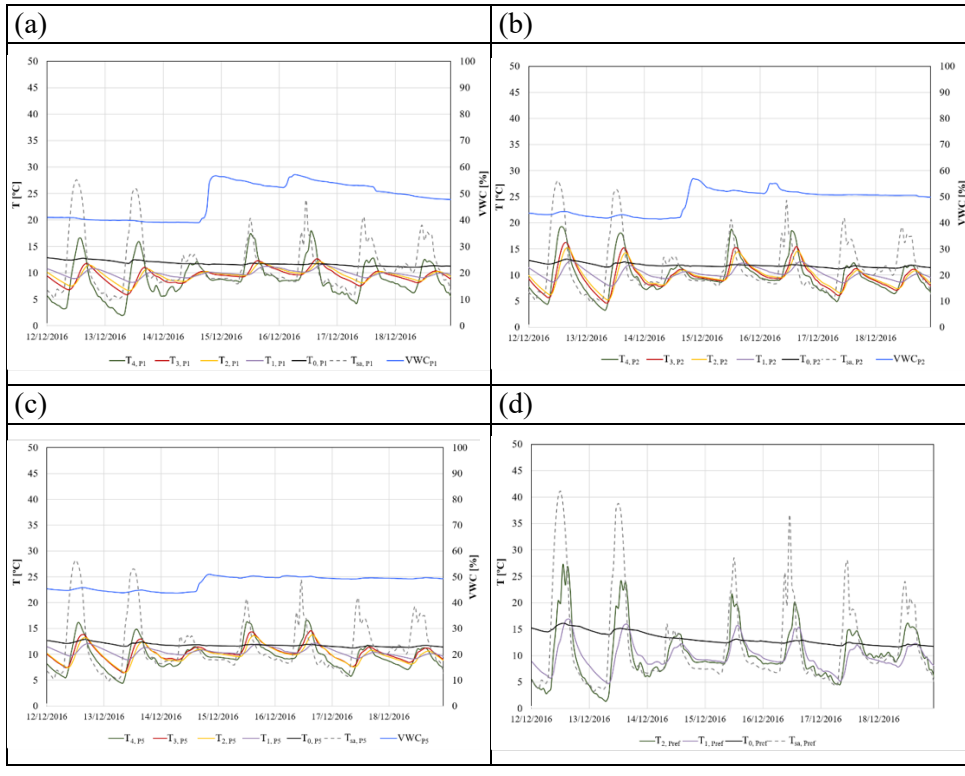

Figure 20. Temperature and water content values in the substrate of (a) P1; (b) P2; (c) P5; (d) Pref, in the winter period.

5.3.2 Weekly analysis of time lag and decrement factor

The values of DF and TL for the three plots with green roof and the reference plot were calculated using Eqs. (15) and (17), respectively. The results of both parameters throughout the selected winter period are shown in Figure 21.

It can be observed that Pref always presented the highest DF values, with an average weekly value of 0.30. These values were significantly reduced in the plots with green roofs, as was already observed in the summer week. The lowest DF values were obtained for P1 and P5, with weekly average values of 0.11 and 0.12, respectively. The highest DF values for the plots with green roof were achieved for P2, with a weekly average value of 0.19, due to the oscillations of $T_{1,P2}$, see Figure 20b, since the T_{sa} values were similar for the three plots with green roof.

Regarding TL, this parameter measured the difference in time between the minimum daily $T_{sa,Pi}$ values and the minimum daily $T_{1,Pi}$ values for the winter climatic conditions, see Eq. (17). The results showed that the lowest values were achieved in Pref, with an average weekly value of 3:17 h, as shown in Figure 21b, and the highest values were almost always obtained for P1, with an average weekly value of 6:34 h, mainly due to the higher amount of plants in P1. These TL values, usually reduced in P2 and P5, with average weekly value of 5:42 h and 5:25 h, respectively.

In winter, the green roofs allowed a significant reduction in the DF values and an increase in the TL values, compared to the Pref results, despite the high amount of water in the substrates, around 48%, see Figure 20a, Figure 20b and Figure 20c. In fact, for rainy and cold climatic conditions in the winter period considered, the trends of DF and TL were mainly due to the vegetation coverage and the composition of the substrates each plot, achieving a reduction in the oscillation of the slab temperature and delaying the minimum peaks of temperature in winter.

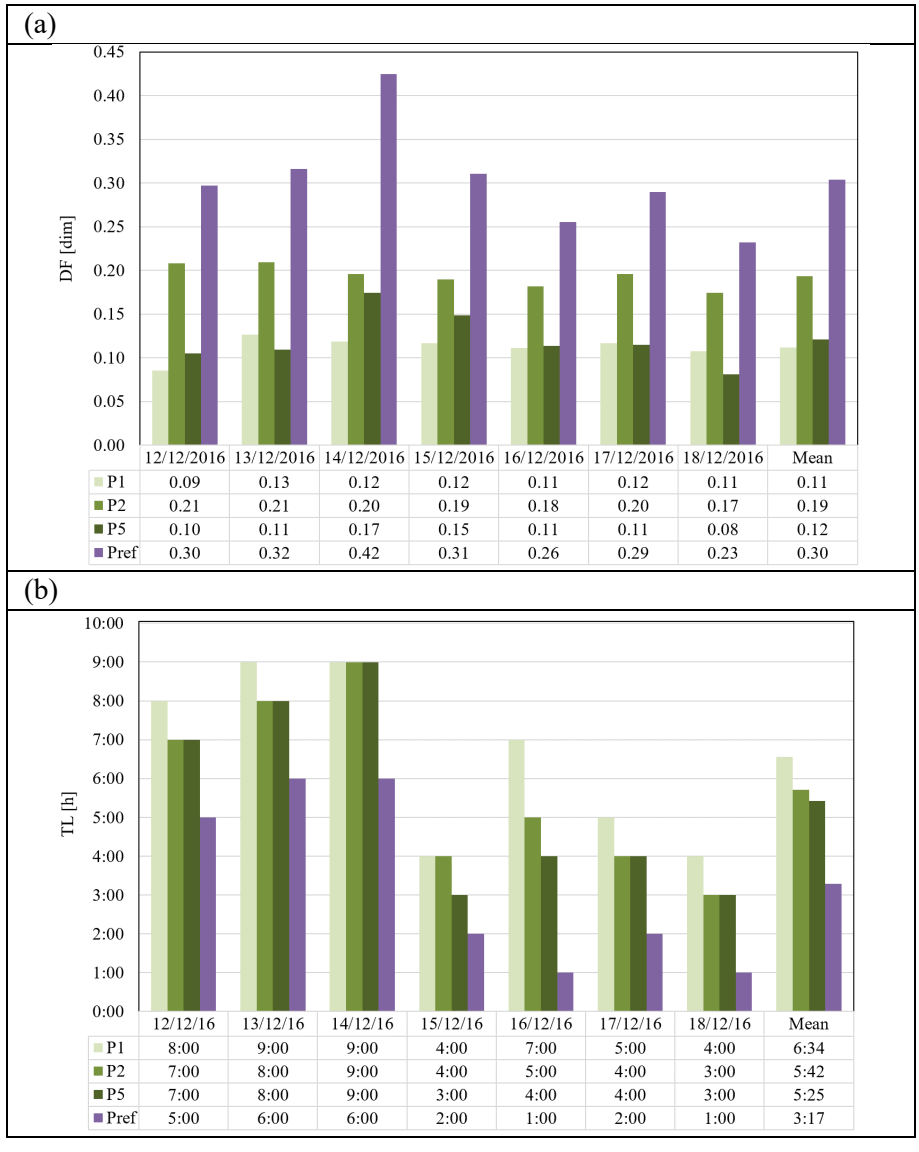

	12/12/2016	13/12/2016	14/12/2016	15/12/2016	16/12/2016	17/12/2016	18/12/2016	Mean
P1	0.09	0.13	0.12	0.12	0.11	0.12	0.11	0.11
P2	0.21	0.21	0.20	0.19	0.18	0.20	0.17	0.19
P5	0.10	0.11	0.17	0.15	0.11	0.11	0.08	0.12
Pref	0.30	0.32	0.42	0.31	0.26	0.29	0.23	0.30

	12/12/16	13/12/16	14/12/16	15/12/16	16/12/16	17/12/16	18/12/16	Mean
P1	8:00	9:00	9:00	4:00	7:00	5:00	4:00	6:34
P2	7:00	8:00	9:00	4:00	5:00	4:00	3:00	5:42
P5	7:00	8:00	9:00	3:00	4:00	4:00	3:00	5:25
Pref	5:00	6:00	6:00	2:00	1:00	2:00	1:00	3:17

Figure 21. Values of (a) decrement factor and (b) time lag for P1, P2, P5 and Pref in the selected winter period.

5.4 Heat flux analysis

A monthly and annual heat flux analysis for the plots with green roofs and the reference plot was performed. For this analysis, the transfer of heat flux between the roofs and the interior of the building was measured.

5.4.1 Monthly analysis of heat flux

Monthly cumulative heat flux gains and losses for P1, P2, P5 and Pref for 2016 are shown in Figure 22.The net energy is also shown in Figure 22, which indicates the difference between the gains and losses of heat through the plot. First, the results obtained in July were analysed, in order to relate them to the parameters previously studied in the summer week. It can be observed that for this month the highest decrease of energy gains was achieved in P1, with a value equal to 11.9 kW h m^{-2}, 83% less than Pref, 69.6 kW h m^{-2}, see Figure 22a and Figure 22d. For P5, it was also possible to significantly reduce the energy gains in respect to Pref in July, with a value of 24.7 kW h m^{-2}, 64.5% less than Pref, see Figure 22c. For the same month, P2 achieved the lowest reduction of energy gains, with a value equal to 26.6 kW h m^{-2}, 61.8% less than Pref, see Figure 22b. This trend, for the month of July, agreed with the dynamic parameters previously studied, DF and CP, due to the capacity to retain water in the substrate, attenuating the maximum roof temperature peaks during a very warm month. Therefore, the lower DF and the higher CP, the lower heat flux gain is. This trend was similar to that obtained in August, because both months had similar climatic conditions, see Table 7. For June and September, P1 also achieved the highest reduction of energy gains, up to 84% less than Pref, however, P5 achieved lower reduction of energy gains than P2, mainly due to the reduction of the ambient temperature, 4.2 ºC less than in July.

For the cold months, the results obtained in December were first analysed, to relate them to the parameters previously studied in the winter week. The highest decrease of energy losses was obtained in P1, with a value of -9.1 kWh m^{-2}, 65.3% less than Pref in the same month, see Figure 22a and Figure 22d. For P2, the value of energy losses was -14.1 kW h m^{-2}, 46.0% less than Pref in the same month, see Figure 22b and Figure 22d. For the same month, P5 achieved the lowest reduction of energy losses, -17.5 kW h m^{-2}, 33.7% less than Pref, see Figure 22c and Figure 22d. This trend was in accordance with the previous TL results, see Figure 21b, which were related to σ_f and LAI in each plot. For the other cold months, such as January and February, the trend was similar for all plots. The maximum reduction of energy losses was obtained in P1 during the month of February, with a value equal to -6.7 kW h m^{-2}, 77.4% less than Pref, see Figure 22a and Figure 22d.

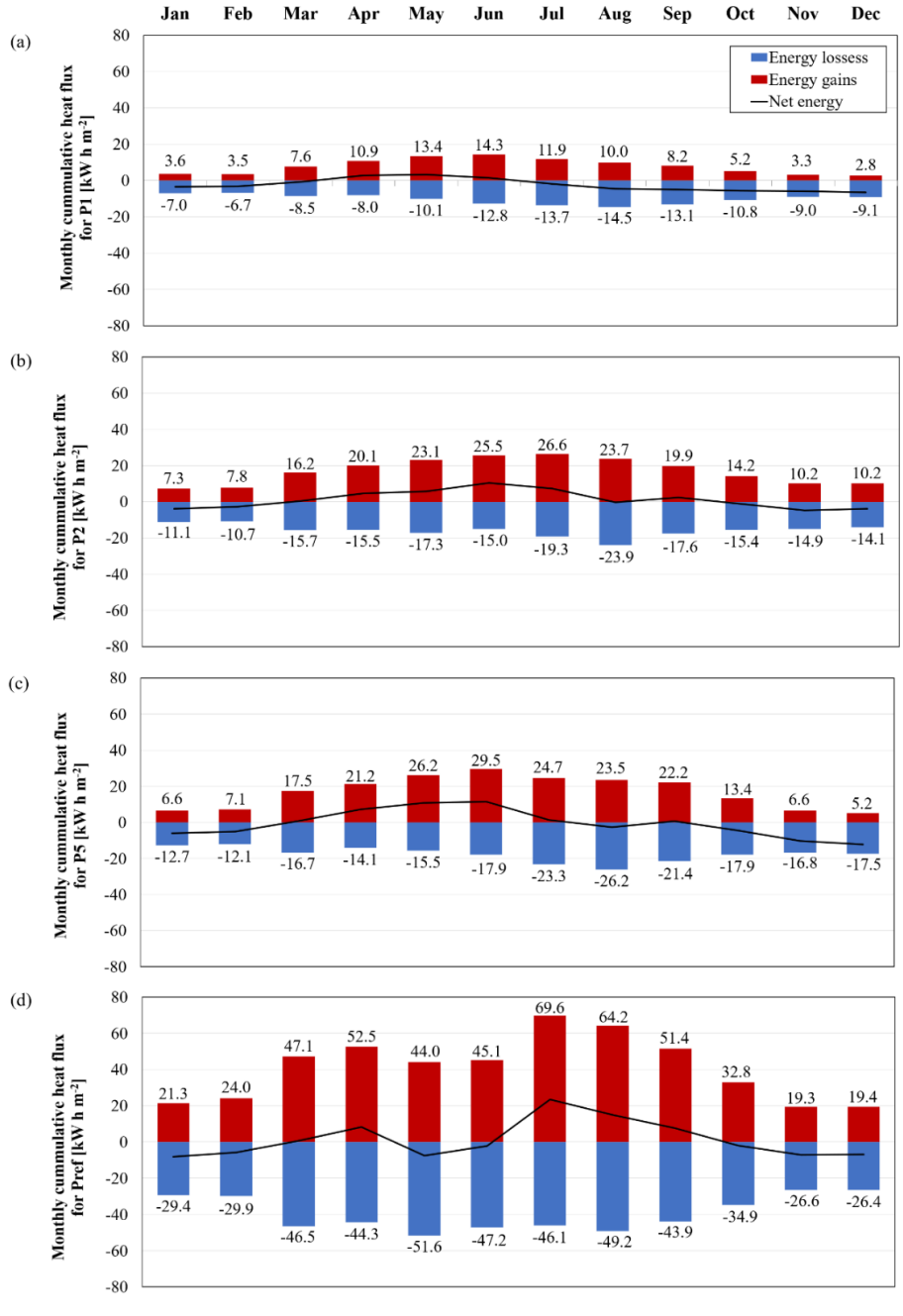

Figure 22. Monthly cumulative heat flux for (a) P1, (b) P2, (c) P5, (d) Pref.

5.4.2 Annual analysis of heat flux

In this section, the annual cumulative heat flux for P1, P2, P5 and Pref for years 2016 and 2017 are shown. The heat gains and losses values for 2017 were slightly higher than the results of the 2016 in all plots, see Figure 23. This increase was mainly due to the slight rise in annual average ambient temperature and annual average solar radiation and to the reduction in annual average rainfall during the 2017, see Table 7. The values of heat gains and losses in Pref for 2016 were of 490.7 kWh/m^2 and -476.0 kW h m^{-2}, respectively, and for 2017 of 549 kWh/m^2 and -507.6 kW h m^{-2}, respectively. Comparing these results with those obtained in the plots with green roof, it can be observed that significant reductions in both heat gains and energy losses were achieved. P1 presented the maximum reduction of heat gains and losses, with 81% and 74%, respectively, for year 2016, and with 80% and 70%, respectively, for year 2017. P5 was the plot with the lowest reduction in heat gains and losses, with a 58% and 55%, respectively, for 2016, and a 56% and 57%, respectively, for 2017, see Figure 23.

These result show that the extensive green roofs under warm climatic conditions achieved high reduction of heat gains, between 56% and 81%, and heat losses, between 55% and 74%, depending on the type of substrate and the fractional vegetation coverage of the plot. The green roof with commercial substrate, P1, obtained the best thermal performance, due to the high capacity to retain water in the substrate.

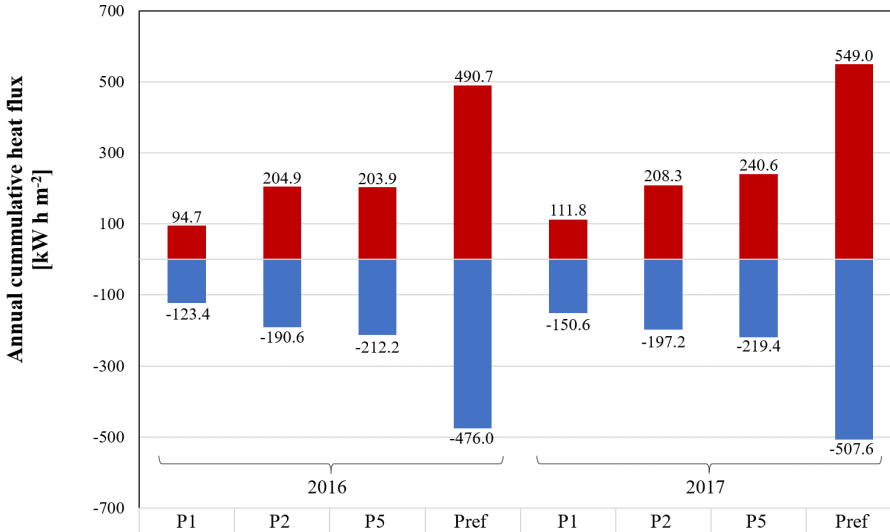

	P1	P2	P5	Pref	P1	P2	P5	Pref
Gains reduct.[%]	81	58	58	0	80	62	56	0
Losses reduct.[%]	74	60	55	0	70	61	57	0

Figure 23. Annual cumulative heat flux in P1, P2, P5 and Pref for 2016 and 2017.

5.5 Conclusion of the chapter

In this chapter, the thermal performance of three plots with green roofs, P1, P2 and P5, with different types of substrates were studied and compared with a traditional gravel ballasted roof, Pref. The substrate of P1 was composed of 100% of commercial growing medium, P2 of 75% of commercial growing medium and 25% of recycled construction materials, and finally, P5 of 50% of commercial growing medium and 50% of recycled construction materials. All the plots were provided with the experimental irrigation strategy, 10 min of watering every day in the morning.

The thermal performance of these three green roofs under warm climatic conditions were studied in Córdoba (Spain), for two years, 2016 and 2017. A dynamic analysis based on decrement factor, DF, time lag, TL, cooling potential, CP, was performed.

The experimental results showed that the three plots with green roof achieved high reduction of DF and high increases of CP, compared to Pref for warm and dry climate, especially in P1 with a weekly average reduction of DF equal to 0.24 and a weekly average increase of CP equal to 16.3 °C. This behaviour was mainly due

to the capacity to retain water in the substrate. The results indicated that, for warm and dry climatic conditions, the higher the capacity to retain water in the substrate, the higher the reduction of DF and the higher the increase of CP was.

Significant increases of TL for the green roofs were obtained, up to 6:08 h and 6:34 h for P1 during the hot and cold periods considered, respectively, compared to Pref. The TL results were related to the fractional vegetation coverage, the leaf area index, the composition of the substrates and their capacity to retain water and the water accumulated in the drainage layer, that gave a delayed the maximum slab temperature peak.

Respect to the heat flux results, significant reductions of energy gains during the hot period and energy losses during the cold period were obtained in the three green roofs, compared to Pref, due to the capacity to retain water in the substrates and the fractional vegetation coverage of these plots. The annual average reductions in heat gains and losses were between 56% and 81%, 55% and 74%, respectively. These important reductions were obtained during two particularly warm years in Córdoba (Spain).

Chapter 6

Energy analysis

In this chapter, a weekly and annual energy analysis of the reduction of energy demand, ED_w and ED_y, of the eco-roof under 20 irrigation strategies and of the green roofs with different substrates, was studied The results were obtained with the simulations performed with the calibrated numerical models.

6.1 Eco-roof energy analysis

A weekly analysis of reduction of energy demand, ED_w, of the eco-roof under different irrigation strategies, from 15/08/2015 to 21/08/2015, was performed. Furthermore, an annual analysis of the reduction of energy demand, ED_y, and performance, P_{eco}, of the eco-roof for all the irrigation strategies was carried out. This analysis was performed from 01/01/2015 to 31/12/2015, when the T_o exceeded the 18 °C, see Table 7. The irrigation strategies were planned from 01/05/2015 to 31/10/2015.

6.1.1 Weekly results

The reduction of Q due to the irrigation strategies, led to weekly reduction of energy demand, ED_w, in the studied roof. The ED_w results of the eco-roof compared to the gravel ballasted roof for the selected summer week, are shown in Figure 24. ED_w was calculated by Eq. (5). The results showed that the ED_w values were always higher than 40% for all the case studies, even for C0 that had no irrigation schedule.

Therefore, the eco-roof had a higher thermal insulation than the considered traditional gravel ballasted roof.

Comparing the irrigation strategies with the same watering schedule and different amount of water, it can be observed that watering in the morning, cases C1, always allowed higher ED_w values than those obtained at other schedules to be achieved. The highest ED_w value was achieved with $C1_{80}$, 95.8%. Nevertheless, there was no substantial improvement of the ED_w value between 60 min and 80 min of irrigation, a difference of 0.3%. Therefore, these results suggest that the irrigation strategy C1 allows the maximum ED_w values to be obtained for the week of August studied.

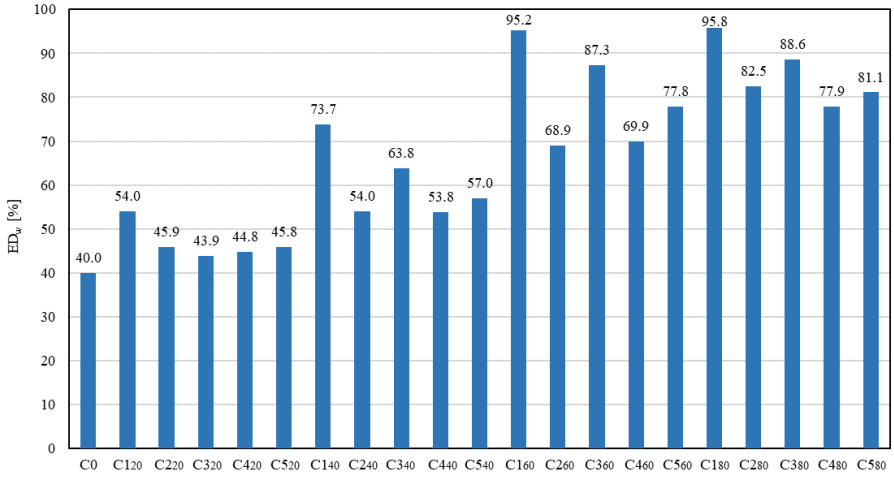

Figure 24. Weekly results of the reduction of energy demand of the eco-roof.

6.1.2 Annual results

The annual results of ED_y and the amount of irrigation and drained water are shown in Figure 25. It can be observed that all the case studies achieved ED_y values higher than 43%. The strategy that achieved the highest ED_y value was $C1_{80}$, 78.7%, with 2660 l/m^2 of annual irrigation water, see Figure 25. However, this strategy also presented a significant annual drainage value, 191 l/m^2, so 7.2% of water was not totally used to reduce the heat flux of the roof. The strategy $C1_{60}$ also achieved a high annual ED_y value, 76.6%, even with a lower amount of annual irrigation water, 1995 l/m^2, and lower annual drainage, 159 l/m^2, than those of $C1_{80}$. A significant annual ED_y value was obtained with the strategy $C1_{40}$, 62.8%. The amount of annual irrigation water used for $C1_{40}$ was 1330 l/m^2, 50% and 33.3% less than the amount of annual water used for $C1_{80}$ and $C1_{60}$, respectively. Furthermore, a low annual drainage value was found for $C1_{40}$, a 5% of irrigation water was drained. The case C0, that had no irrigation schedule, also achieved a significant annual ED value, 43.3%, due to the insulation effect of the substrate, see Figure 25. Therefore, the installation of an eco-roof significantly improved the thermal performance of the building compared to a traditional gravel ballasted roof, achieving a high percentage of ED_y. In addition, adequate irrigation strategies allowed a further increase of this ED, up to 78.7% for $C1_{80}$.

The annual P_{eco} results are also shown in Figure 25. This parameter was used to evaluate the irrigation strategies that had the highest reduction of energy demand with respect to the lowest quantity of irrigation water, expressed by Eq. (6). It can be observed that the strategy with the highest P_{eco} value was $C5_{20}$, 153.9 [kWh/l year], mainly due to the low quantity of irrigation water, 380 l/m^2, see Figure 25. $C5_{20}$ also presented the lowest annual drainage, only 1 l/m^2. Among the cases with the same irrigation schedule, the highest P_{eco} values were always found for C5, the strategies with irrigation in alternate days. For the remaining cases with the same irrigation schedule, the highest P_{eco} values were obtained for C1, the cases with irrigation once a day at 8:30 am, as shown in Figure 25, due to the high reduction of energy demand achieved with the eco-roof with respect to the traditional roof. The lowest P_{eco} values were found for C4, the cases with irrigation once a day at 1:00 pm.

Therefore, it has been found that an irrigation strategy on alternate days watering for 20 min in the morning, allowed an ED_y value up to 46.7 % respect to the traditional gravel ballasted roof, and with a low waste of irrigation water to be achieved.

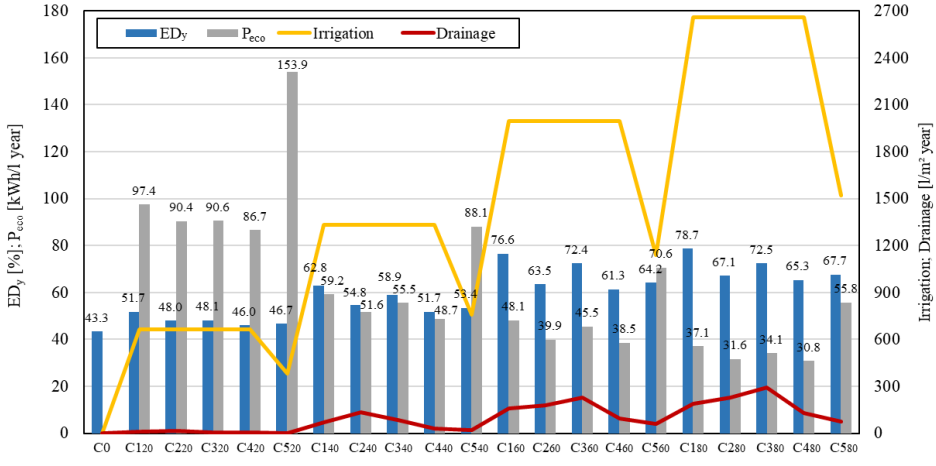

Figure 25. Annual results of the reduction of energy demand, energy performance, irrigation and drainage.

6.2 Green roofs energy analysis

A weekly and annual analysis of the reduction of energy demand, ED_w and ED_y, of the green roofs with different substrates was carried out. The weekly analysis was performed from 15/08/2016 to 21/08/2016. During all the year the green roofs were provided with the experimental irrigation schedule of 10 min of watering twice a day, which corresponded to the irrigation strategy $C3_{20}$ of the eco-roof analysis.

6.2.1 Weekly analysis

The ED_w results of the green roofs with different substrates, P1, P2 and P5, compared to the gravel ballasted roof for the selected summer week, are shown in Figure 26. ED_w was calculated by Eq. (5). The results showed that the ED_w values were always higher than 58.6% for all the three plots.

P1 was always the plot that achieved the highest reduction of energy demand, with a weekly average value of 82.1%. The highest reduction was obtained on 21/08 with a value of 85.6%, while the lowest one on 18/08 with a value of 78.5%. P2 and P5 always obtained similar results, with weekly average values of 65.0% and 65.8%, respectively. P2 achieved the highest reduction of ED_w on 16/08 with a value of 69.7%, while the lowest one on 20/08 with a value of 58.6%. P5 achieved

the highest reduction of ED_w on 17/08, with a value of 67.9%, while the lowest reduction of ED_w was obtained on 20/08 with a value of 61.1%. These results were in line with the analysis of TL, DF and CP showed in the Chapter 5.

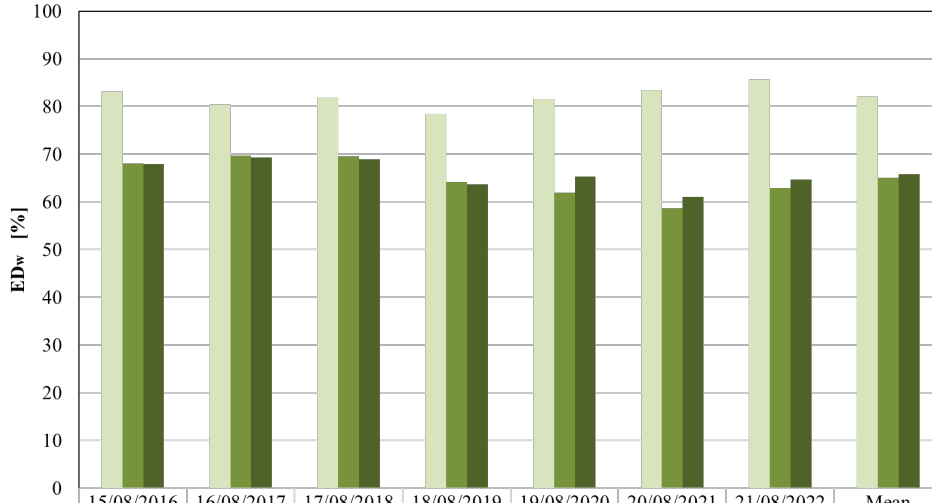

	15/08/2016	16/08/2017	17/08/2018	18/08/2019	19/08/2020	20/08/2021	21/08/2022	Mean
P1	83.15	80.38	81.85	78.48	81.53	83.44	85.66	82.1
P2	68.02	69.68	69.60	64.15	61.95	58.63	62.97	65.0
P5	67.89	69.32	68.93	63.62	65.28	61.06	64.73	65.8

Figure 26. Weekly results of the reduction of energy demand of the green roofs with different substrates

6.2.2 Annual analysis

The annual results of ED_y for the three plots with green roofs are shown in Figure 27. The analysis was carried out for the 2016 and 2017 years. It can be observed that all the case studies achieved ED_y values higher than 56.2%.

The plot that always achieved the highest reduction of ED throughout the 2016 and 2017 was P1, with values of 80.7% and 79.6%, respectively. P2 and P5 also obtained high reduction of energy demand, 58.2% and 62.1%, for P2 and 58.4% and 56.2% for P5, for the years 2016 and 2017, respectively.

Comparing these results with the eco-roof results analysed in section 6.1, it can be observed that the green roofs always achieved higher reduction of ED_y. In particular, for the experimental irrigation strategy $C3_{20}$, the eco-roof achieved an

ED_y of 48.1% while the green roof P1, that had the same commercial substrate, achieved a value of 80.7% for 2016 and 79.6% for 2017, a 40.4% and 39.6% more respect to the eco-roof, respectively. P2 and P5, that presented different substrates, also achieved always higher reduction of ED_y respect to the eco-roof, under the same experimental irrigation strategy, 17.3% and 17.6% more for the 2016, and 22.5% and 14.4% more for the 2017, respectively.

Therefore, it can be said that plants can help to further reduce the ED_y and the installation of a green roof with plants significantly improved the thermal performance of the building compared to a traditional gravel ballasted roof, achieving a high percentage of ED_y, more than an eco-roof with only substrate under the same irrigation strategy.

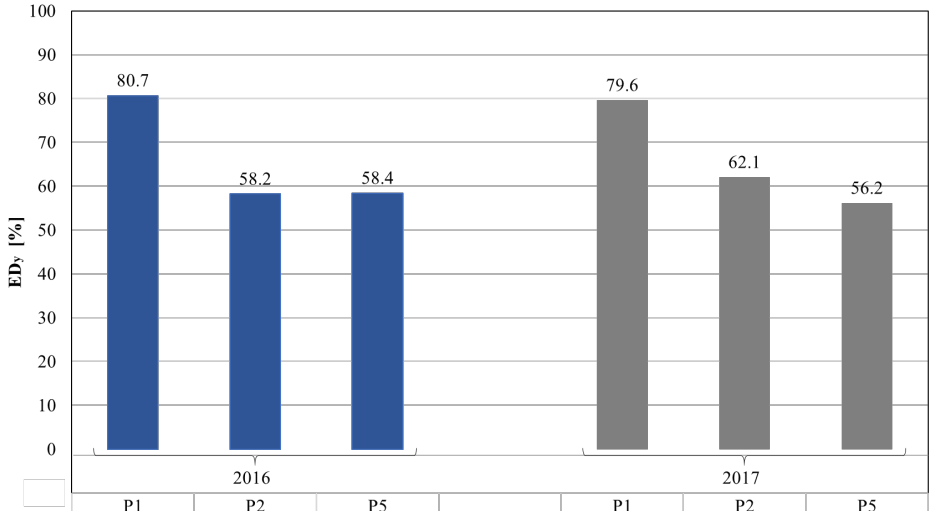

Figure 27. Annual results of the reduction of energy demand of the green roofs with different substates.

6.3 Conclusion of the chapter

In this chapter, a weekly an annual energy analysis of the reduction of energy demand, ED_w and ED_y, of the eco-roof under 20 irrigation strategies and of the green roofs with different substrates, was performed.

The results showed that during the selected summer week, the eco-roof achieved a reduction of ED_w up to 95.8%, while achieved an annual reduction of ED_y up to 78.7%. Both results were obtained watering every day 80 min in the morning. In addition to this, it was studied the irrigation strategy that allowed the highest reduction of ED_y with the low waste of water, through the ratio P_{eco}. The results showed that it was possible to obtain a reduction ED_y of 46.7% with respect to the traditional gravel ballasted roof, irrigating on alternate days for 20 min in the morning. Strategy $C3_{20}$, that represented the real irrigation of the experimental eco-roof, allowed to achieve a reduction of ED_y of 48.1%, respect to the traditional gravel ballasted roof. Without irrigation strategy, it is also possible achieve a great reduction of ED_y, up to 43.3%.

Then, the same weekly and annual ED analysis were realised for the three experimental green roofs with different substrates. The results showed that the commercial substrate obtained the highest reduction of ED_w, with an average weekly value of 82.1%. Respect to the annual analysis, the green roof with commercial substrate also achieved the highest reduction of ED_y, 80.7% with the irrigation strategy $C3_{20}$, that represented the real irrigation of the experimental green roofs, a 59.6% more than the eco-roof in the same conditions.

It can be concluded that this type of installation only with substrate and with a proper irrigation strategy, is a great solution for the rehabilitation of old buildings, achieving high reduction of energy demand respect to a traditional roof. Moreover, plants can help further to reduce the energy demand, up to 40.4% more respect to the installation with only substrate under the same irrigation strategy.

Chapter 7

Conclusions and future work

In this chapter are reported the conclusions and the proposals for future works that are deduced from the research work developed in the frame of this thesis. The conclusions were based on the hypothesis presented in 1.5.

7.1 Conclusions

An eco-roof only with substrate and three green roofs with plants and different substrates were proposed as passive systems of low environmental impact for the rehabilitation of old buildings in south European climates. The study was carried out throughout two years warmer than average years, 2016 and 2017. All the results were compared to a traditional gravel ballasted roof.

Evapotranspiration and volumetric water content were demonstrated to have a great impact on the heat flux reduction of the eco-roof. Moreover, evapotranspiration values depended on the climatic conditions, since that evapotranspiration values increased when the values of outdoor air temperature, wind speed and solar radiation rose and outdoor air relative humidity values decreased.

The highest reduction of annual energy demand for the eco-roof, 95.8%, was obtained with 80 min of irrigation every day in the morning, respect to the traditional gravel ballasted roof. The irrigation strategy that allowed to achieve the highest reduction of annual energy demand with the lowest waste of water was irrigating 10 min in the morning in alternate days, 46.7% with 380 l/m^2 year.

Without irrigation high reductions of annual energy demand also were achieved, 40%, respect to the traditional roof.

The analysis of green roofs with different substrates showed that the substrate with 100% commercial growing medium, managed to retain more water in summer than the rest of the plots, using the same amount of watering. Despite this, all the plots showed a decrease in the temperature profile respect to the traditional roof, depending on the capacity of the substrate to retain water. The minimum temperature values for the three plots with green roofs were obtained for the probes placed in the upper side of the roof slab.

The dynamic variables used for the green roofs analysis strongly depended on the volumetric water content of the substrate. The lowest decrement factor values were always achieved in the plot with 100% of commercial substrate and the higher the capacity to retain water in the substrate, the higher the reduction in the oscillation of the slab temperature was. Time lag, in addition to the water content in the substrate, also depended on the fractional vegetation coverage, the leaf area index, the composition of the substrates and the water accumulated in the drainage layer. The analysis of time lag results confirmed the green roof benefits for the retrofit of buildings without insulation by delaying the peak in the maximum surface temperature. The highest values of time lag were achieved by the plot with 100% of commercial substrate. Finally, the analysis of the cooling potential showed that the higher the capacity to retain water in the substrate, the higher the cooling potential was. The plot with 100% of commercial substrate also achieved the best results of cooling potential. Despite this, all the plots with green roofs always allowed the slab temperature to reduce by more than 12.7 ºC, compared to the traditional roof.

The energy analysis demonstrated that the green roof with commercial substrate achieved the highest reduction of annual energy demand, 80.7% with the experimental irrigation strategy, 10 min every day in the morning. Comparing these results with the eco-roof results, it can be observed that the green roofs always achieved higher reduction of annual energy demand. In particular, for the experimental irrigation strategy, the eco-roof achieved an annual reduction of energy demand of 48.1%, a 40.4% less than the green roof with the same substrate. The other plots, that presented different substrates, also achieved always higher reduction of annual energy demand respect to the eco-roof, under the same experimental irrigation strategy.

These results demonstrated that both eco-roof and green roof are passive installations that allow to achieve a significant reduction of energy demand for the rehabilitation of old buildings. A proper irrigation strategy and the presence of plants can help further to improve the energy performance of the roof.

7.2 Future works

The present thesis focused on the experimental and numerical study of the potential of energy demand reduction in buildings with eco-roofs and green roofs with different substrates, under climatic conditions of Southern Europe.

This type of installation allowed to achieve high reduction of energy demand in the building and a proper irrigation strategy helped further to improve the energy performance of the roof.

In the future, it could be interesting to investigate if the best irrigation strategy found for the commercial substrate could also be valid for the other substrates studied. Then, the thickness of the substrate could be variated in order to investigate how it influence the energy behaviour of the roof.

Green roofs could be complemented with other passive systems, such as a ventilated façade. In this way, the simultaneous action of more passive systems to reduce the energy demand for the rehabilitation of old buildings would be evaluated.

It would also be interesting to study the effect of green roofs in buildings with different transmittance values and in new sustainable constructions. Then, a study on the capacity of the green roof to capture CO_2, in line with the EU *Renovation Wave* and the necessity to create a link between the built environment and the ecosystems, could be carry out.

Bibliography

[1] F. Ardente, M. Beccali, M. Cellura, M. Mistretta, Energy and environmental benefits in public buildings as a result of retrofit actions, Renew. Sustain. Energy Rev. 15 (2011) 460–470. doi:10.1016/j.rser.2010.09.022.

[2] J.E. Oliver, Kyoto protocol, in: Encycl. Earth Sci. Ser., 2005. doi:10.1007/1-4020-3266-8_118.

[3] European Commission, 2020 climate & energy package | Climate Action, 2020 Clim. Energy Packag. (2009).

[4] European Commission, 2030 climate & energy framework - Climate Action, 2030 Clim. Energy Framew. (2018).

[5] European Commission, Directive 2002/91/EC of the European Parliament and of the Council of 16 December 2002 on the energy performance of buildings, 2002. doi:10.1039/ap9842100196.

[6] European Parliament, European Directive 2010/31/EU on the Energy Performance of Buildings, 2010. doi:doi:10.3000/17252555.L_2010.153.eng.

[7] European Union, Directive 2012/27/EU - "Energy Efficiency Directive," Off. J. Eur. Union. (2012).

[8] European Commission, Directive (EU) 2018/844 of the European Parliament and of the Council of 30 May 2018 amending Directive 2010/31/EU on the energy performance of buildings and Directive 2012/27/EU on energy efficiency, (2018).

[9] Directive (EU) 2018/2001 of the European Parliament and of the Council of 11 December 2018 on the promotion of the use of energy from renewable sources (recast), 2018 (2018).

[10] Paris Agreements, United Nations Climate Change Conference. <http://www.cop21.gouv.fr/en/>, (2015).

[11] Communication from the Commission to the European Parliament, the Council, the European Economic and Social Committee of the Regions, A Renovation Wave for Europe - greening our buildings, creating jobs, improving lives, (2020).

[12] S. Committee, COMMISSION RECOMMENDATION (EU) 2020/1563 of

14 October 2020 on energy poverty, (2020) 35–41.

[13] Eurostat, https://ec.europa.eu/eurostat/en/web/products-eurostat-news/-/ddn-20210106-1?redirect=/eurostat/en/news/whats-new, Accessed 25.04.21. (2021).

[14] European Commission, Comprehensive study of building energy renovation activities and the uptake of nearly zero-energy buildings in the EU Final report, 2019.

[15] D. Sadhukhan, S. Peri, N. Sugunaraj, A. Biswas, D.F. Selvaraj, K. Koiner, A. Rosener, M. Dunlevy, N. Goveas, D. Flynn, P. Ranganathan, Estimating surface temperature from thermal imagery of buildings for accurate thermal transmittance (U-value): A machine learning perspective, J. Build. Eng. 32 (2020) 101637. doi:10.1016/j.jobe.2020.101637.

[16] L. Hao, D. Herrera-Avellanosa, C. Del Pero, A. Troi, What are the implications of climate change for retrofitted historic buildings? A literature review, Sustain. 12 (2020) 1–17. doi:10.3390/su12187557.

[17] L. Kranzl, A. Toleikyte, A. Müller, M. Hummel, E. Heiskanen, K. Matschoss, C. Rohde, J. Kockat, J. Steinbach, M. Pietrobon, R. Armani, L. Pagliano, P. Zahradnik, J. Karasek, Policies to enforce the transition to nZEB : Synthesis report and policy recommendations from the project, (2014).

[18] Ministerio de Fomento (España), Documento Básico HE Ahorro de Energía 2019, Código Técnico La Edif. (2019) 1–129.

[19] M. Abuseif, Z. Gou, A review of roofing methods: Construction features, heat reduction, payback period and climatic responsiveness, Energies. 11 (2018). doi:10.3390/en11113196.

[20] J. Al Dakheel, C. Del Pero, N. Aste, F. Leonforte, Smart buildings features and key performance indicators: A review, Sustain. Cities Soc. 61 (2020) 102328. doi:10.1016/j.scs.2020.102328.

[21] Z. Ghaddar, K. Ghali, N. Ghaddar, Impact of integrating desiccant dehumidification processes to conventional AC system on urban microclimate and energy use in Beirut city, Energy Convers. Manag. 153 (2017) 374–390. doi:10.1016/j.enconman.2017.10.024.

[22] H. Li, L. Yang, H.Q. Dong, Groundwater Source Heat Pump Technology Use for Heating and Air-Conditioning of a Commercial Building, Adv. Mater. Res. 608–609 (2012) 994–997. doi:10.4028/www.scientific.net/AMR.608-609.994.

[23] N. Aste, R.S. Adhikari, M. Manfren, Cost optimal analysis of heat pump

technology adoption in residential reference buildings, Renew. Energy. 60 (2013) 615–624. doi:10.1016/j.renene.2013.06.013.

[24] L. Belussi, B. Barozzi, A. Bellazzi, L. Danza, A. Devitofrancesco, C. Fanciulli, M. Ghellere, G. Guazzi, I. Meroni, F. Salamone, F. Scamoni, C. Scrosati, A review of performance of zero energy buildings and energy efficiency solutions, J. Build. Eng. 25 (2019) 100772. doi:10.1016/j.jobe.2019.100772.

[25] M. Shafique, R. Kim, M. Rafiq, Green roof benefits, opportunities and challenges – A review, Renew. Sustain. Energy Rev. 90 (2018) 757–773. doi:10.1016/j.rser.2018.04.006.

[26] M. Shafique, R. Kim, M. Rafiq, Green roof benefits, opportunities and challenges – A review, Renew. Sustain. Energy Rev. 90 (2018) 757–773. doi:10.1016/j.rser.2018.04.006.

[27] M. Karteris, I. Theodoridou, G. Mallinis, E. Tsiros, A. Karteris, Towards a green sustainable strategy for Mediterranean cities: Assessing the benefits of large-scale green roofs implementation in Thessaloniki, Northern Greece, using environmental modelling, GIS and very high spatial resolution remote sensing data, Renew. Sustain. Energy Rev. 58 (2016) 510–525. doi:10.1016/j.rser.2015.11.098.

[28] H. Akbari, C. Cartalis, A. Muscio, Local climate change and Urban heat island mitigation techniques – the state of the art, 22 (2020) 1–16. doi:10.3846/13923730.2015.1111934.

[29] O. Saadatian, K. Sopian, E. Salleh, C.H. Lim, S. Riffat, E. Saadatian, A. Toudeshki, M.Y. Sulaiman, A review of energy aspects of green roofs, Renew. Sustain. Energy Rev. 23 (2013) 155–168. doi:10.1016/j.rser.2013.02.022.

[30] W.C. Li, K.K.A. Yeung, A comprehensive study of green roof performance from environmental perspective, Int. J. Sustain. Built Environ. 3 (2014) 127–134. doi:10.1016/j.ijsbe.2014.05.001.

[31] K. Vijayaraghavan, D.H.K. Reddy, Y.S. Yun, Improving the quality of runoff from green roofs through synergistic biosorption and phytoremediation techniques: A review, Sustain. Cities Soc. 46 (2019). doi:10.1016/j.scs.2018.12.009.

[32] A.F. Speak, J.J. Rothwell, S.J. Lindley, C.L. Smith, Reduction of the urban cooling effects of an intensive green roof due to vegetation damage, Urban Clim. 3 (2013) 40–55. doi:10.1016/j.uclim.2013.01.001.

[33] FAO, Evapotranspiración del cultivo Guías para la determinación de los requerimientos de agua de los cultivos, 2006. doi:M-56.

[34] A.B. Besir, E. Cuce, Green roofs and facades: A comprehensive review, Renew. Sustain. Energy Rev. 82 (2018) 915–939. doi:10.1016/j.rser.2017.09.106.

[35] E. Schroll, J. Lambrinos, T. Righetti, D. Sandrock, The role of vegetation in regulating stormwater runoff from green roofs in a winter rainfall climate, Ecol. Eng. 37 (2011) 595–600. doi:10.1016/j.ecoleng.2010.12.020.

[36] T.C. Liu, G.S. Shyu, W.T. Fang, S.Y. Liu, B.Y. Cheng, Drought tolerance and thermal effect measurements for plants suitable for extensive green roof planting in humid subtropical climates, Energy Build. 47 (2012) 180–188. doi:10.1016/j.enbuild.2011.11.043.

[37] Y.Y. Huang, C.T. Chen, W.T. Liu, Thermal performance of extensive green roofs in a subtropical metropolitan area, Energy Build. 159 (2018) 39–53. doi:10.1016/j.enbuild.2017.10.039.

[38] Y. He, H. Yu, A. Ozaki, N. Dong, S. Zheng, Long-term thermal performance evaluation of green roof system based on two new indexes : A case study in Shanghai area, 120 (2017).

[39] J. Yang, M. Kumar, A. Pyrgou, A. Chong, M. Santamouris, D. Kolokotsa, S. Eang, Green and cool roofs ' urban heat island mitigation potential in tropical climate, (2018).

[40] N. Hien, Y. Chen, C. Leng, A. Sia, Investigation of thermal beneÿts of rooftop garden in the tropical environment, 38 (2003) 261–270.

[41] M. Mungur, Y. Poorun, D. Juggurnath, Y.B. Ruhomally, R. Rughooputh, M.Z. Dauhoo, A. Khoodaruth, H. Shamachurn, M. Gooroochurn, N. Boodia, M. Chooneea, S. Facknath, A numerical and experimental investigation of the effectiveness of green roofs in tropical environments: The case study of Mauritius in mid and late winter, Energy. 202 (2020) 117608. doi:10.1016/j.energy.2020.117608.

[42] J.M. Huang, L.C. Chen, A numerical study on mitigation strategies of urban heat islands in a tropical megacity: A case study in Kaohsiung city, Taiwan, Sustain. 12 (2020). doi:10.3390/SU12103952.

[43] H. Zhang, S. Lu, X. Fan, J. Wu, Y. Jiang, L. Ren, J. Wu, H. Zhao, Is sustainable extensive green roof realizable without irrigation in a temperate monsoonal climate? A case study in Beijing, Sci. Total Environ. 753 (2021) 142067. doi:10.1016/j.scitotenv.2020.142067.

[44] C.M. Silva, M.G. Gomes, M. Silva, Green roofs energy performance in Mediterranean climate, Energy Build. 116 (2016) 318–325. doi:10.1016/j.enbuild.2016.01.012.

[45] I. Andr, Hydrological Performance of Green Roofs at Building and City Scales under Mediterranean Conditions, (2018) 1–15. doi:10.3390/su10093105.

[46] C.F. Chen, Performance evaluation and development strategies for green roofs in Taiwan: A review, Ecol. Eng. 52 (2013) 51–58. doi:10.1016/j.ecoleng.2012.12.083.

[47] S.B. Mickovski, K. Buss, B.M. McKenzie, B. Sökmener, Laboratory study on the potential use of recycled inert construction waste material in the substrate mix for extensive green roofs, Ecol. Eng. 61 (2013) 706–714. doi:10.1016/j.ecoleng.2013.02.015.

[48] A.J. Bates, J.P. Sadler, R.B. Greswell, R. Mackay, Effects of recycled aggregate growth substrate on green roof vegetation development: A six year experiment, Landsc. Urban Plan. 135 (2015) 22–31. doi:10.1016/j.landurbplan.2014.11.010.

[49] A. Nagase, N. Dunnett, The relationship between percentage of organic matter in substrate and plant growth in extensive green roofs, Landsc. Urban Plan. 103 (2011) 230–236. doi:10.1016/j.landurbplan.2011.07.012.

[50] B. Raji, M.J. Tenpierik, A. Van Den Dobbelsteen, The impact of greening systems on building energy performance: A literature review, Renew. Sustain. Energy Rev. 45 (2015) 610–623. doi:10.1016/j.rser.2015.02.011.

[51] H.F. Castleton, V. Stovin, S.B.M. Beck, J.B. Davison, Green roofs; Building energy savings and the potential for retrofit, Energy Build. 42 (2010) 1582–1591. doi:10.1016/j.enbuild.2010.05.004.

[52] M.G. Gomes, C.M. Silva, A.S. Valadas, M. Silva, Impact of vegetation, substrate, and irrigation on the energy performance of green roofs in a Mediterranean climate, Water (Switzerland). 11 (2019). doi:10.3390/w11102016.

[53] J. Goussous, H. Siam, H. Alzoubi, Prospects of green roof technology for energy and thermal benefits in buildings: Case of Jordan, Sustain. Cities Soc. 14 (2015) 425–440. doi:10.1016/j.scs.2014.05.012.

[54] Y. He, H. Yu, A. Ozaki, N. Dong, S. Zheng, Influence of plant and soil layer on energy balance and thermal performance of green roof system, Energy. 141 (2017) 1285–1299. doi:https://doi.org/10.1016/j.energy.2017.08.064.

[55] A. Gagliano, T. Poli, G. Sciuto, Thermal performance assessment of extensive green roofs investigating realistic vegetation-substrate configurations, Build. Simul. (2019) 379–393.

[56] C.L. Tan, P.Y. Tan, N.H. Wong, H. Takasuna, T. Kudo, Y. Takemasa, C.V.J.

Lim, H.X.V. Chua, Impact of soil and water retention characteristics on green roof thermal performance, Energy Build. 152 (2017) 830–842. doi:10.1016/j.enbuild.2017.01.011.

[57] A.L.S. Chan, T.T. Chow, Energy and economic performance of green roof system under future climatic conditions in Hong Kong, Energy Build. 64 (2013) 182–198. doi:10.1016/j.enbuild.2013.05.015.

[58] I. Ziogou, A. Michopoulos, V. Voulgari, T. Zachariadis, Energy, environmental and economic assessment of electricity savings from the operation of green roofs in urban office buildings of a warm Mediterranean region, J. Clean. Prod. 168 (2017) 346–356. doi:10.1016/j.jclepro.2017.08.217.

[59] F.E. Boafo, J.T. Kim, J.H. Kim, Evaluating the impact of green roof evapotranspiration on annual building energy performance, Int. J. Green Energy. 14 (2017) 479–489. doi:10.1080/15435075.2016.1278375.

[60] S. Yuan, D. Rim, Cooling energy saving associated with exterior greenery systems for three US Department of Energy (DOE) standard reference buildings, Build. Simul. 11 (2018) 625–631. doi:10.1007/s12273-018-0427-y.

[61] S. Vera, C. Pinto, P.C. Tabares-velasco, W. Bustamante, F. Victorero, J. Gironás, C.A. Bonilla, Influence of vegetation , substrate , and thermal insulation of an extensive vegetated roof on the thermal performance of retail stores in semiarid and marine climates, Energy Build. 146 (2017) 312–321.

[62] K.C. Dahanayake, C.L. Chow, Comparing reduction of building cooling load through green roofs and green walls by EnergyPlus simulations, Build. Simul. 11 (2018) 421–434. doi:10.1007/s12273-017-0415-7.

[63] T.E. Morakinyo, K.W.D. Kalani, C. Dahanayake, E. Ng, C.L. Chow, Temperature and cooling demand reduction by green-roof types in different climates and urban densities: A co-simulation parametric study, Energy Build. 145 (2017) 226–237. doi:10.1016/j.enbuild.2017.03.066.

[64] F. Fantozzi, C. Bibbiani, C. Gargari, R. Rugani, G. Salvadori, Do green roofs really provide significant energy saving in a Mediterranean climate ? Critical evaluation based on different case studies, Front. Archit. Res. (2021). doi:10.1016/j.foar.2021.01.006.

[65] K. Vijayaraghavan, Green roofs: A critical review on the role of components, benefits, limitations and trends, Renew. Sustain. Energy Rev. 57 (2016) 740–752. doi:10.1016/j.rser.2015.12.119.

[66] P. Bevilacqua, J. Coma, G. Pérez, C. Chocarro, A. Juárez, C. Solé, M. De

Simone, L.F. Cabeza, Plant cover and floristic composition effect on thermal behaviour ofextensive green roofs, Build. Environ. 92 (2015) 305–316. doi:10.1016/j.buildenv.2015.04.026.

[67] J. Coma, G. Pérez, C. Solé, A. Castell, L.F. Cabeza, Thermal assessment of extensive green roofs as passive tool for energy savings in buildings, Renew. Energy. 85 (2016) 1106–1115. doi:10.1016/j.renene.2015.07.074.

[68] L.L.H. Peng, C.Y. Jim, Green-roof effects on neighborhood microclimate and human thermal sensation, Energies. 6 (2013) 598–618. doi:10.3390/en6020598.

[69] M. Vaz Monteiro, T. Blanuša, A. Verhoef, M. Richardson, P. Hadley, R.W.F. Cameron, Functional green roofs: Importance of plant choice in maximising summertime environmental cooling and substrate insulation potential, Energy Build. 141 (2017) 56–68. doi:10.1016/j.enbuild.2017.02.011.

[70] S. Kemp, P. Hadley, T. Blanuša, The influence of plant type on green roof rainfall retention, Urban Ecosyst. 22 (2019) 355–366. doi:10.1007/s11252-018-0822-2.

[71] D. Wolf, J.T. Lundholm, Water uptake in green roof microcosms: Effects of plant species and water availability, Ecol. Eng. 33 (2008) 179–186. doi:10.1016/j.ecoleng.2008.02.008.

[72] B. Dvorak, A. Volder, Green roof vegetation for North American ecoregions: A literature review, Landsc. Urban Plan. (2010). doi:10.1016/j.landurbplan.2010.04.009.

[73] L.W. Zhou, Q. Wang, Y. Li, M. Liu, R.Z. Wang, Green roof simulation with a seasonally variable leaf area index, Energy Build. 174 (2018) 156–167. doi:10.1016/j.enbuild.2018.06.020.

[74] S. Cascone, J. Coma, A. Gagliano, G. Pérez, The evapotranspiration process in green roofs: A review, Build. Environ. 147 (2019) 337–355. doi:10.1016/j.buildenv.2018.10.024.

[75] Y. Chen, B. Zheng, Y. Hu, Numerical simulation of local climate zone cooling achieved through modification of trees, albedo and green roofs-a case study of changsha, China, Sustain. 12 (2020). doi:10.3390/su12072752.

[76] P. Ferrante, M. La Gennusa, G. Peri, G. Rizzo, G. Scaccianoce, Vegetation growth parameters and leaf temperature: Experimental results from a six plots green roofs' system, Energy. 115 (2016) 1723–1732. doi:10.1016/j.energy.2016.07.085.

[77] G. Pérez, C. Chocarro, A. Juárez, J. Coma, Evaluation of the development of five Sedum species on extensive green roofs in a continental Mediterranean climate, Urban For. Urban Green. 48 (2020) 126566. doi:10.1016/j.ufug.2019.126566.

[78] M. Mobasheri, Green roofs-construction and functional requirements for four buildings on the IST campus Architecture Examination Committee, (2014) 96.

[79] C. Butler, C.M. Orians, Sedum cools soil and can improve neighboring plant performance during water deficit on a green roof, Ecol. Eng. 37 (2011) 1796–1803. doi:10.1016/j.ecoleng.2011.06.025.

[80] G. Zanin, L. Bortolini, Performance of Three Different Native Plant Mixtures for Extensive Green Roofs in a Humid Subtropical Climate Context, Water. 12 (2020) 3484. doi:10.3390/w12123484.

[81] M. Meetam, N. Sripintusorn, W. Songnuan, U. Siriwattanakul, A. Pichakum, Assessment of physiological parameters to determine drought tolerance of plants for extensive green roof architecture in tropical areas, Urban For. Urban Green. 56 (2020) 126874. doi:10.1016/j.ufug.2020.126874.

[82] S. Cascone, Green roof design: State of the art on technology and materials, Sustain. 11 (2019). doi:10.3390/su11113020.

[83] K.L. Getter, D.B. Rowe, J.A. Andresen, I.S. Wichman, Seasonal heat flux properties of an extensive green roof in a Midwestern U.S. climate, Energy Build. 43 (2011) 3548–3557. doi:10.1016/j.enbuild.2011.09.018.

[84] D. Morau, T. Libelle, F. Garde, Performance evaluation of green roof for thermal protection of buildings in reunion Island, Energy Procedia. 14 (2012) 1008–1016. doi:10.1016/j.egypro.2011.12.1047.

[85] M. Xiao, Y. Lin, J. Han, G. Zhang, A review of green roof research and development in China, Renew. Sustain. Energy Rev. 40 (2014) 633–648. doi:10.1016/j.rser.2014.07.147.

[86] G. yu QIU, H. yong LI, Q. tao ZHANG, W. CHEN, X. jian LIANG, X. ze LI, Effects of Evapotranspiration on Mitigation of Urban Temperature by Vegetation and Urban Agriculture, J. Integr. Agric. 12 (2013) 1307–1315. doi:10.1016/S2095-3119(13)60543-2.

[87] K.J. Kontoleon, D.K. Bikas, The effect of south wall's outdoor absorption coefficient on time lag, decrement factor and temperature variations, Energy Build. 39 (2007) 1011–1018. doi:10.1016/j.enbuild.2006.11.006.

[88] R. Fathipour, A. Hadidi, Analytical solution for the study of time lag and decrement factor for building walls in climate of Iran, Energy. 134 (2017)

167–180. doi:10.1016/j.energy.2017.06.009.

[89] P. Bevilacqua, D. Mazzeo, R. Bruno, N. Arcuri, Experimental investigation of the thermal performances of an extensive green roof in the Mediterranean area, Energy Build. 122 (2016) 63–69. doi:10.1016/j.enbuild.2016.03.062.

[90] T. Susca, Green roofs to reduce building energy use? A review on key structural factors of green roofs and their effects on urban climate, Build. Environ. 162 (2019). doi:10.1016/j.buildenv.2019.106273.

[91] S. Cascone, J. Coma, A. Gagliano, G. Pérez, The evapotranspiration process in green roofs: A review, Build. Environ. 147 (2019) 337–355. doi:10.1016/j.buildenv.2018.10.024.

[92] W. Yang, Z. Wang, J. Cui, Z. Zhu, X. Zhao, Comparative study of the thermal performance of the novel green(planting) roofs against other existing roofs, Sustain. Cities Soc. 16 (2015) 1–12. doi:10.1016/j.scs.2015.01.002.

[93] L.S.H. Lee, C.Y. Jim, Thermal-cooling performance of subtropical green roof with deep substrate and woodland vegetation, (2018).

[94] C.Y. Jim, L.L.H. Peng, Substrate moisture effect on water balance and thermal regime of a tropical extensive green roof, Ecol. Eng. 47 (2012) 9–23. doi:10.1016/j.ecoleng.2012.06.020.

[95] R. Djedjig, E. Bozonnet, R. Belarbi, Analysis of thermal effects of vegetated envelopes: Integration of a validated model in a building energy simulation program, Energy Build. 86 (2015) 93–103. doi:10.1016/j.enbuild.2014.09.057.

[96] D. Kaiser, M. Köhler, M. Schmidt, F. Wolff, Increasing Evapotranspiration on Extensive Green Roofs by Changing Substrate Depths, Construction, and Additional Irrigation, Buildings. 9 (2019) 173. doi:10.3390/buildings9070173.

[97] M. Santamouris, Cooling the cities - A review of reflective and green roof mitigation technologies to fight heat island and improve comfort in urban environments, Sol. Energy. 103 (n.d.) 682–703. doi:10.1016/j.solener.2012.07.003.

[98] A.M. Coutts, E. Daly, J. Beringer, N.J. Tapper, Assessing practical measures to reduce urban heat: Green and cool roofs, Build. Environ. 70 (2013) 266–276. doi:10.1016/j.buildenv.2013.08.021.

[99] V. Azeñas, J. Cuxart, R. Picos, H. Medrano, G. Simó, A. López-Grifol, J. Gulías, Thermal regulation capacity of a green roof system in the mediterranean region: The effects of vegetation and irrigation level, Energy

Build. 164 (2018) 226–238. doi:10.1016/j.enbuild.2018.01.010.

[100] C. Van Mechelen, T. Dutoit, M. Hermy, Adapting green roof irrigation practices for a sustainable future : A review, Sustain. Cities Soc. 19 (2015) 74–90. doi:10.1016/j.scs.2015.07.007.

[101] A.G.N. Bandara, B.M.A.N. Balasooriya, H.G.I.W. Bandara, K.S. Buddhasiri, Smart Irrigation Controlling System for Green Roofs Based on Predicted Evapotranspiration, (2016) 31–36.

[102] Y. Lin, H. Lin, Thermal performance of different planting substrates and irrigation frequencies in extensive tropical rooftop greeneries, Build. Environ. 46 (2011) 345–355. doi:10.1016/j.buildenv.2010.07.027.

[103] H. Qin, Y. Peng, Q. Tang, S. Yu, A HYDRUS model for irrigation management of green roofs with a water storage layer, Ecol. Eng. 95 (2016) 399–408. doi:10.1016/j.ecoleng.2016.06.077.

[104] J. Heusinger, D.J. Sailor, S. Weber, Modeling the reduction of urban excess heat by green roofs with respect to different irrigation scenarios, Build. Environ. 131 (n.d.) 174–183. doi:10.1016/j.buildenv.2018.01.003.

[105] M. Kottek, J. Grieser, C. Beck, B. Rudolf, F. Rubel, World Map of the Köppen-Geiger climate classification updated, Meteorol. Zeitschrift. 15 (2006) 259–263. doi:10.1127/0941-2948/2006/0130.

[106] DesignBuilder, (2014). doi:Available from: https://designbuilder.co.uk.

[107] EnergyPlus, US Dep. Energy. (2014). doi:Available from: https://energyplus.net.

[108] S. Frankenstein, G. Koenig, ERDC / CRREL TR-04-25 FASST Vegetation Models Cold Regions Research and Engineering Laboratory, (2004).

[109] S. Frankenstein, G.G. Koenig, Fast All-season Soil STrength (FASST) Cold Regions Research, (2004).

[110] D.J. Sailor, A green roof model for building energy simulation programs, Energy Build. 40 (2008) 1466–1478. doi:10.1016/j.enbuild.2008.02.001.

[111] G.E. Myers, Long-Time solutions to heat- conduction transients with time-dependent inputs, J. Heat Transfer. 102 (1980) 115–120. doi:10.1115/1.3244221.

[112] J.E. Seem, Modeling of Heat Transfer in Buildings ". Ph.D. Thesis , University of Wisconsin, Ph.D. Thesis , Univ. Wisconsin. (1987) 1987.

[113] P.W. O'Callaghan, S.D. Probert, Sol-air temperature, Appl. Energy. 3 (1977) 307–311. doi:10.1016/0306-2619(77)90017-4.

[114] Ashrae Standard, ASHRAE Handbook 2001 Fundamentals, in: Ashrae Stand., 2001. doi:10.1017/CBO9781107415324.004.

[115] M. Martin, P. Berdahl, Characteristics of infrared sky radiation in the United States, Sol. Energy. (1984). doi:10.1016/0038-092X(84)90162-2.

Appendix A

Long term experimental analysis of thermal performance of extensive green roofs with different substrates in Mediterranean climate

The paper presented in this appendix is published in *Energy and Buildings* (doi: 10.1016/j.enbuild.2019.05.041)

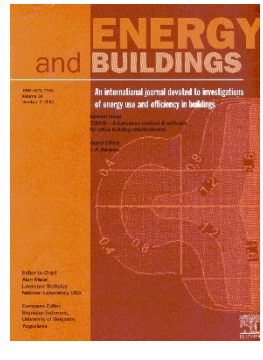

Energy & Buildings 197 (2019) 18–33

Contents lists available at ScienceDirect

Energy & Buildings

journal homepage: www.elsevier.com/locate/enbuild

Long term experimental analysis of thermal performance of extensive green roofs with different substrates in Mediterranean climate

M. Porcaro[a,*], M. Ruiz de Adana[a], F. Comino[a], A. Peña[b], E. Martín-Consuegra[c], T. Vanwalleghem[d]

[a] Departamento de Química-Física y Termodinámica Aplicada, Escuela Politécnica Superior, Universidad de Córdoba, Campus de Rabanales, Antigua Carretera Nacional IV, km 396, Córdoba 14072, Spain
[b] Área de Ingeniería de Proyectos, Universidad de Córdoba, Campus de Rabanales, Antigua Carretera Nacional IV, km 396, Córdoba 14072, Spain
[c] Departamento de Biología Vegetal y Ecología, Div. Botánica, Facultad de Ciencias, Universidad de Córdoba, Campus de Rabanales, Antigua Carretera Nacional IV, km 396, Córdoba 14072, Spain
[d] Área de Ingeniería Hidráulica, Universidad de Córdoba, Campus de Rabanales, Antigua Carretera Nacional IV, km 396, Córdoba 14072, Spain

ARTICLE INFO

Article history:
Received 27 December 2018
Revised 18 April 2019
Accepted 18 May 2019
Available online 18 May 2019

Keywords:
Green roofs
Energy demand
Time lag
Decrement factor
Cooling potential

ABSTRACT

Green roofs are passive construction systems that can contribute to reduce the energy demand of buildings and achieve the European goal of nearly zero energy buildings. The main objective of this work was to determine experimentally the thermal performance of extensive green roofs with different substrates, compared to a traditional gravel ballasted roof. Hence, a study on the annual reduction of energy demand throughout two years warmer than average years, 2016 and 2017, and a dynamic analysis based on decrement factor, DF, time lag, TL, cooling potential, CP, for these three green roofs were carried out.

The results showed that significant reductions of DF and increases of TL and CP were achieved, especially in the green roof with 100% of commercial growing medium substrate. Annual reductions of energy gains and losses were obtained in the three green roofs, with annual average reductions of 66% and 63%, respectively, compared to the traditional roof. These results were mainly related to the composition of the substrates, their capacity to retain water and the quantity of vegetation in each plot. This study indicates that the use of green roofs contributes significatively to reduce the energy demand of existing buildings under warm climatic conditions.

1. Introduction

EU Directives [1,2] reinforce the goal of reducing energy consumption and introduce the concept of nearly zero energy buildings (nZEB) for the retrofitting of existing buildings and the construction of new buildings. An nZEB is a building that has a very high performance, with constructive systems of low environmental impact combined with installations that promote the use of renewable energies [3,4].

One of the possible passive construction systems of low environmental impact are green roofs. Some of the advantages of a green roof are that it has a good thermal insulation capacity, retains meteoric water, absorbs CO_2 and local noise pollution and minimises the heat island effects in cities [5–7]. Green roofs ensure less energy losses in winter and the maintenance of the internal temperature in summer [8]. There are three types of green roof: intensive, semi-intensive and extensive. An intensive green roof usually has a higher thickness, between 150 and 400 mm, and the plant species used require a lot of maintenance and irrigation [9]. A semi-intensive green roof needs periodically maintenance and irrigation and has a thickness of 120–250 mm, while an extensive green roof is used mainly to cover large non-walkable roofs, has a thickness of 60–200 mm and the plant species require low maintenance [9]. The present work focused on extensive green roofs.

Previous research studies on extensive green roofs analysed experimentally and numerically their behaviour under different climatic conditions. An extensive green roof was studied in the cool wet climate of the Pacific Northwest [10], showing the necessity of plants that retain a great quantity of water to counter the environmental constraints imposed by regional climate. In tropical climate, green roofs showed good thermal benefits and urban heat island mitigation potential [11,12]. Other research focused on subtropical climate, showing the importance to choose droughts tolerant plants [13] and a high deep of the substrate [14], to obtain good thermal benefits. Some authors achieved a reduction of the surface temperature of a bare rooftop for subtropical climatic con-

* Corresponding author.
E-mail address: z72popom@uco.es (M. Porcaro).

https://doi.org/10.1016/j.enbuild.2019.05.041
0378-7788/

Nomenclature

C_{cover}	cloudiness factor of the sky
CDW	construction and demolition waste
CP	cooling potential [°C]
DF	decrement factor [dim]
E	East
F_{gnd}	view factor from surface to ground
F_{sky}	view factor from surface to sky
H	heat flux [W m^{-2}]
h_c	mean convective heat transfer coefficient [W m^{-2} K^{-1}]
$h_{c,f}$	foliage convective heat transfer coefficient [W m^{-2} K^{-1}]
$h_{c,s}$	soil convective heat transfer coefficient [W m^{-2} K^{-1}]
h_o	heat transfer coefficient by radiation and convection at the outer surface [W m^{-2} K^{1}]
h_r	mean radiative heat transfer coefficient [W m^{-2} K^{-1}]
LAI	leaf area index [dim]
nZEB	nearly zero energy buildings
P	plot
RA	recycled aggregates
RF	rain fall [mm/h]
RH	relative humidity [%]
SR	solar radiation [W m^{-2}]
t	time [h]
T	temperature [°C]
T_{hs}	average temperature between the plot surface temperature and the sky temperature [K]
TL	time lag [h]
W	West
VWC	volumetric water content [m^3 m^{-3}]
WD	wind direction [°]
WS	wind speed [m s^{-1}]

Greek letters

ΔR	infrared radiation difference between surface and sky and surroundings [W m^{-2}]
α	product of the solar absorptance of the exterior surface and the rate of total solar radiation incident per unit area upon surface [W m^{-2}]
α_o	solar absorptance of exterior surface
σ	Stefan-Boltzmann constant [W m^{-2} K^{-4}]
σ_f	fractional vegetation coverage
ε	infrared emittance of surface
ε_0	emittance of the clear sky
ε_f	emissivity of canopy
ε_g	emissivity of the ground surface

Subscripts

a	air
amb	ambient air
e	exterior
E	East
g	ground surface
Glob,H	global on the horizontal axis
i	interior
min	minimum value
max	maximum value
n	probe number
sa	sol air
sky	sky
W	West

ditions [15], although the relative humidity affected negatively the reduction of surface temperature. Long term studies about thermal performances of green roofs in subtropical climates showed that the best cooling effects were obtained in summer. However, an improve of the thickness of substrate layer helped to reach better insulation, both in summer and winter [16]. Other works focused on weekly studies of green roofs in Mediterranean climate [17,18] achieving suitable reduction of the total transferred energy. A long term study in Mediterranean climate showed the hydrological efficiency of the green roofs as effective systems to control the volume of rainfall [19].

Different types of substrates in extensive green roofs were studied by other authors. Commercial substrates showed to be very suitable for these type of installations [20,21]. Other studies analysed the performance of extensive green roofs with substrates composed of low-cost and waste materials, such as materials from the construction sector, to reduce their economic costs, achieving acceptable performances [22–24]. In other studies, it was seen that the amount of water in the substrate helps to minimise the cooling demand in summer [25,26].

The overall performance of extensive green roofs has been studied from several dynamic parameters. Many authors studied the heat flux through the layers of the roof as a performance parameter [27,28], where they obtained significant reductions compared to traditional roofs. The cooling potential of the surface temperature of the green roof was another dynamic parameter analysed. This parameter was related to the mitigation of the effects of urban heat islands [29,30]. Two dynamic parameters used to study other passive construction systems, such as green façades, are time lag, TL, and decrement factor, DF, [31,32]. Both parameters were used to study the heat storage capabilities of any materials and the reduction of energy demand [32]. Recently, these parameters were studied for a green roof with different plants during a summer week for the climatic conditions in the south of Italy [33], achieving an increase of TL and a reduction of DF in respect to a roof with only substrate.

Most of the previous studies carried out weekly analyses of green roofs. However, it would be interesting to evaluate the thermal performance of green roofs with different substrates over a long period of time.

The main objective of this work was to determine the thermal performance of three green roofs with different substrates for the retrofitting of existing buildings, compared to a traditional gravel ballasted roof. The substrates used were a combination of different percentages of commercial growing medium and recycled construction materials. Hence, several dynamic parameters were studied for each roof, such as decrement factor, DF, time lag, TL, sol-air temperature, T_{sa}, cooling potential, CP, and annual reduction of energy demand. The green roofs were installed in an office building at the University of Córdoba (Spain) and studied throughout two warmer than average years, 2016 and 2017, in Córdoba (Spain).

2. Methodology

2.1. Climatic conditions and degree days

The University of Córdoba is located in Southern Spain, where the climatic conditions are typically Mediterranean, defined as subtype Csa dry-summer subtropical, according to Köppen-Geiger climate classification [34]. Córdoba has relatively mild winters and very warm summers. The daily and yearly temperature fluctuations

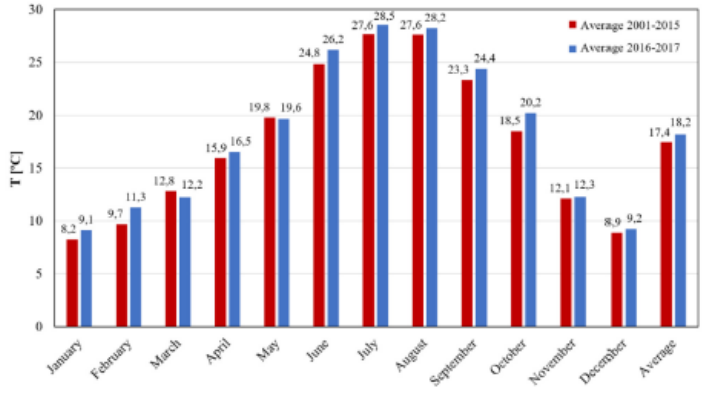

Fig. 1. Monthly average temperature values from 2011 to 2015 and from 2016 to 2017 in Córdoba, Spain.

Table 1
Climatic data of Córdoba, 2016 and 2017.

Year 2016	Units	Jan	Feb	Mar	Apr	May	Jun	Jul	Aug	Sep	Oct	Nov	Dec	Average
Monthly average temperature	°C	10.6	10.9	11.4	15.7	18.6	24.9	29.1	28.5	24.9	19.6	12.5	10.4	18.1
Maximum monthly average temperature	°C	15.7	16.4	19.0	22.0	25.1	33.1	37.3	36.9	33.0	26.5	18.4	16.5	25.0
Minimum monthly average temperature	°C	6.4	5.6	4.5	10.0	12.6	16.3	20.5	20.2	16.8	14.2	8.1	6.2	11.8
Monthly average rainfall	mm/month	59.6	42.6	30.2	115.4	92.4	0.2	0.4	0.2	3.0	84.0	142.2	469.0	86.6
Number of rainy days	days	19.0	12.0	13.0	12.0	11.0	1.0	1.0	1.0	1.0	10.0	15.0	24.0	10.0
Monthly average solar radiation on the horizontal surface	MJ/m²	7.7	10.3	17.2	19.5	22.2	28.1	27.5	25.7	21.0	13.9	9.5	8.7	17.6
Reference evapotranspiration	mm	1.2	1.8	2.8	3.9	5.5	6.7	7.6	6.7	4.5	2.8	1.5	1.1	3.8
Year 2017	**Units**	**Jan**	**Feb**	**Mar**	**Apr**	**May**	**Jun**	**Jul**	**Aug**	**Sep**	**Oct**	**Nov**	**Dec**	**Average**
Monthly average temperature	°C	7.6	11.7	13.1	17.4	20.7	27.4	28.0	27.9	23.9	20.8	12.1	8.1	18.2
Maximum monthly average temperature	°C	15.4	17.3	20.8	25.9	28.4	35.9	37.0	36.4	32.6	30.0	20.8	15.0	26.3
Minimum monthly average temperature	°C	2.0	7.1	6.7	9.7	13.3	18.4	18.6	18.9	15.1	13.8	6.0	3.2	11.1
Monthly average rainfall	mm/month	20.0	50.8	73.6	67.7	46.2	9.2	0.2	7.8	0.2	27.4	52.4	235.1	49.2
Number of rainy days	days	13.0	15.0	14.0	7.0	6.0	1.0	1.0	7.0	1.0	5.0	7.0	12.0	7.4
Monthly average solar radiation on the horizontal surface	MJ/m²	10.6	9.9	16.8	22.4	25.8	29.3	27.9	24.4	20.9	15.7	11.0	8.5	18.6
Reference evapotranspiration	mm	1.2	1.7	2.9	3.9	5.1	7.3	7.7	6.6	5.0	3.1	1.7	1.1	3.9

are very high. Summers tend to be dry with less than one-third of the precipitation of the wettest winter month. This study was developed in the period 2016–2017. The monthly average temperatures from 2011 to 2015 and from 2016 to 2017 in Córdoba are shown in Fig. 1. It can be observed that the average temperatures from 2016 to 2017 increased 0.72 °C compared to the previous 15 years, 2001–2015. The greatest difference between the monthly average temperatures was obtained in June, 1.4°C. The monthly average maximum and minimum values and other significant climatic parameters of 2016 and 2017 are reported in Table 1.

2.2. Green roof experimental setup

An existing office building constructed in 1956 located Lat 37.9° N, Long 4.7° W was selected for this study. The office building had a rectangular footprint (27.7 m length, 9.5 m width, 7 m height) and a flat roof, as shown in Fig. 2. There was not a climate control program in the building, therefore, the indoor air conditions were in free evolution.

The experimental extensive green roofs were installed in May 2015. Six plots were located on the building roof with a surface of 14.78 m² each. One additional plot was used as the reference roof, Pref. The green roof plots layout is shown in Fig. 3. The roof did not have shadows of trees or other buildings and the main façade of the building faces south.

Table 2
Growing media composition of experimental green roof plots.

Plot	P1	P2	P5
Commercial growing medium	100%	75%	50%
Recycled aggregates construction materials	0	25%	50%

In this work, experimental results corresponding to P1, P2, P5 and Pref were analysed. The three green roofs consisted of the following layers, ordered from top to bottom: Mediterranean vegetation, growing medium (0.1 m), filter sheet, a drainage and water storage layer, a root-barrier waterproof layer, water proof membrane and a roof assembly (0.3 m concrete), see Figs. 4a and 5a. Pref consisted of the following layers, ordered from top to bottom: layer of gravel ballasted (0.03 m), waterproof membrane and roof assembly (0.3 m concrete), see Figs. 4b and 5b. The substrate composition in each plot was different, as indicated in Table 2, where different percentages (by volume) of commercial growing medium and recycled construction materials were used. Recycled aggregates construction material is defined as material derived from construction and demolition waste (CDW) of buildings. These new

Fig. 2. Aerial view of the building (before the green roof was installed) [35].

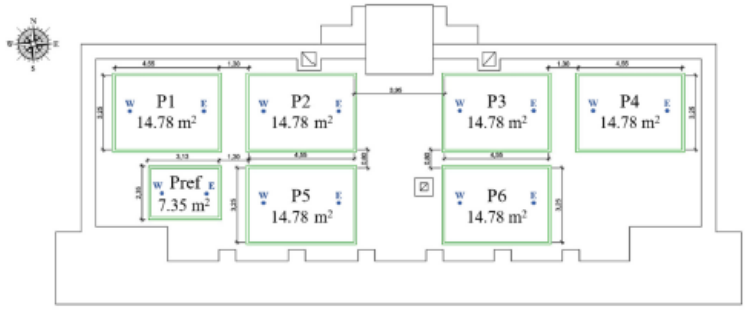

Fig. 3. Roof plan with green roof plots. *Note: E and W refer to East and West.

Table 3
Properties of the used materials.

	Commercial growing medium	Recycled aggregates construction materials
Saturated-surface-dry density [g/cm³]	1.5	2.6
Dry density [g/cm³]	1.1	2.5
Dry bulk density [g/cm³]	0.3	1.4
Water absorption [%]	41.3	3.6
pH	7.3–7.7	10.8
Electric conductivity [mS/cm]	2.0	1.7

materials are then called Recycled Aggregates (RA). Their composition can be various in nature, depending on the origin of the waste. Generally, they are composed of different percentages of ceramic particles, concrete, gypsum, etc. Extensive green roofs with fine mixed recycled aggregate as growth substrate could revalue construction and demolition wastes, which currently present low added value.

The properties of both materials are summarised in Table 3. These properties were obtained by UNE-EN 1097–06:2014 Standard. The granulometry was obtained according to the UNE-EN 933–1: 2012 Standard. The maximum granulometry of the commercial growing medium was 8 mm and of the recycled aggregates construction materials was 9 mm. The RA material was prepared with a sand-sized granulometry. The values of pH and electrical conductivity of each substrate were 7.8 and 2.0 mS/cm for P1, 8.6 and 1.9 mS/cm for P2 and 9.4 and 1.7 mS/cm for P5.

Twelve autochthonous Mediterranean plant species were planted in P1, P2 and P5. These were selected by their adaptation to tolerate drought stress, intense lighting, extreme heat and shallow substrates, which are exactly the biological and ecological characteristics needed for green roofs in urban Mediterranean ecosystems. The species used were: Acinos alpinus, Bellis perennis, Brachypodium retusum, Cerastium tomentosum, Dianthus arenarius, Lobularia maritima, Lotus corniculatus, Paronychia argentea, Phagnalon saxatile, Sanguisorba minor, Sedum sediforme and Trifolium repens.

The area of each plot was divided into 18 experimental micro-plots of 0.75 m². 12 plants were planted in each micro-plot, 1 unit of each selected species. The placement of the different species was not carried out randomly. It was based on the premise that all the species interacted with each other, in order to evaluate these interactions. The number of units planted in the available area of

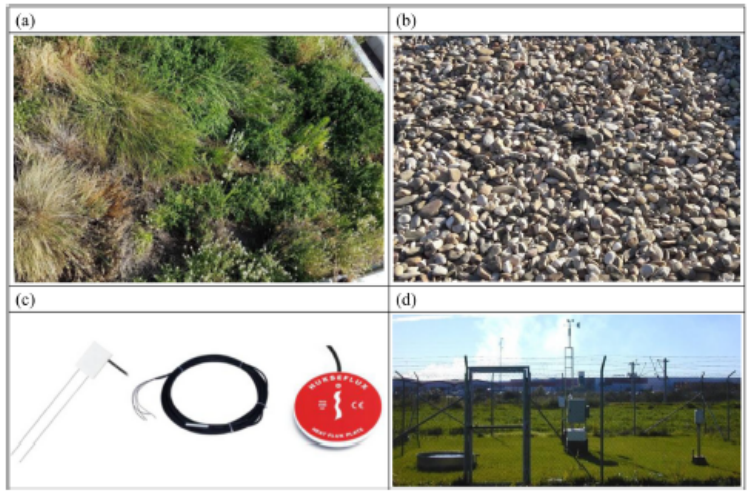

Fig. 4. Images of a) P1, b) Pref, c) probes used, d) weather station.

Table 4
Equipment and variables measured in the experimental campaign.

Equipment	Models	Accuracy	Variable	Name	Unit	City
Thermistors	Campbell 109	±0.25°C (−10 to 70 °C)	Temperature	T	[°C]	Logan (USA)
Heat flux plate	Campbell HFP01	±5%	Heat Flux	H	[W/m² K]	Logan (USA)
Water content reflectometer	Campbell CS616	±2.5% (0 to 50%)	Volumetric Water content	VWC	[%]	Logan (USA)
Platinum resistance temperature	Vaisala HMP45C	0.2°C (−40 to 70°C)	Air temperature	Ta	[°C]	Vantaa, (Finland)
Capacitive relative humidity	Vaisala HMP45C	2% (0 to 100%)	Air relative humidity	RH	[%]	Vantaa, (Finland)
Silicon photocell solar radiation	Campbell SP1110 pyranometer	5% (350 nm to 1100 nm)	Solar radiation	SR	[W/m²]	Logan (USA)
Wind speed and direction sensor	RM Young 05103	1% (0 to 100 m/s) 3° (0 to 360°)	Wind speed and direction	WS WD	[m/s] [°]	Traverse (USA)
Rain gauge	Campbell ARG100	98% at 20 mm/h	Rainfall	RF	[m³/m³]	Logan (USA)

the plot resulted in a planting density of 15.34 plants/m^2, density very close to that recommended by the German Guideline FLL [36], 16 plants/m^2.

The experimental extensive green roofs were installed in May 2015. The experimental results were collected after obtaining all the vegetation coverage of each plot. The fractional vegetation coverage, σ_f, and the leaf area index, LAI, were estimated through direct measurements on each green roof plot, obtaining values of $\sigma_f = 0.59$ and LAI = 2 for P1, $\sigma_f = 0.56$ and LAI = 1.7 for P2, and $\sigma_f = 0.53$ and LAI = 1.5 for P5. These values were considered constant throughout the period studied. This method of direct measurement was based on obtaining the areas using the Image J software [37].

2.3. Description of monitoring system

Meteorological data were monitored by a weather station, placed near the experimental installation, see Fig. 4d. The data recorded were: ambient air temperature, relative humidity, rainfall, atmospheric pressure, speed and direction of the wind and solar radiation, see Fig. 4c. The specification of measuring devices, the type of sensor and its accuracy are shown in Table 4.

Two acquisition point (East and West) properly spaced from their edges to avoid boundary effects, were installed in P1, P2 and P5, for the monitoring of the main variables, see Figs. 3 and 5. In each acquisition point, along the vertical profile, five probes of temperature were installed. The temperature probes were located under the roof slab, $T_{W0,\,Pi}$ and $T_{E0,\,Pi}$, between the roof slab and the root barrier, $T_{W1,\,Pi}$ and $T_{E1,\,Pi}$, between the drainage layer and the bottom part of the growing media, $T_{W2,\,Pi}$ and $T_{E2,\,Pi}$, in the middle height of growing media, $T_{W3,\,Pi}$ and $T_{E3,\,Pi}$, and in the upper part of the growing media, $T_{W4,\,Pi}$ and $T_{E4,\,Pi}$, as shown in Fig. 5a.

Volumetric water content, VWC, was measured using a water content reflectometer in each acquisition point, $VWC_{W,\,Pi}$ and $VWC_{E,\,Pi}$, as shown in Fig. 5a. Heat flux was measured using a heat flux plate in each acquisition point in the middle of the growing media, $H_{W,\,Pi}$ and $H_{E,\,Pi}$, as shown in Fig. 5a. Two acquisition points (East and West) were also installed in Pref to monitoring the main variables, Fig. 5b. In each acquisition point, along the vertical profile, three temperature probes were installed. The temperature

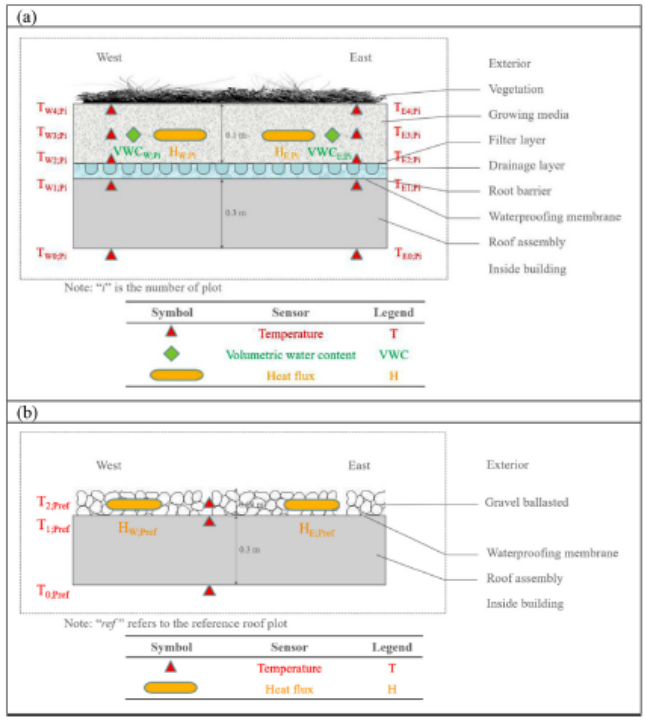

Fig. 5. Plots layers and sensors; a) P1, P2 and P5; where "i" is the number of the plot; b) Pref.

probes were located under the roof slab, $T_{0,Pref}$, between the roof slab and the gravel ballasted layer, $T_{1,Pref}$, and in the upper part of the gravel ballasted, $T_{2,Pref}$, as shown in Fig. 5b. Heat flux was measured in Pref using a heat flux plate in each acquisition point in the middle of the gravel ballasted, $H_{W,Pref}$ and $H_{E,Pref}$, as shown in Fig. 5b. The characteristics of the equipment of the experimental installation are shown in Table 4.

The green roof was equipped with a drip irrigation system managed by a time schedule module. The irrigation was provided during the warmest months in summer to prevent water stress in plants. The irrigation system operated twice a day in P1, P2 and P5, for 10 min and fed by 27 l each time.

A dedicated data acquisition system was used to sample the information of the sensors every 15 min. The experimental data was recorded for two years, from January 2016 to December 2017. The measured values were filtered and then, analysed in spreadsheets for time steps of 15 min. For the values measured at two points, East and West, $T_{n,Pi}$, VWC_{Pi} and H_{Pi}, a mean value was calculated, where n is the probe number with respect to Fig. 5 and Pi is P1, P2, P5 or Pref. These mean values were used to calculate the dynamic parameters, with the same time steps. Finally, daily average values were obtained for the dynamic parameters. Important hiatus was not produced during the period studied, less than 0.3% of the data collected. Appropriate interpolation methods were used in order to fill the gaps of the data.

2.4. Dynamic variables used in the energy analysis

The experimental green roof analysis was evaluated according to several dynamic parameters used in previous studies [33,38]. The dynamic parameters evaluated were the following:

- Sol-air temperature, T_{sa}, which is defined as the outside air temperature which, in the absence of solar radiation, would give the same temperature distribution and rate of heat transfer through a roof as exists due to the combined effects of the actual outdoor temperature distribution plus the incident solar radiation [39]. T_{sa} was calculated with Eq. (1) for a traditional roof [40]. This equation was characterized to calculate T_{sa} for plots with green roofs, Eq. (2), taking into account evapotranspiration contribution, according to [33,38].

$$T_{sa} = T_{amb} + \frac{\Delta R}{h_o} + \frac{\alpha}{h_o} \quad (1)$$

$$T_{sa} = \frac{h_c}{h_c + h_r} T_{amb} + \frac{h_r}{h_c + h_r} T_{sky} + \frac{\alpha}{h_c + h_r} \quad (2)$$

Where T_{amb} is the external air temperature; ΔR is the infrared radiation difference between surface and sky and surroundings, ex-

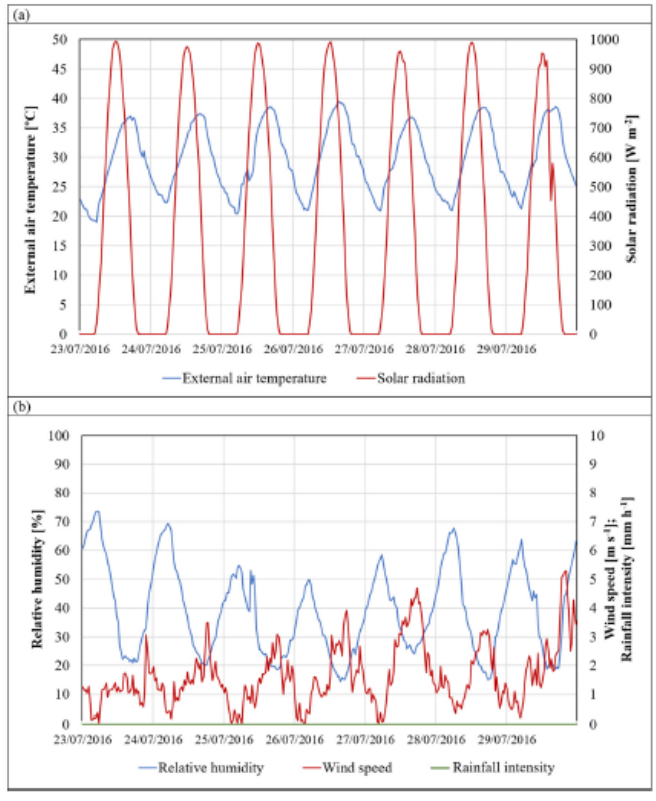

Fig. 6. Climatic conditions of the selected summer period. (a) Solar radiation and external air temperature. (b) Rainfall, windspeed and relative humidity.

pressed by Eq. (3); h_o is the heat transfer coefficient by radiation and convection at the outer surface, expressed by Eq. (4); h_c is the mean convective heat transfer coefficient, expressed by Eq. (5); h_r is the mean radiative heat transfer coefficient, expressed by Eq. (6); α is the product of the solar absorptance of the exterior surface and the rate of total solar radiation incident per unit area upon surface expressed by Eq. (7); T_{sky} is the sky temperature, which was calculated considering the sky as a black body [41], expressed by Eq. (8).

$$\Delta R = \varepsilon \cdot \sigma \cdot \left(F_{sky} \cdot \left(T_{sky}^4 - T_{amb}^4\right) + F_{gnd} \cdot \left(T_g^4 - T_{amb}^4\right)\right) \quad (3)$$

$$h_o = 10.08 + 10.8 \cdot WS \quad (4)$$

$$h_c = \sigma_f \cdot h_{c_f} + \left(1 - \sigma_f\right) \cdot h_{c,s} \quad (5)$$

$$h_r = \frac{\varepsilon_f \cdot \varepsilon_g}{\varepsilon_g + \varepsilon_f - \varepsilon_g \cdot \varepsilon_f} \cdot \left(4 \cdot \sigma \cdot T_m^3\right) \quad (6)$$

$$\alpha = \alpha_o \cdot SR_{Qab,H} \quad (7)$$

$$T_{sky} = T_{amb} \cdot \left(\varepsilon_0 + 0.8 \cdot (1 - \varepsilon_0) \cdot C_{cover}\right)^{0.25} \quad (8)$$

- Decrement factor, DF, is defined as the ratio between the maximum daily excursions of the internal and external temperature fluctuations [31], expressed by Eq. (9).

$$DF = \frac{T_{i,max} - T_{i,min}}{T_{e,max} - T_{e,min}} \quad (9)$$

- Time lag, TL, is defined as the time difference between the maximum peak of the internal temperature and the maximum peak of the external temperature for summer climatic conditions, expressed by Eq. (10), and the time difference between the minimum peak of the internal temperature and the minimum peak of the external temperature for winter climatic conditions, expressed by Eq. (11), [31].

$$TL_{summer} = t_{Ti,max} - t_{Te,max} \quad (10)$$

$$TL_{winter} = t_{Ti,min} - t_{Te,min} \quad (11)$$

DF and TL were evaluated considering $T_{sa,\,Pi}$ as the external boundary temperature for all the plots and $T_{i,\,Pi}$ as the internal bound-

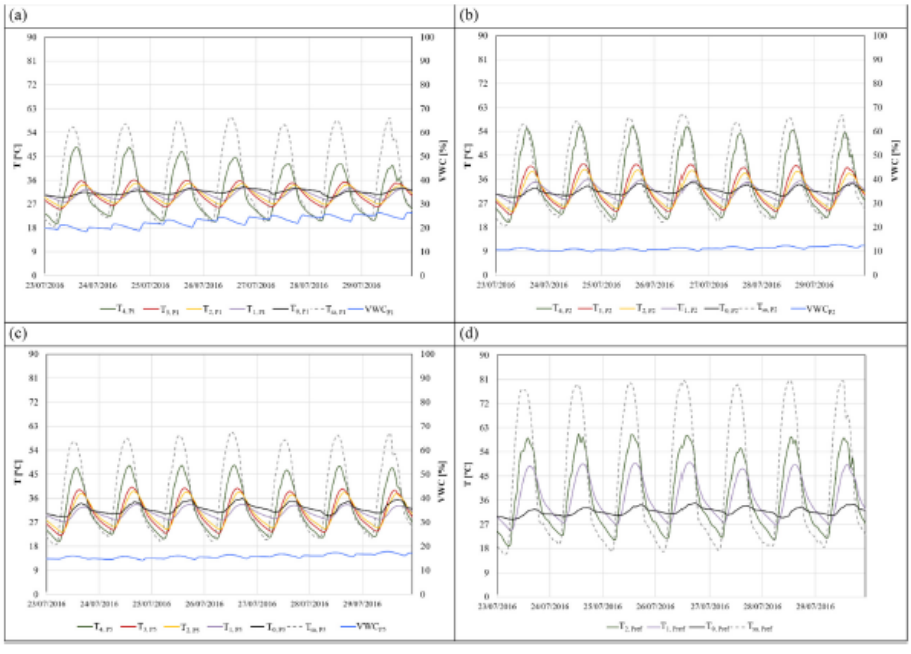

Fig. 7. Temperature profile measured, sol-air temperature and water content measured in the substrate for (a) P1; (b) P2; (c) P5; (d) Pref, in the summer period.

ary temperature for P1, P2 and P5, see Fig. 5a. $T_{1,Pref}$ was considered the internal boundary temperature for the reference plot, see Fig. 5b.

- Cooling potential, CP, is defined as the difference between the maximum internal boundary temperature of the reference plot and the maximum internal boundary temperature of the green roofs, according to Eq. (12).

$$CP = T_{1,Pref,max} - T_{1,Pi,max} \quad (12)$$

Where $T_{1,Pref,max}$ is the maximum slab temperature value for Pref and $T_{1,Pi,max}$ is the maximum slab temperature value for P1, P2 and P5. CP was only calculated for the considered summer period.

- Heat flux, measured in the growing medium in the plots with green roofs and in the gravel ballasted layer in the reference plot, see Fig. 5. The heat flux sensors were placed such that a positive and negative reading signifies heat entering and leaving the building, respectively.

3. Results and analysis

Three different green roof plots were studied throughout the years 2016 and 2017. The analysis of the experimental results for 2016 is presented in weekly, monthly and annual analysis to correctly understand the behaviour of the extensive green roof plots for the climatic conditions of Córdoba. Nevertheless, the analysis of the experimental results for 2017 is presented in annual analysis, because the monthly average temperature values were similar for both years.

3.1. Summer behaviour of the extensive green roof

A typical summer week was selected for the study of the summer behaviour of the green roof plots, analysing in depth the climatic conditions, the substrate temperature profile and the TL, DF and CP parameters.

The climatic conditions for the selected summer period, from 23/07/2016 to 29/07/2016, are shown in Fig. 6. The values of total horizontal solar radiation and external air temperature were similar for each day of the week, reaching peaks of 994 W/m² and 39.4 °C, respectively, see Fig. 6a. It can also be observed a weekly oscillation of relative humidity between 14.5% and 73.7%, a weekly variation of wind speed between 0 m/s and 4.8 m/s and absence of rainfall, see Fig. 6b.

3.1.1. Analysis of the temperature profile and water content in the plots

The temperature values measured and sol-air temperature calculated, T_{sa}, for the four plots, and VWC in the substrates of P1, P2 and P5, for the selected summer period are shown in Fig. 7. The T_{sa} and VWC values were obtained from the average value measured by the two probes located in the same horizontal profile. Regarding the water content in the substrate, it can be observed an increase in its value in the three green roofs when the irrigation was operating. For P1, VWC values oscillated between 18.3% and 26.4% during the week, with a weekly average value of 22.8%, see Fig. 7a. For P2, the variation was less than for P1, between 9.7% and 12.8%, with a weekly average value of 11.1%, see Fig. 7b, and finally, for

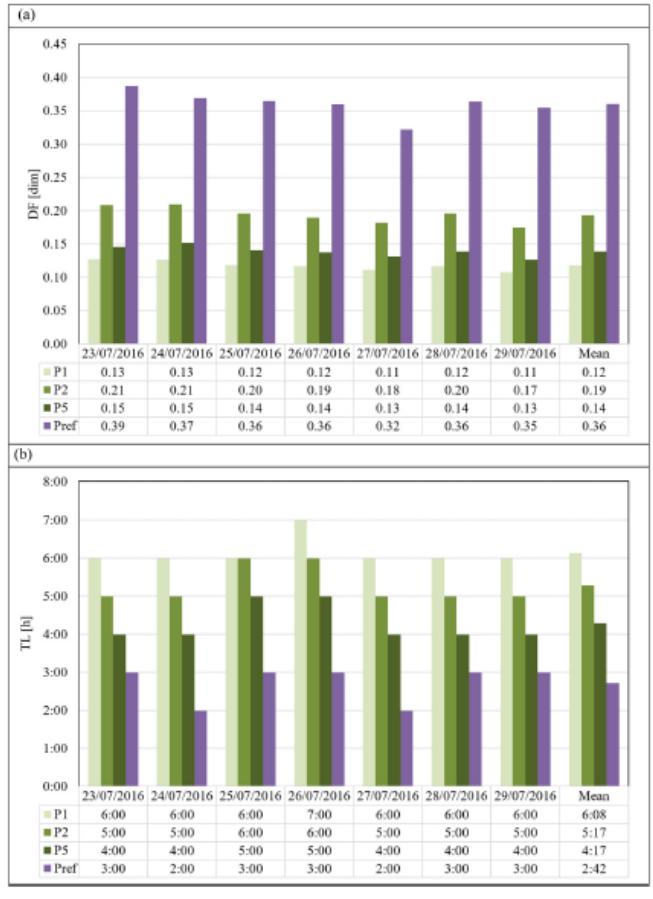

	23/07/2016	24/07/2016	25/07/2016	26/07/2016	27/07/2016	28/07/2016	29/07/2016	Mean
P1	0.13	0.13	0.12	0.12	0.11	0.12	0.11	0.12
P2	0.21	0.21	0.20	0.19	0.18	0.20	0.17	0.19
P5	0.15	0.15	0.14	0.14	0.13	0.14	0.13	0.14
Pref	0.39	0.37	0.36	0.36	0.32	0.36	0.35	0.36

	23/07/2016	24/07/2016	25/07/2016	26/07/2016	27/07/2016	28/07/2016	29/07/2016	Mean
P1	6:00	6:00	6:00	7:00	6:00	6:00	6:00	6:08
P2	5:00	5:00	6:00	6:00	5:00	5:00	5:00	5:17
P5	4:00	4:00	5:00	5:00	4:00	4:00	4:00	4:17
Pref	3:00	2:00	3:00	3:00	2:00	3:00	3:00	2:42

Fig. 8. Values of (a) decrement factor and (b) time lag for P1, P2, P5 and Pref in the selected summer period.

P5, the oscillation obtained was between 14.1% and 17.9%, with a weekly average value of 15.9%, see Fig. 7c.

These results showed that the substrate of P1, with 100% commercial growing medium, managed to retain more water in summer than the rest of the plots, using the same amount of watering. The substrate of P2, with 75% commercial growing medium and 25% recycled construction materials, was the one that retained the least water, with values lower than the substrate of P5, with 50% commercial growing medium and 50% recycled construction materials, see Figs. 7b and 6c. It can also be seen that the maximum temperatures in the green roofs were achieved for T_4, measured in the upper part of the substrate, with values of 48,5 °C, 55,7 °C and 48,2 °C for P1, P2 and P5, respectively. For the last days of the week, the highest T_4 values of the green roofs decreased as the water content in the substrate increased, especially in P1, see Figs. 7a, 6b and 6c. However, the highest $T_{2,Pref}$ values were stable throughout the week, because there was no irrigation and the highest external temperatures was also constant, see Fig. 6a. Therefore, these results show the relation between the substrate used and VWC.

The temperature values measured decreased according to the depth of the four plots. The minimum temperature values for the three plots with green roofs were obtained for T_1, measured below the drainage layer, oscillating between 27.6 °C and 34.8 °C for P1, see Fig. 7a, between 27.2 °C and 35.9 °C for P2, see Fig. 7b, and between 27.3 °C and 33.6 °C for P5, see Fig. 7c. For Pref, $T_{1,Pref}$ values variated between 30.1 °C and 50.1 °C.

Regarding T_{sa}, similar values were obtained for the three plots with green roofs, with maximum and minimum values of 60.0 °C and 18.5 °C, respectively. However, T_{sa} values for Pref increased significantly during the morning, up to 80.5 °C, and decreased during the night, up to 16.0 °C.

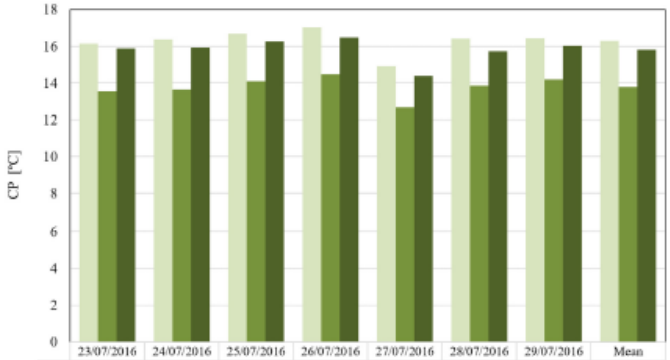

	23/07/2016	24/07/2016	25/07/2016	26/07/2016	27/07/2016	28/07/2016	29/07/2016	Mean
P1	16.1	16.4	16.7	17.0	14.9	16.4	16.4	16.3
P2	13.6	13.6	14.1	14.5	12.7	13.8	14.2	13.8
P5	15.9	15.9	16.3	16.5	14.4	15.7	16.0	15.8

Fig. 9. Cooling potential values for P1, P2 and P5 in the selected summer period.

3.1.2. Time lag and decrement factor analysis

The values of decrement factor, DF, and time lag, TL, for the four plots were calculated using Eqs. (3) and (4), respectively. The daily results of DF and TL for the summer week are shown in Fig. 8.

The parameter DF showed the oscillations of $T_{i,Pi}$ (ΔT_i), temperature values between the roof slab and the root barrier, respect to the oscillations of $T_{sa,Pi}$ (ΔT_e), see Eq. (9). The higher ΔT_e or the lower ΔT_i, the lower DF is. In Fig. 7, it can be observed that ΔT_e values were similar for the three green roofs, because the T_{sa} values were similar. The ΔT_i values varied in each plot with green roofs, mainly due to the capacity of the substrate to retain water, VWC, during daily irrigation. Therefore, the higher capacity to retain water, lower values of ΔT_i and DF were obtained, see Fig. 7. The lowest DF values were always achieved in P1, with an average weekly value of 0.12, see Fig. 8a, in agreement with the lowest values of $T_{i,P1}$, as shown in Fig. 7a, mainly due to the high capacity of the substrate to retain water. Comparing the three plots with green roofs, the highest DF values were obtained in P2, with an average weekly value of 0.19, see Fig. 8a, mainly due to the low capacity of retaining water in its substrate, so the oscillations of $T_{i,\,P2}$ were higher, see Fig. 7b. The DF values increased significantly in Pref. It can be observed that Pref presented the highest DF values throughout the selected period, with an average weekly value of 0.36, see Fig. 8a, mainly due to the fluctuation of the slab temperature, $T_{i;Pref}$, see Fig. 7d. These results indicated that, for very warm and dry climatic conditions, the higher the capacity to retain water in the substrate, the higher the reduction in the oscillation of the slab temperature, $T_{i,Pi}$, and DF is.

The TL parameter measured the difference in time between the maximum daily $T_{sa,Pi}$ values and the maximum daily $T_{i,Pi}$ values for the summer climatic conditions, see Eq. (10). The TL results were mainly related to the fractional vegetation coverage, the leaf area index, the composition of the substrates and their capacity to retain water and the water accumulated in the drainage layer.

The TL values shown in Fig. 8b could be divided into several part of TL according to the layers of the plots. There was a TL from the maximum daily $T_{sa,Pi}$ value to the maximum daily $T_{4,Pi}$ value (vegetation layer), see Fig. 7, another TL of maximum daily temperatures from $T_{4,Pi}$ to $T_{2,Pi}$ (substrate layer), see Fig. 7, and finally, another TL of maximum daily temperatures from $T_{2,Pi}$ to $T_{i,Pi}$ (water accumulation layer), see Fig. 7. The TL values due to the vegetation layer were similar for the three plots, between 1 h and 2 h. The TL values due to the substrate layer were higher for P1 than P2 and P5, due to volumetric water content of the substrates. Finally, the highest TL values due to the water accumulation layer were for P2, see Fig. 7. In this case, the substrate drained more water than the other substrates and consequently there was more water accumulated in this layer. As a result, the order of the plots that presented from the highest to the lowest values of TL were P1, P2, P5 and Pref, with average weekly values of 6:08 h, 5:17 h, 4:17 h and 2:42 h, respectively, see Fig. 8b, mainly due the cross-effects of the different layer of the plots. Previous studies also showed the importance of vegetation and composition of the substrate in the dynamic characterization of a green roof [33], with maximum weekly average TL values of 4:20 h. Nevertheless, in the present work higher TL values were found, up to 6.08 h, as shown in Fig. 8b. The TL values confirm the green roof benefits for the retrofit of buildings without insulation by delaying the peak in the maximum surface temperature.

3.1.3. Cooling potential

The cooling potential, CP, of the three plots with green roofs was evaluated for the selected summer period, according to Eq. (12). The results of daily CP and a weekly average value for each plot are shown in Fig. 9. It can be seen that the highest CP values were obtained in P1, with a weekly average value of 16.3 °C. The second plot with the highest CP was P5, with a weekly average of 15.8 °C, 3% less than P1. Finally, P2 had the lowest CP values compared to the rest of the plots with green roofs, a 15% less than P1. This study showed that the plots with green roofs always allowed the slab temperature to reduce by more than 12.7 °C, compared to Pref. These results were inversely proportional to the DF values, Fig. 8a, where the green roof that had the greatest capacity to retain water in the substrate, P1, achieved the best results. Therefore, the higher the capacity to retain water in substrate, the higher CP is.

3.2. Winter behaviour of the extensive green roof

A weekly analysis for a typical winter week, similar to that performed in Section 3.1, was carried out. The winter week selected

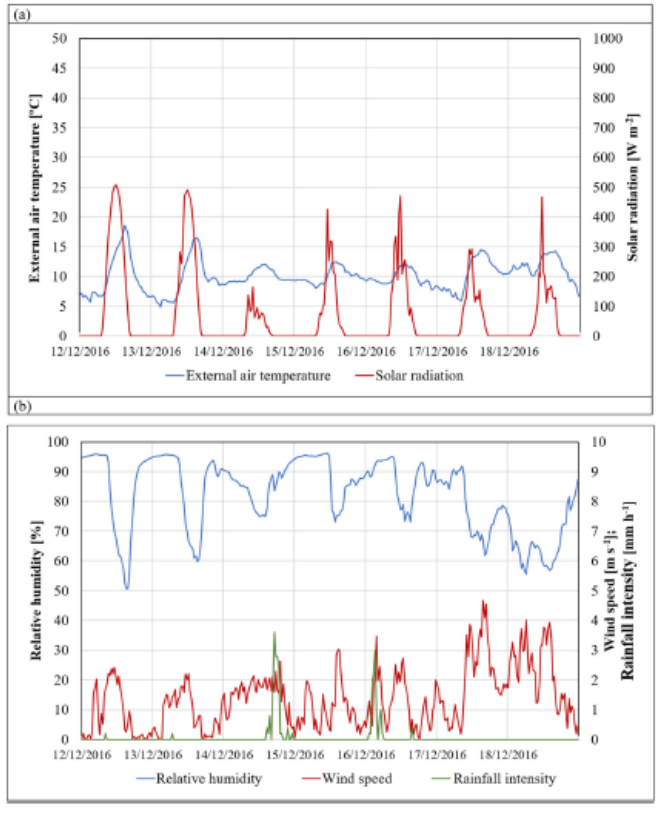

Fig. 10. Climatic conditions of the selected winter period. (a) Solar radiation and external air temperature. (b) Rainfall, wind speed and relative humidity.

was from 12/12/2016 to 18/12/2016. The climatic conditions, the substrate temperature profile and the TL and DF parameters were also analysed for this week. The climatic conditions for the selected winter period are shown in Fig. 10. The peak values of total horizontal solar radiation and external air temperature varied each day, with maximum values of 507.7 W/m^2 and 18.6 °C during the first day, respectively, see Fig. 10a. The selected week also had some rainy days, with a total weekly rainfall of 26.8 mm/h, see Fig. 10b. The minimum values of total horizontal solar radiation and external air temperature were obtained for day 14/12/2016, see Fig. 10a, coinciding with the day with the highest rainfall, see Fig. 10b. It can also be observed an oscillation of relative humidity between 50.7% and 96.1% and wind speed between 0 m/s and 4.7 m/s.

3.2.1. Analysis of the temperature profile and water content in the plots

Temperature profile, sol-air temperature and volumetric water content in the substrate of the four plots for the selected winter week are shown in Fig. 11. The irrigation during this week wasn't planned, so the percentage of water present in the substrate depended on the air humidity and the amount of rainfall, see Fig. 10b. It can be observed that the weekly average VWC values for the three plots with green roofs were similar, 47.6%, 48.2% and 47.7% for P1, P2 and P5, respectively. For the first two days, that had low rainfall, the VWC values oscillated between 39.5% and 43.6%. However, these values increased in the following days, that had high rainfall, up to 56.8%, 56.7% and 51.2% for P1, P2 and P5, respectively. Regarding the temperatures measured, the T_4 values for green roofs and the T_2 values for Pref oscillated each day, more than the rest of the temperature values measured, due to the fact that the climatic conditions had more influence on their reading. The maximum T_4 values obtained were 17.8 °C, 19.8 °C and 17.1 °C for P1, P2 and P5, respectively, and the maximum T_2 values obtained for Pref was 27.2°C. These temperature peaks decreased as a function of the depth measured for the four plots, as well as for the summer period studied, obtaining the lowest oscillations for T_1 for all plots. The maximum values of T_1 for P1, P2, P5 and Pref were 11.6 °C, 12.6 °C, 12.2 °C and 16.5 °C, respectively.

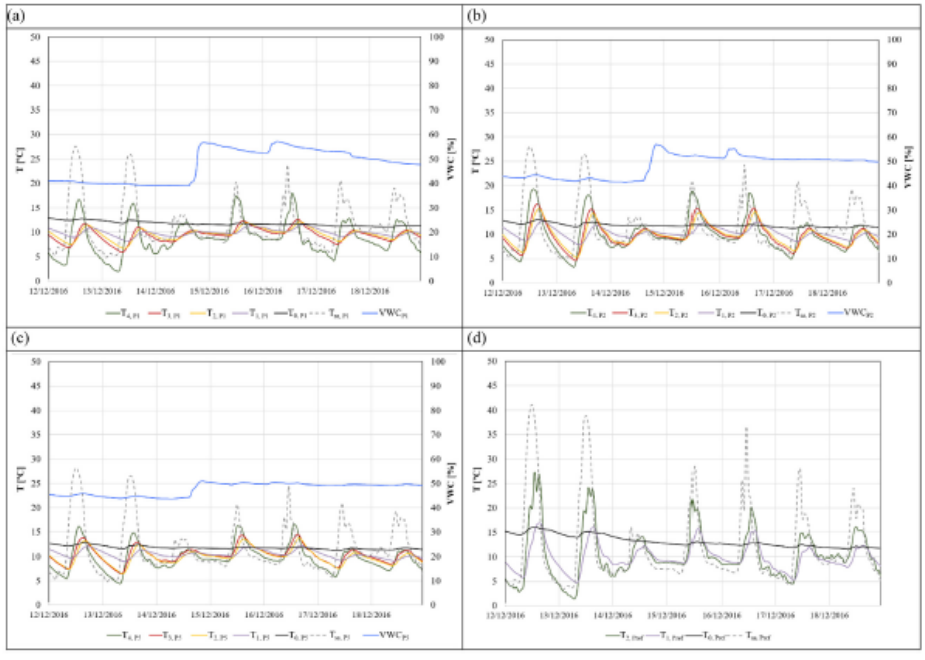

Fig. 11. Temperature and water content values in the substrate of (a) P1; (b) P2; (c) P5; (d) Pref, in the winter period.

In Fig. 11, it can also be seen that the T_{sa} values for the plots with green roofs were similar, with maximum and minimum values of 28.2 °C and 4.8 °C, respectively. However, T_{sa} values for Pref increased significantly during the morning, up to 41.2 °C, and decreased during the night, up to 3.2 °C.

3.2.2. Time lag and decrement factor analysis

The values of DF and TL for the four plots were calculated using Eqs. (9) and (11), respectively. The results of both parameters throughout the selected winter period are shown in Fig. 12. It can be observed that Pref always presented the highest DF values, with an average weekly value of 0.30. These values were significantly reduced in the plots with green roofs, as was already observed in the summer week. The lowest DF values were obtained for P1 and P5, with weekly average values of 0.11 and 0.12, respectively. The highest DF values for the plots with green roof were achieved for P2, with a weekly average value of 0.19, due to the oscillations of $T_{I,P2}$, see Fig. 11b, since the T_{sa} values were similar for the three plots with green roof.

Regarding TL, this parameter measured the difference in time between the minimum daily $T_{sa,Pi}$ values and the minimum daily $T_{I,Pi}$ values for the winter climatic conditions, see Eq. (11). The results showed that the lowest values were achieved in Pref, with an average weekly value of 3:17 h, as shown in Fig. 12b, and the highest values were almost always obtained for P1, with an average weekly value of 6:34 h, mainly due to the higher amount of plants in P1. These TL values, usually reduced for P2 and P5, with average weekly value of 5:42 h and 5:25 h, respectively.

The green roofs allowed a significant reduction in the DF values and an increase in the TL values, compared to the Pref results, despite the high amount of water in the substrates, around 48%, see Figs. 11a–11c. In fact, for rainy and cold climatic conditions in the winter period considered, the trends of DF and TL were mainly due to the vegetation coverage and the composition of the substrates each plot, achieving a reduction in the oscillation of the slab temperature and delaying the minimum peaks of temperature in winter.

3.3. Energy flux analysis

A monthly and annual energy analysis for the plots with green roofs and the reference plot was performed. For this analysis, the transfer of heat flux between the roofs and the interior of the building was measured.

3.3.1. Monthly energy flux analysis

Monthly cumulative energy flux gains and losses for P1, P2, P5 and Pref for 2016 are shown in Fig. 13. The net energy is also shown in Fig. 13, which indicates the difference between the gains and losses of heat through the plot. First, the results obtained in July were analysed, in order to relate them to the parameters previously studied in the summer week. It can be observed that for this month the highest decrease of energy gains was achieved in P1, with a value equal to 11.9 kW h m^{-2}, 83% less than Pref, 69.6 kW h m^{-2}, see Figs. 13a and 13d. For P5, it was also possible to significantly reduce the energy gains in respect to Pref in July, with a value of 24.7 kW h m^{-2}, 64.5% less

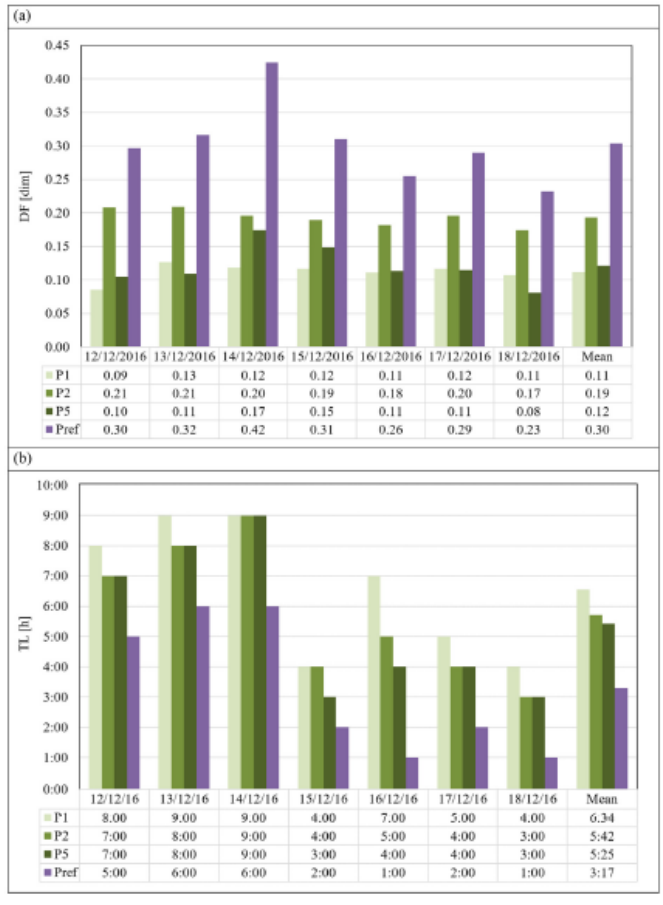

	12/12/2016	13/12/2016	14/12/2016	15/12/2016	16/12/2016	17/12/2016	18/12/2016	Mean
P1	0.09	0.13	0.12	0.12	0.11	0.12	0.11	0.11
P2	0.21	0.21	0.20	0.19	0.18	0.20	0.17	0.19
P5	0.10	0.11	0.17	0.15	0.11	0.11	0.08	0.12
Pref	0.30	0.32	0.42	0.31	0.26	0.29	0.23	0.30

	12/12/16	13/12/16	14/12/16	15/12/16	16/12/16	17/12/16	18/12/16	Mean
P1	8:00	9:00	9:00	4:00	7:00	5:00	4:00	6:34
P2	7:00	8:00	9:00	4:00	5:00	4:00	3:00	5:42
P5	7:00	8:00	9:00	3:00	4:00	4:00	3:00	5:25
Pref	5:00	6:00	6:00	2:00	1:00	2:00	1:00	3:17

Fig. 12. Values of (a) decrement factor and (b) time lag for P1, P2, P5 and Pref in the selected winter period.

than Pref, see Fig. 13c. For the same month, P2 achieved the lowest reduction of energy gains, with a value equal to 26.6 kW h m^{-2}, 61.8% less than Pref, see Fig. 13b. This trend, for the month of July, agreed with the dynamic parameters previously studied, DF and CP, due to the capacity to retain water in the substrate, attenuating the maximum roof temperature peaks during a very warm month. Therefore, the lower DF and the higher CP, the lower heat flux gain is. This trend was similar to that obtained in August, because both months had similar climatic conditions, see Table 1. For June and September, P1 also achieved the highest reduction of energy gains, up to 84% less than Pref, however, P5 achieved lower reduction of energy gains than P2, mainly due to the reduction of the ambient temperature, 4.2 °C less than in July.

For the cold months, the results obtained in December were first analysed, in order to relate them to the parameters previously studied in the winter week. The highest decrease of energy losses was obtained in P1, with a value of −9.1 kW h m^{-2}, 65.3% less than Pref in the same month, see Figs. 13a and 13d. For P2, the value of energy losses was −14.1 kW h m^{-2}, 46.0% less than Pref in the same month, see Figs. 13b and 12d. For the same month, P5 achieved the lowest reduction of energy losses, −17.5 kW h m^{-2}, 33.7% less than Pref, see Figs. 13c and 12d. This trend was in accordance with the previous TL results, see Fig. 12b, which were related to σ_f and LAI in each plot. For the other cold months, such as January and February, the trend was similar for all plots. The maximum reduction of energy losses was obtained in P1 during the month of February, with a value equal to −6.7 kW h m^{-2}, 77.4% less than Pref, see Figs. 13a and 12d.

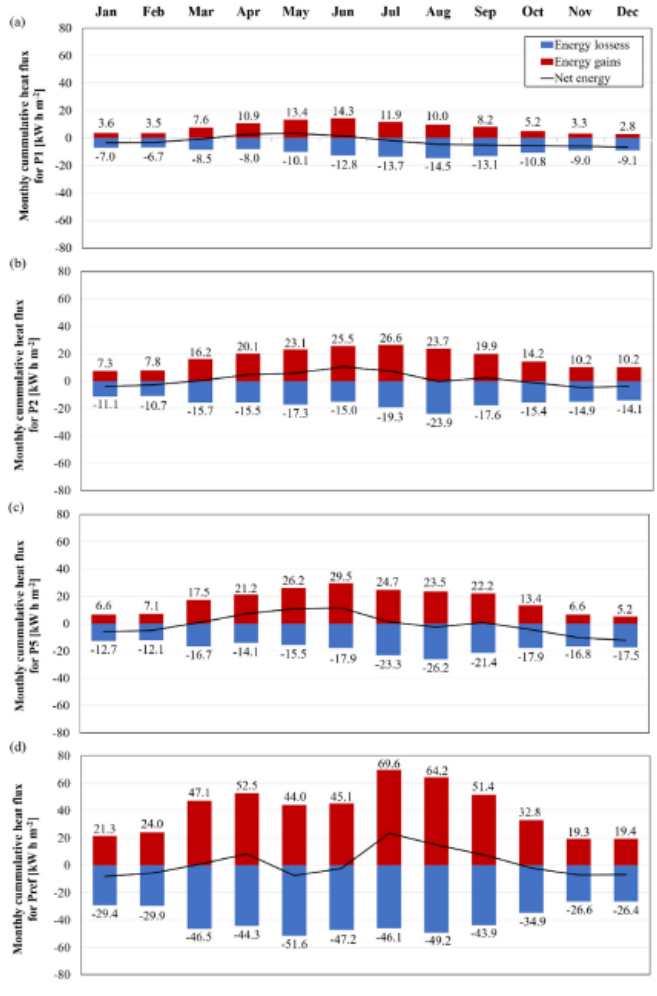

Fig. 13. Monthly cumulative energy flux for (a) P1, (b) P2, (c) P5, (d) Pref.

3.3.2. Annual energy flux analysis

In this section, the annual cumulative energy flux for P1, P2, P5 and Pref for years 2016 and 2017 are shown. The energy gains and losses values for 2017 were slightly higher than the results of the 2016 in all plots, see Fig. 14. This increase was mainly due to the slight rise in annual average ambient temperature and annual average solar radiation and, to the reduction in annual average rainfall during the 2017, see Table 1. The values of energy gains and losses in Pref for 2016 were of 490.7 kWh/m^2 and −476.0 kW h m^{-2}, respectively, and for 2017 of 549 kWh/m^2 and −507.6 kW h m^{-2}, respectively. Comparing these results with those obtained in the plots with green roofs, it can be observed that significant reductions in both energy gains and energy losses were achieved. As shown in Fig. 14, P1 presented the maximum reduction of energy gains and losses, with 81% and 74%, respectively, for year 2016, and with 80% and 70%, respectively, for year 2017. P5 was the plot with the lowest reduction in energy gains and losses, with a 58% and 55%, respectively, for 2016, and a 56% and 57%, respectively, for 2017.

These result show that the extensive green roofs under warm climatic conditions achieved high energy savings, between 55% and 81%, depending on the type of substrate and the fractional vegeta-

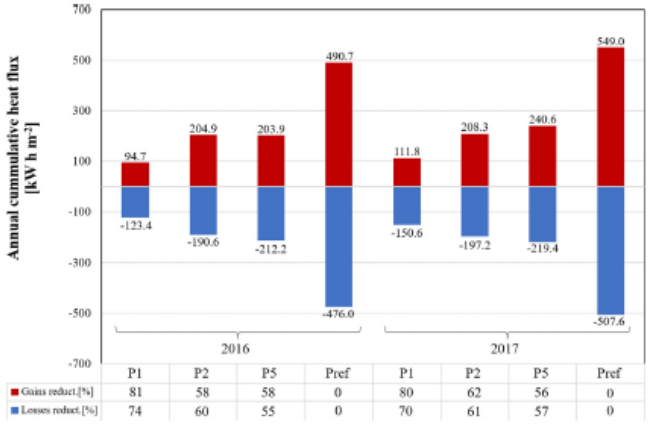

Fig. 14. Annual cumulative energy flux in P1, P2, P5 and Pref for 2016 and 2017.

tion coverage of the plot. Green roofs with commercial substrate, as P1, obtained the best thermal performance, due to the capacity to retain water in the substrate.

4. Conclusion

In this work, the thermal performance of three plots with green roofs, P1, P2 and P5, with different types of substrates were studied and compared with a traditional gravel ballasted roof, Pref. The substrate of P1 was composed of 100% of commercial growing medium, P2 of 75% of commercial growing medium and 25% of recycled construction materials, and finally, P5 of 50% of commercial growing medium and 50% of recycled construction materials. The thermal performance of these three green roofs under warm climatic conditions were studied in Córdoba (Spain), during two years, 2016 and 2017. The potential of green roofs for retrofitting of existing buildings was studied. A dynamic analysis based on decrement factor, DF, time lag, TL, cooling potential, CP, and annual reduction of energy demand for these green roofs was performed.

The experimental results showed that the three plots with green roofs achieved high reduction of DF and high increases of CP, compared to Pref for warm and dry climate, especially in P1 with a weekly average reduction of DF equal to 0.24 and a weekly average increase of CP equal to 16.3 °C. This behaviour was mainly due to the capacity to retain water in the substrate. The results indicated that, for warm and dry climatic conditions, the higher the capacity to retain water in the substrate, the higher the reduction of DF and the higher the increase of CP is.

Significant increases of TL for the green roofs were obtained, up to 6:08 h and 6:34 h for P1 during the hot and cold periods considered, respectively, compared to Pref. The TL results were related to the fractional vegetation coverage, the leaf area index, the composition of the substrates and their capacity to retain water and the water accumulated in the drainage layer, that gave a delayed the maximum slab temperature peak.

Finally, significant reductions of energy gains during the hot period and energy losses during the cold period were obtained in the three green roofs, compared to Pref, due to the capacity to retain water in the substrates and the fractional vegetation coverage of these plots. The annual average reductions in energy gains and losses of the three green roofs were 66% and 63%, respectively. These important energy savings were obtained during two particularly warm years in Córdoba (Spain).

It can be concluded that the use of green roofs could be considered for the retrofit of existing buildings under warm climatic conditions, as a measurement to achieve nZEB requirements.

Conflict of interest

We have no conflict of interest to declare.

Acknowledgements

Weather data from the Agroclimatic Information Network of Andalusia which have been supplied by the Institute of Research and Agricultural and Fisheries Training of the CAPDR of the Andalucía Regional Administration, Junta de Andalucía.

The authors would like to express appreciation for the financial support of the European Regional Development Fund (ERDF) through the project GGI3003IDIB "Optimizing the potential of green roofs for building retrofit: interaction between recycled substrates, water properties and energy efficiency", by the Agency of Public Works of Andalucía, Junta de Andalucía, Spain.

References

[1] European Commission, Directive 2002/91/EC of the European Parliament and of the Council of 16 December 2002 on the energy performance of buildings, 2002. doi:10.1039/zp9842100196.
[2] European Parliament, European directive 2010/31/EU on the energy performance of buildings, 2010. doi:10.3000/17252555.L_2010.153.eng.
[3] A. de Gracia, L. Navarro, J. Coma, S. Serrano, J. Romaní, G. Pérez, L.F. Cabeza, Experimental set-up for testing active and passive systems for energy savings in buildings – Lessons learnt, Renew. Sustain. Energy Rev. 82 (2018) 1014–1026, doi:10.1016/j.rser.2017.09.109.
[4] D.H.W. Li, L. Yang, J.C. Lam, Zero energy buildings and sustainable development implications - A review, Energy 54 (2013) 1–10, doi:10.1016/j.energy.2013.01.070.
[5] M. Shafique, R. Kim, M. Rafiq, Green roof benefits, opportunities and challenges – A review, Renew. Sustain. Energy Rev. 90 (2018) 757–773, doi:10.1016/j.rser.2018.04.006.
[6] M. Karteris, I. Theodoridou, G. Mallinis, E. Tsiros, A. Karteris, Towards a green sustainable strategy for Mediterranean cities: assessing the benefits of large-scale green roofs implementation in Thessaloniki, Northern Greece, using environmental modelling, GIS and very high spatial resolution remote sensing data, Renew. Sustain. Energy Rev. 58 (2016) 510–525, doi:10.1016/j.rser.2015.11.098.

[7] H. Akbari, C. Cartalis, A. Muscio, Local climate change and urban heat island mitigation techniques – the state of the art 22 (2020) 1–16, doi:10.3846/13923730.2015.1111934.
[8] O. Saadatian, K. Sopian, E. Salleh, C.H. Lim, S. Riffat, E. Saadatian, A. Toudeshki, M.Y. Sulaiman, A review of energy aspects of green roofs, Renew. Sustain. Energy Rev. 23 (2013) 155–168, doi:10.1016/j.rser.2013.02.022.
[9] A.B. Besir, E. Cuce, Green roofs and facades: a comprehensive review, Renew. Sustain. Energy Rev. 82 (2018) 915–939, doi:10.1016/j.rser.2017.09.106.
[10] E. Schroll, J. Lambrinos, T. Righetti, D. Sandrock, The role of vegetation in regulating stormwater runoff from green roofs in a winter rainfall climate, Ecol. Eng. 37 (2011) 595–600, doi:10.1016/j.ecoleng.2010.12.020.
[11] J. Yang, D.Jiamathy Mohan Kumar, A. Pyrgou, A. Chong, M. Santamouris, D. Kolokotsa, S.E. Lee, Green and cool roofs' urban heat island mitigation potential in tropical climate, Sol. Energy 173 (2018) 597–609, doi:10.1016/j.solener.2018.08.006.
[12] N. Hien, Y. Chen, C. Leng, A. Sia, Investigation of thermal benefits of rooftop garden in the tropical environment 38 (2003) 261–270.
[13] T.C. Liu, G.S. Shyu, W.T. Fang, S.Y. Liu, B.Y. Cheng, Drought tolerance and thermal effect measurements for plants suitable for extensive green roof planting in humid subtropical climates, Energy Build. 47 (2012) 180–188, doi:10.1016/j.enbuild.2011.11.043.
[14] L.S.H. Lee, C.Y. Jim, Thermal-cooling performance of subtropical green roof with deep substrate and woodland vegetation, (2018).
[15] Y.Y. Huang, C.T. Chen, W.T. Liu, Thermal performance of extensive green roofs in a subtropical metropolitan area, Energy Build. 159 (2018) 39–53, doi:10.1016/j.enbuild.2017.10.039.
[16] Y. He, H. Yu, A. Ozaki, N. Dong, S. Zheng, Long-term thermal performance evaluation of green roof system based on two new indexes : A case study in Shanghai area, 120 (2017).
[17] V. Azeñas, J. Cuxart, R. Picos, H. Medrano, G. Simó, A. López-Grifol, J. Gallas, Thermal regulation capacity of a green roof system in the mediterranean region: the effects of vegetation and irrigation level, Energy Build. 164 (2018) 226–238, doi:10.1016/j.enbuild.2018.01.010.
[18] C.M. Silva, M.G. Gomes, M. Silva, Green roofs energy performance in Mediterranean climate, Energy Build. 116 (2016) 318–325, doi:10.1016/j.enbuild.2016.01.012.
[19] I. Andr, Hydrological performance of green roofs at building and city scales under Mediterranean conditions, (2018) 1–15. doi:10.3390/su10093105.
[20] K. Vijayaraghavan, Green roofs: a critical review on the role of components, benefits, limitations and trends, Renew. Sustain. Energy Rev. 57 (2016) 740–752, doi:10.1016/j.rser.2015.12.119.
[21] C.F. Chen, Performance evaluation and development strategies for green roofs in Taiwan: a review, Ecol. Eng. 52 (2013) 51–58, doi:10.1016/j.ecoleng.2012.12.083.
[22] S.B. Mickovski, K. Buss, B.M. McKenzie, B. Sökmener, Laboratory study on the potential use of recycled inert construction waste material in the substrate mix for extensive green roofs, Ecol. Eng. 61 (2013) 706–714, doi:10.1016/j.ecoleng.2013.02.015.
[23] A.J. Bates, J.P. Sadler, R.B. Greswell, R. Mackay, Effects of recycled aggregate growth substrate on green roof vegetation development: a six year experiment, Landsc. Urban Plan. 135 (2015) 22–31, doi:10.1016/j.landurbplan.2014.11.010.
[24] A. Nagase, N. Dunnett, The relationship between percentage of organic matter in substrate and plant growth in extensive green roofs, Landsc. Urban Plan. 103 (2011) 230–236, doi:10.1016/j.landurbplan.2011.07.012.
[25] B. Raji, M.J. Tenpierik, A. Van Den Dobbelsteen, The impact of greening systems on building energy performance: a literature review, Renew. Sustain. Energy Rev. 45 (2015) 610–623, doi:10.1016/j.rser.2015.02.011.
[26] H.F. Castleton, V. Stovin, S.B.M. Beck, J.B. Davison, Green roofs; Building energy savings and the potential for retrofit, Energy Build. 42 (2010) 1582–1591, doi:10.1016/j.enbuild.2010.05.004.
[27] K.L. Getter, D.B. Rowe, J.A. Andresen, I.S. Wichman, Seasonal heat flux properties of an extensive green roof in a Midwestern U.S. climate, Energy Build. 43 (2011) 3548–3557, doi:10.1016/j.enbuild.2011.09.018.
[28] D. Morau, T. Libelle, F. Garde, Performance evaluation of green roof for thermal protection of buildings in reunion Island, Energy Procedia. 14 (2012) 1008–1016, doi:10.1016/j.egypro.2011.12.1047.
[29] M. Xiao, Y. Lin, J. Han, G. Zhang, A review of green roof research and development in China, Renew. Sustain. Energy Rev. 40 (2014) 633–648, doi:10.1016/j.rser.2014.07.147.
[30] G.Yu Qiu, H.Yong Li, Q.Tao Zhang, W. Chen, X.Jian Liang, X.Ze Li, Effects of evapotranspiration on mitigation of urban temperature by vegetation and urban agriculture, J. Integr. Agric. 12 (2013) 1307–1315, doi:10.1016/S2095-3119(13)60543-2.
[31] K.J. Kontoleon, D.K. Bikas, The effect of south wall's outdoor absorption coefficient on time lag, decrement factor and temperature variations, Energy Build. 39 (2007) 1011–1018, doi:10.1016/j.enbuild.2006.11.006.
[32] R. Fathipour, A. Hadidi, Analytical solution for the study of time lag and decrement factor for building walls in climate of Iran, Energy 134 (2017) 167–180, doi:10.1016/j.energy.2017.06.009.
[33] P. Bevilacqua, D. Mazzeo, R. Bruno, N. Arcuri, Experimental investigation of the thermal performances of an extensive green roof in the Mediterranean area, Energy Build. 122 (2016) 63–69, doi:10.1016/j.enbuild.2016.03.062.
[34] M. Kottek, J. Grieser, C. Beck, B. Rudolf, F. Rubel, World Map of the Köppen-Geiger climate classification updated, Meteorol. Zeitschrift. 15 (2006) 259–263, doi:10.1127/0941-2948/2006/0130.
[35] GoogleMaps, https://www.google.com/maps, (2018).
[36] Forschungsgesellschaft Landschaftsentwicklung Landschaftsbau, Guidelines for the Planning, Execution and Upkeep of Green-roof sites, 2002. http://greenroofsouth.co.uk/FLLGuidelines.pdf.
[37] C.A. Schneider, W.S. Rasband, K.W. Eliceiri, C. Instrumentation, NIH Image to ImageJ mageJ age]yeaimage analysis 9 (2017) 671–675.
[38] D.J. Sailor, A green roof model for building energy simulation programs 40 (2008) 1466–1478, doi:10.1016/j.enbuild.2008.02.001.
[39] P.W. O'Callaghan, S.D. Probert, Sol-air temperature, Appl. Energy 3 (1977) 307–311, doi:10.1016/0306-2619(77)90017-4.
[40] Ashrae Standard, ASHRAE Handbook 2001 Fundamentals, 2001 in: Ashrae Stand., doi:10.1017/CBO9781107415324.004.
[41] M. Martin, P. Berdahl, Characteristics of infrared sky radiation in the United States, Sol. Energy (1984), doi:10.1016/0038-092X(84)90162-2.

Appendix B

Exploring the reduction of energy demand of a building with an eco-roof under different irrigation strategies

The paper presented in this appendix has been submitted in *Sustainable Cities and Society* (December 2020).

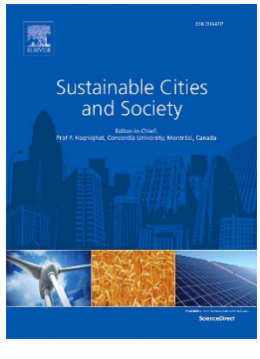

Exploring the reduction of energy demand of a building with an eco-roof under different irrigation strategies

ABSTRACT

A passive system widely used to reduce the energy consumption of a building is the green roof. The main objective of this work was to determine the reduction of energy demand of a building with a green roof without plants, eco-roof, for 20 different irrigation strategies, compared to a traditional roof, in southern Europe.

The results of the eco-roof showed that the evapotranspiration, ET, value increased when outdoor temperature, wind speed, solar radiation and volumetric water content of the substrate rose, and when outdoor relative humidity decreased. The increase in ET had a significant energy influence on the heat flux, $\dot{Q}$, such that the higher the ET, the lower the $\dot{Q}$.

The annual $\dot{Q}$ results showed that the eco-roof improved the thermal performance of the building compared to the traditional roof, achieving a high reduction of energy demand, ED, up to 78.7%. The strategy that had the highest ratio between the annual ED to the lowest use of water was watering in alternate days for 20 min in the morning, obtaining an ED value of 46.7%. These results indicate that eco-roofs with a proper irrigation strategy could be used as an efficient passive system for the rehabilitation of old buildings.

Keywords: passive system, energy demand, evapotranspiration, irrigation strategies

Nomenclature

A	area [m^2]
C	case study
C_e^g	bulk transfer coefficient [-]
C_h^g	bulk transfer coefficient [-]
c_p	specific heat [J kg^{-1} K^{-1}]
D	drainage [l m^{-2}]
ED	energy demand [%]
ET	evapotranspiration [l m^{-2}]
F_g	net heat flux to ground surface [W m^{-2}]
$I_{ir}^{\downarrow}$	total incoming long-wave radiation [W m^{-2}]
$I_s^{\downarrow}$	total incoming short-wave radiation [W m^{-2}]
l_g	latent heat of vaporization at the ground surface temperature [J kg^{-1}]
K	hydraulic conductivity [m s^{-1}]
P	performance of the eco-roof [W h l^{-1}]
q_a	mixing ratio of the air [-]
q_g	mixing ratio at the ground surface [-]
Q	cumulative energy gains [W h m^{-2}]
$\dot{Q}$	heat flux [W m^{-2}]
$\dot{Q}_S$	sensible heat flux [W m^{-2}]
$\dot{Q}_L$	latent heat flux [W m^{-2}]
R	rainfall [l m^{-2}]
RH	relative humidity [%]
SR	solar radiation [W m^{-2}]
T_a	air temperature near the soil [K]
T_f	foliage temperature [K]
T_g	ground surface temperature [K]
T_o	outdoor temperature [K]
U	transmittance [W m^{-2} K^{-1}]
VWC	volumetric water content [m^3 m^{-3}]
W	quantity of irrigation water [l m^{-2}]
W_a	wind speed [m s^{-1}]
WD	wind direction [º]
WS	wind speed [m s^{-1}]
z	depth [m]

Greek letters

α_g	albedo of ground surface [-]
ε_f	emissivity of the foliage [-]
ε_g	emissivity of the ground surface [-]
λ	thermal conductivity [W m^{-1} K^{-1}]
ρ_{ag}	density of air at ground surface temperature [kg m^{-3}]
σ	Stefan-Boltzmann constant [W m^{-2} K^{-4}]
σ_f	fractional vegetation coverage [-]

Subscripts

a	air
eco	eco-roof
exp	experimental
f	foliage
g	ground
num	numerical
o	outdoor
trad	traditional roof
w	week
y	year

1. INTRODUCTION

Over the last few years, awareness about global warming and energy-efficient buildings has increased exponentially. The building sector has a large environmental impact and in Europe it represents 50% of the total energy consumption (Dutil, Rousse, & Quesada, 2011). Many studies have been carried out in order to reduce the use of fossil fuel and increase the renewable energy consumption, promoting passive systems and efficient envelopes in buildings (Daly, Cooper, & Ma, 2014), in line with the EU Directives (European Parliament, 2010; European Union, 2012).

A passive system widely used globally to reduce the energy consumption of a building is the green roof. In Europe, green roofs are very popular in the Nordic countries and Germany, where this technology has been implemented in more than the 10% of all new buildings (Shafique, Kim, & Rafiq, 2018). They are also commonly used in the rehabilitation of old buildings (Cascone, Catania, Gagliano, & Sciuto, 2018). Green roofs are categorized as extensive, intensive and semi-

intensive, based on the thickness of the substrate, the type of plants used and the maintenance required (Cascone, 2019; Mahdiyar, Tabatabaee, Abdullah, & Marto, 2018; Naranjo, Mesa, & Maury, 2020). Previous green roofs research showed notable benefits such as the absorption of CO2, the reduction of noise pollution and the minimization of the heat island effect in cities (Akbari, Cartalis, & Muscio, 2015; Ziogou, Michopoulos, Voulgari, & Zachariadis, 2018). Some studies showed that green roofs reduce the heating and cooling demands of the buildings (Ran & Tang, 2018; Zhang, He, & Dewancker, 2020). Plants of a green roof can decrease the solar radiation transmitted to the soil and function as a wind barrier. Consequentially, the heat conducted to the indoor of the building is reduced and the energy losses due to the wind convection are minimized (Besir & Cuce, 2018; Vaz Monteiro et al., 2017). Furthermore, green roofs contribute to a delay in the storm peak runoff to the drainage system and also enrich biodiversity in cities (Kemp, Hadley, & Blanuša, 2019; Li & Yeung, 2014; Vijayaraghavan, Reddy, & Yun, 2019).

One of the major energy benefits of the green roofs is the cooling effect on the indoor conditions due to the evapotranspiration, ET (Speak, Rothwell, Lindley, & Smith, 2013). ET is the combination of two separate processes whereby water is lost on the one hand from the soil surface by evaporation and on the other hand from the plants by transpiration (FAO, 2006). Several studies analysed the influence of ET on the energy behaviour of green roofs (Cascone, Coma, Gagliano, & Pérez, 2019; Susca, 2019; Yang, Wang, Cui, Zhu, & Zhao, 2015). While the different variables affecting ET are well known (FAO, 2006), the relative importance of each of these variables differs depending on the environmental conditions. An experimental study in subtropical Hong Kong native-woodland intensive green roof found that solar radiation had the strongest correlation with ET (Lee & Jim, 2018). Another experimental study in a tropical extensive green roof showed that ET was largely dependent on solar radiation, relative humidity and wind speed, but found little influence of substrate moisture (Jim & Peng, 2012). A numerical model of a green roof was developed to determine the ET effects on the heat transfer of a building (Djedjig, Bozonnet, & Belarbi, 2015). The model suggested that a green roof installation is able to decrease the heat flux of the building envelope and the ET reduces further the temperature of the roof surface, providing a greater cooling effect. Other authors evaluated numerically the behaviour of green roofs focusing on the correlation between ET and the volumetric water content, VWC, of the growing media (Kaiser, Köhler, Schmidt, & Wolff, 2019; Santamouris, n.d.). These results showed that the irrigation of a green roof

increased ET values and mitigated the urban heat island effect, especially during the warmer periods. An experimental study also evaluated the effect of ET on VWC of both a green roof and a bare substrate for four summer days in Melbourne (Coutts, Daly, Beringer, & Tapper, 2013), suggesting that during the summer period the lack of water in the substrates halted the ET and the cooling effect of the roofs was reduced. The irrigation of green roofs helps to reduce the heat transfer between the exterior and the interior of a building, during the warmer months, and increases its thermal insulation capacity (Azeñas et al., 2018). Some researchers demonstrated that in the coming 30 years many areas in the world will be water stressed, so the goal of irrigation installations of green roofs will be to achieve the maximum energy savings with minimum water consumption (Mechelen, Dutoit, & Hermy, 2015). In recent literature some numerical studies proposed an irrigation controlling method based on the predicted ET and daily weather variables, in order to maximize the efficient use of water (Bandara, Balasooriya, Bandara, & Buddhasiri, 2016). Other types of irrigation strategies were analysed in experimental research studies to identify the optimal irrigation frequency (Lin & Lin, 2011). The results indicated that a substrate which is irrigated twice a week is able to reduce the heat amplitude under the roof slab surface up to 91.6%. A numerical model of a green roof was developed to study the irrigation management (Qin, Peng, Tang, & Yu, 2016), showing that irrigation every 3 days to the field capacity and irrigation every 7 days to the saturation moisture content are two efficient watering schemes for the climatic condition of Shenzhen, China. A green roof model was simulated in EnergyPlus software to analyse the sensible heat flux reduction potential of several irrigation scenarios under different climatic conditions (Heusinger, Sailor, & Weber, n.d.). For cities with low excess heat and high annual precipitations, such as London and New York, a sensible heat reduction up to 75% was obtained. However, the irrigation strategies of these models were carried out with equal amount of water in all case studies.

Research indicated that the type and characteristics of the substrate play an important role in the insulation of buildings (Gomes, Silva, Valadas, & Silva, 2019; Goussous, Siam, & Alzoubi, 2015; Saadatian et al., 2013). A numerical simulation of different soil thickness showed that the ET of the substrate had a significant effect on the thermal performance of the green roof, expecially in summer (He, Yu, Ozaki, Dong, & Zheng, 2017). Several energy simulations were performed in EnergyPlus software to investigate the thermal performance of five types of green roofs substrates (Gagliano, Poli, & Sciuto, 2019). It was found that the thermal performance of green roofs strongly depended on the thermophysical properties of

the substrate used. An experimental annual study analysed three different substrates under the Mediterranean climate (Porcaro et al., 2019), showing that a substrate composed of commercial growing medium achieved higher heat flux reduction than substrates composed of recycled construction materials. An experimental study was carried out to evaluate the impact of the substrate and irrigation on the thermal performance of green roofs (Tan et al., 2017). This study suggested that the substrate and the soil moisture reduced the roof temperature and improved the thermal performance of the building. An experimental research study analysed the temperature below the concrete of an eco-roof and of a traditional gravel ballasted roof for a summer week in the south of Italy (Bevilacqua, Mazzeo, Bruno, & Arcuri, 2016). The substrate was not provided with irrigation system. The results showed that this temperature was reduced compared to the traditional roof. In this study, an eco-roof was defined as a green roof without plants.

The results obtained in recent literature have shown that irrigation strategies could improve the thermal performance of a building with a green roof. However, most of these studies have focused on a limited number of irrigation strategies with the same amount of water in all cases. Therefore, a detailed analysis of the reduction of energy demand of a building with an eco-roof for different irrigation strategies under Mediterranean climatic conditions could be carried out.

The main objective of this work was to determine the reduction of energy demand of a building with an eco-roof under different irrigation strategies compared to a traditional roof. To achieve this, a model of an eco-roof and another of a traditional gravel ballasted roof were calibrated with experimental data and annual energy simulations were carried out to evaluate 20 different irrigation strategies.

2. METHODOLOGY

Experimental setup and monitoring system

The energy performance of an eco-roof and a traditional gravel ballasted roof were analysed for the climatic conditions of Córdoba, 37°53'29.6" N 4°46'21.9" O. This city is located in the south of Spain and its climate is Mediterranean, subtype Csa dry-summer, as defined in the Koppen-Geiger climate classification (Kottek, Grieser, Beck, Rudolf, & Rubel, 2006).

An experimental setup composed of an eco-roof and a traditional gravel ballasted roof were installed on the rooftop of an old office building from the 1950s, located in the University of Córdoba. The dimensions of the rooftop were 27.7 m

length and 9.5 m width and no shadows of trees or other buildings fell on it. The building didn't have a climate control program, so the indoor air conditions were maintained in free evolution.

A representation of the eco-roof and the gravel ballasted roof is shown in Fig. 1. The layers of the eco-roof, from bottom to top, were: roof slab (λ= 2.3 W/mK; c_p= 1000 J/kgK), waterproof membrane, root-barrier, water storage layer (λ= 0.17 W/mK; c_p= 900 J/kgK), filter sheet and commercial growing medium (λ= 0.52 W/mK; c_p= 1840 J/kgK) with a maximum granulometry of 8 mm, see Fig. 1a. The properties of the substrate are shown in Table 1. The layers of the gravel ballasted roof, from bottom to top, were roof slab, waterproof membrane and a layer of gravel ballasted (λ= 0.55 W/mK; c_p= 1000 J/kgK), see Fig. 1b.

Table 1. Properties of the commercial growing medium substrate.

	Value
Saturated-surface-dry density	1.5 [g/cm^3]
Dry density	1.1 [g/cm^3]
Dry bulk density	0.3 [g/cm^3]
Water absorption	41.3 [%]
pH	7.3-7.7
Electric conductivity	2.0 [mS/cm]

Ten temperature, T, probes along the vertical profile, two volumetric water content, VWC, probes and two heat flux, $\dot{Q}$, probes were installed in the eco-roof, as shown in Fig. 1a. Three temperature, T, probes along the vertical profile and two heat flux, $\dot{Q}$, probes were installed in the gravel ballasted roof, as shown in Fig. 1b.

All the data were recorded every 15 min, from 1/01/2015 to 31/12/2015, by a dedicated acquisition system. The technical specification of all the devices used to record the data are summarized in Table 2.

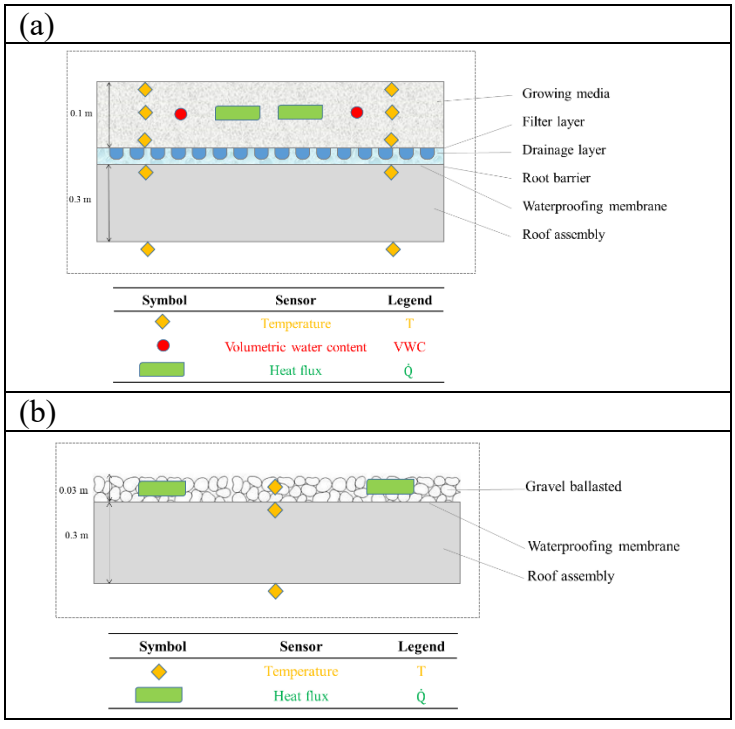

Fig. 1. Layers of (a) the eco-roof and (b) the gravel ballasted roof

Table 2. Equipment and variables measured in the experimental campaign.

Equipment	Accuracy	Variable	Unit
Thermistors	±0,25ºC (-10 to 70 ^{0}C)	Temperature	[ºC]
Heat flux plate	±5%	Heat flux	[W/m^{2}K]
Water content reflectometer	±2.5% (0 to 50%)	Volumetric water content	[%]
Platinum resistance temperature	0.2ºC (-40 to 70ºC)	Air temperature	[ºC]
Capacitive relative humidity	2% (0 to 100%)	Air relative humidity	[%]
Silicon photocell solar radiation	5% (350 nm to 1100 nm)	Solar radiation	[W/m^2]
Wind speed and direction sensor	1% (0 to 100 m/s) 3º (0 to 360º)	Wind speed and direction	[m/s] [º]
Rain gauge	98% at 20 mm/h	Rainfall	[m^3/m^3]

The experimental setup shown in Fig. 1 was used to calibrate two models of a building with a gravel ballasted roof and an eco-roof. In order to calibrate these models, a climatic file with the weather conditions of Córdoba was used. The climatic data were measured throughout 2015 by a weather station situated near the

experimental set up. The probes used by the weather station are shown in Table 2. The data collected were: atmospheric pressure, outdoor air temperature, To, outdoor relative humidity, RH_o, rainfall, R, solar radiation, SR, wind speed, WS, and wind direction, WD. The monthly average meteorological data of 2015 are shown in Table 3.

Table 3. Monthly meteorological data.

Month	T_o [C]	RH_o [%]	SR [Wh/m²]	WD [°]	WS [m/s]	R [mm]
January	10.6	89.9	90	171.5	1.6	0.041
February	10.9	81.9	116.5	184.4	2.2	0.035
March	11.4	71.9	200.6	201.6	1.5	0.021
April	15.8	66.4	227.1	199.1	1.7	0.072
May	18.6	61.3	257.5	192.6	1.9	0.054
June	24.9	43.5	323.7	206.7	2	0
July	29.1	40.5	318.3	206.9	1.9	0.001
August	27.6	45	265.6	207.8	2	0.002
September	22.5	53.5	221.7	201.2	1.8	0.008
October	18.5	73.8	146.2	155.9	1.3	0.057
November	12.8	77.5	137.1	135.8	1.1	0.043
December	10.2	77.6	95.9	110	1	0.008

Building models

Two building models were designed in order to simulate the energy behaviour of two roofs: a traditional gravel ballasted roof and an eco-roof. These models were developed using DesignBuilder software ("DesignBuilder," 2014), which is the graphical interface of EnergyPlus ("EnergyPlus," 2014). The geometrical and thermal characteristics of the building were the same for both models, except for the roof. The characteristics of the building are summarized in Table 4.

Table 4. Geometrical and thermal characteristics of the office building.

Geometrical characteristics	Height	9.0 [m]
	Number of floors	3
	Floor area	264.0 [m^2]
Thermal characteristics	U external walls	3.0 [W/m^2K]
	U ground	2.0 [W/m^2K]
	U traditional roof	2.9 [W/m^2K]
	U eco-roof	1.3 [W/m^2K]
	U windows	5.7 [W/m^2K]

The eco-roof energy analysis of the DesignBuilder software was based on the Army Corps of Engineers' FASST vegetation models (Frankenstein & Koenig, 2004a, 2004b). In this model the energy budget was divided into a budget for the foliage layer, Ff, and a budget for the ground surface, Fg, (Sailor, 2008). The overall energy balance at the soil surface was given by Eq. (1), where the final term is the conduction of heat into the soil. The present work focused on an eco-roof only with substrate, so the energy balance of the roof was calculated without the contributions of the plants.

$$F_g = \left(1 - \sigma_f\right)\left[I_s^{\downarrow}\left(1 - \alpha_g\right) + \varepsilon_g I_{ir}^{\downarrow} - \varepsilon_g \sigma T_g^4\right] - \frac{\sigma_f \varepsilon_g \varepsilon_f \sigma}{\varepsilon_g + \varepsilon_f - \varepsilon_g \varepsilon_f}\left(T_g^4 - T_f^4\right) + \dot{Q}_s + \dot{Q}_L + K \times \frac{\partial T_g}{\partial z} \quad (1)$$

Where σ_f is the fractional vegetation coverage (zero in the eco-roof); $I_s^{\downarrow}$ is the total incoming short-wave radiation; α_g is the albedo of ground surface; $I_{ir}^{\downarrow}$ is the total incoming long-wave radiation; ε_g is the emissivity of the ground surface; T_g is the ground surface temperature; ε_f is the emissivity of the foliage; σ is the Stefan-Boltzmann constant; T_f is the foliage temperature; $\dot{Q}_s$ is the sensible heat flux; $\dot{Q}_L$ is the latent heat flux; K is the hydraulic conductivity and z is the depth.

Sensible heat flux, $\dot{Q}_s$, in an eco-roof depended on the temperature difference between the soil and the external air and the wind speed, as expressed by Eq. (2).

$$\dot{Q}_s = \rho_{ag} C_{p,a} C_h^g W_a \left(T_a - T_g\right) \quad (2)$$

Where ρ_{ag} is the density of air at ground surface temperature; $C_{p,a}$ is the specific heat of air at constant pressure; C_h^g is the bulk transfer coefficient; W_a is the wind speed; T_a is the air temperature near the soil and T_g is the ground surface temperature.

Latent heat flux, $\dot{Q}_L$, in an eco-roof depended on the difference between the mixing ratio of the soil surface and air and the wind speed, as expressed by Eq. (3).

$$\dot{Q}_L = C_e^g \cdot l_g \cdot W_a \cdot \rho_{ag} \cdot \left(q_a - q_g\right) \quad (3)$$

Where C_e^g is the bulk transfer coefficient; l_g is the latent heat of vaporization at the ground surface; q_a is the mixing ratio of the air near to the soil and q_g is the mixing ratio at the ground surface.

Irrigation strategies

Heat flux, $\dot{Q}$, of an eco-roof under different irrigation strategies was evaluated and compared to a traditional gravel ballasted roof. The irrigation strategies consisted of watering at five specific moments of the day with four different quantities of water. The daily irrigation schedules were: (i) once a day in the morning, (ii) once a day during the night, (iii) twice a day with the irrigation quantity divided between morning and evening, (iv) once a day in the afternoon and finally (v) once a day in the morning for alternate days, i.e. it was irrigated on Monday, Wednesday, Friday and Sunday. The quantities of irrigation water were: (i) 3.7 l/m^2·day, (ii) 7.3 l/m^2·day, (iii) 11.0 l/m^2·day, (iv) 14.6 l/m^2·day, considering that 10 minutes of irrigation corresponded to 1.83 l/m^2. The combination of the five schedules and four irrigation quantities resulted in 20 irrigation strategies, $C1_{20}$ to $C5_{80}$, as summarized in Table 5. The numbers 1-5 indicated the daily irrigation schedule and the subscripts 20-80 indicated the daily minutes of irrigation.

The irrigation strategies of the eco-roof were based on a mass balance expressed by Eq. (4).

$$\Delta VWC = W + R - ET - D \quad (4)$$

Where ΔVWC is the variation of the volumetric water content stored in the substrate, W is the quantity of irrigation water, R is rainfall quantity, ET is the evapotranspiration and D is the drainage.

The irrigation aimed to reduce the heat flux through the roof assembly from the exterior to the interior during the summer period for the considered climatic conditions. For this reason, the irrigation strategies were proposed from May to October, when the exterior air temperature exceeded 18 ºC, see Table 3. A case without irrigation strategy, C0, was also studied for the eco-roof, see Table 5.

Table 5. Irrigation strategies.

Case studies	Irrigation period [min/day]	Quantity of water [l/m^2 day]	Irrigation schedule	Schedule
C0	0	0	-	-
$C1_{20}$	20	3.7	8:30 am	Every day
$C2_{20}$	20	3.7	8:30 pm	Every day
$C3_{20}$	20	3.7	8:30 am/8:30 pm	Every day
$C4_{20}$	20	3.7	1:00 pm	Every day
$C5_{20}$	20	3.7	8:30 am	Alternate days
$C1_{40}$	40	7.3	8:30 am	Every day
$C2_{40}$	40	7.3	8:30 pm	Every day
$C3_{40}$	40	7.3	8:30 am/8:30 pm	Every day
$C4_{40}$	40	7.3	1:00 pm	Every day
$C5_{40}$	40	7.3	8:30 am	Alternate days
$C1_{60}$	60	11.0	8:30 am	Every day
$C2_{60}$	60	11.0	8:30 pm	Every day
$C3_{60}$	60	11.0	8:30 am/8:30 pm	Every day
$C4_{60}$	60	11.0	1:00 pm	Every day
$C5_{60}$	60	11.0	8:30 am	Alternate days
$C1_{80}$	80	14.6	8:30 am	Every day
$C2_{80}$	80	14.6	8:30 pm	Every day
$C3_{80}$	80	14.6	8:30 am/8:30 pm	Every day
$C4_{80}$	80	14.6	1:00 pm	Every day
$C5_{80}$	80	14.6	8:30 am	Alternate days

Energy simulation

Detailed energy simulations were carried out with the DesignBuilder software ("DesignBuilder," 2014). The simulations were performed for the climatic conditions of Córdoba throughout the whole year 2015.

The eco-roof under the different irrigation strategies was studied according to the following parameters:

- Evapotranspiration, ET, of the substrate that was calculated directly from the latent heat flux calculations for the substrate, see Eq. (3), and the corresponding values of latent heat of water vaporization (Sailor, 2008). Although the term ET is used throughout the paper, it should be noted that in this study the transpiration term was zero, as the eco-roof was studied without vegetation. Therefore, all transformation of liquid water from the eco-roof to the atmosphere was through evaporation from the bare soil surface only.
- Heat flux, $\dot{Q}$, obtained in the eco-roof and the traditional gravel ballasted roof. Heat flux of the eco-roof, $\dot{Q}_{eco}$, was calculated with the sum of sensible heat

flux and latent heat flux, expressed by Eqs. (2) and (3), respectively. The heat flux of the traditional gravel ballasted roof, $\dot{Q}_{trad}$, was calculated with the transfer model based on the conduction transfer functions, CTFs, (Myers, 1980; Seem, 1987). In addition, $Q^{\cdot}$ was used as calibration parameter of the roof models. The probes used to measure $\dot{Q}$ are shown in Fig. 1. The positive and negative $\dot{Q}$ values indicated heat entering and leaving, respectively. In the present work, the positive $\dot{Q}$ values were evaluated in detail, because the main objective of the eco-roof was to reduce heat flux entering in the building during the warmer seasons, that correspond to the maximum peaks of solar radiation and outdoor air temperature during the day-time, see Table 3.

- Energy demand, ED, of the building with the eco-roof under different irrigation strategies, compared to the traditional gravel ballasted roof. ED was calculated by Eq. (5), where Q_{trad} is the sum of the positive gains of the traditional roof and Q_{eco} is the sum of the positive gains of the eco-roof.

$$ED = \frac{Q_{trad} - Q_{eco}}{Q_{trad}} \cdot 100 \quad (5)$$

- The energy performance of the eco-roof, P_{eco}, was analysed with a ratio, in order to evaluate the irrigation strategies that led the highest reduction of energy demand with respect to the lowest amount of irrigation water, expressed by Eq. (6):

$$P_{eco} = \frac{Q_{trad} - Q_{eco}}{W} \quad (6)$$

3. RESULTS AND ANALYSIS

Calibration of the models

A calibration of the two building models, one with a traditional gravel ballasted roof and one with an eco-roof, was carried out using the heat flux data collected during the experimental campaign, see Fig. 1. The models were calibrated for two typical months under the climatic condition of Córdoba: August, that

presented high values of outdoor air temperature and solar radiation, and December, that presented low values of outdoor air temperature and solar radiation, see Table 3. The irrigation schedule in August was 1.83 l/m^2 twice a day, corresponding to the irrigation strategy $C3_{20}$, while in December no irrigation schedule was considered, C0, see Table 5.

The experimental $\dot{Q}$ values with respect to numerical $\dot{Q}$ values of both roofs for the selected months are shown in Fig. 2. It can be observed that R2 values equal or higher than 0.94 were obtained for both models. Previous studies regarding eco-roof models which were validated experimentally, usually did not provide information on the correlation coefficient R^2.

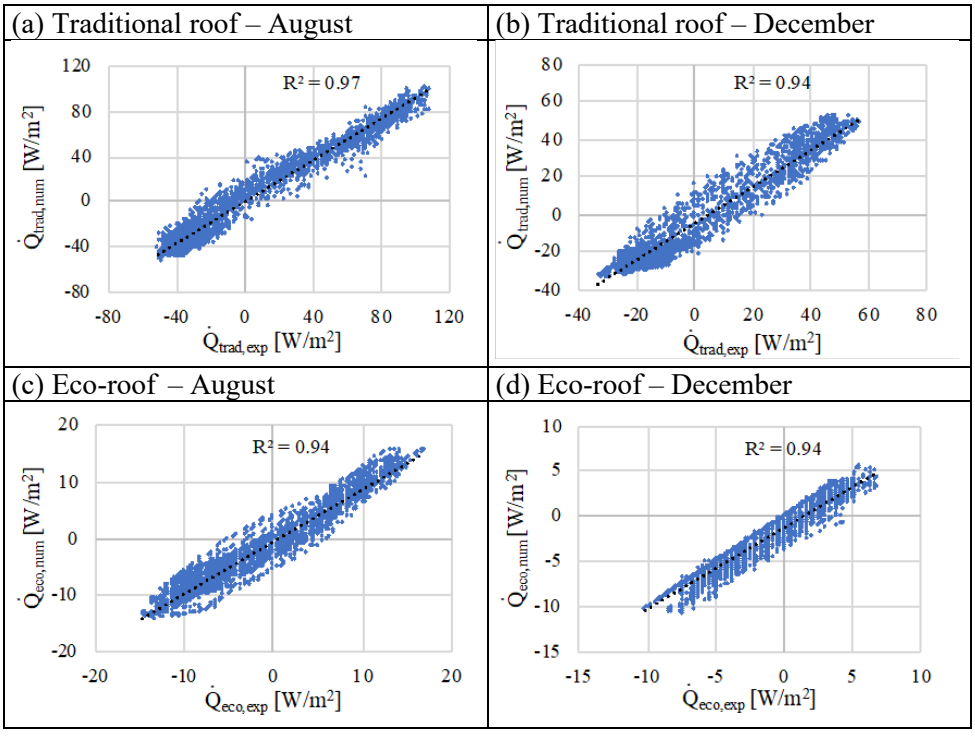

Fig. 2. Calibration of models of the traditional gravel ballasted roof in (a) August and (b) December, and the eco-roof in (c) August and (d) December.

Weekly evapotranspiration analysis

A weekly analysis of the effects of climatic conditions and the VWC of the substrate on the ET of the eco-roof was carried out. Two typical weeks for the

climatic conditions of Córdoba were selected for this study: a summer week from 15/08/2015 to 21/08/2015, where the eco-roof was provided with the irrigation strategy $C3_{20}$ and a winter week from 02/01/2015 to 08/01/2015 with no irrigation schedule, C0, see Table 5.

Effect of climatic variables on evapotranspiration

The effects of the climatic variables on the ET were analysed for the two selected weeks. The climatic variables used were outdoor air temperature, T_o, solar radiation, SR, wind speed, WS, and outdoor relative humidity, RH_o. The results of this analysis are shown in Fig. 3. It can be observed that the trends obtained of the climatic variables on ET were similar for both weeks, although different slopes were obtained. The ET values increased when the values of T_o, WS and SR rose, see Fig. 3a, Fig. 3c and Fig. 3d, respectively. However, the ET values increased when the RH_o values decreased, see Fig. 3b. In previous studies of the effects of climatic conditions on ET, similar trends were obtained (Cascone et al., 2019; FAO, 2006).

For the summer week, the ET values were usually higher than those during the winter week, see Fig. 3, mainly due to the high values of T_o and SR and low values of RH_o achieved with respect to those during the winter week. For the winter week, almost all the ET values were lower than 0.05 mm/h.

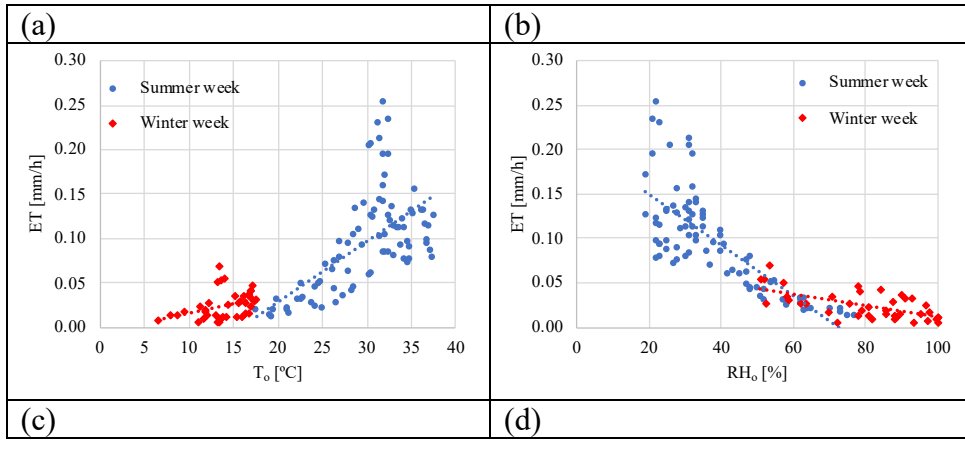

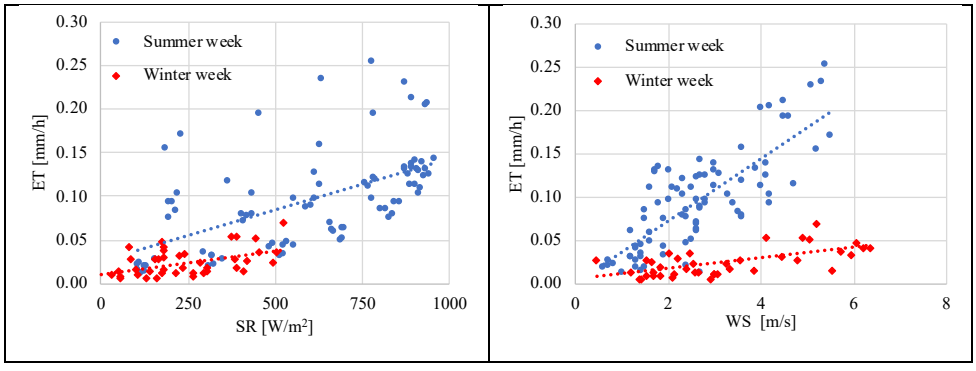

Fig. 3. Effect of climatic conditions (a) T_o; (b) RH_o; (c) SR; (d) WS, on ET.

Effect of volumetric water content of the substrate on evapotranspiration

An analysis of the effects of VWC on ET for all the irrigation strategies was carried out for the two weeks studied. The average weekly results of VWC with respect to ET are represented in Fig. 4. For the summer week, it can be observed that ET values increased when the weekly average of VWC increased. The highest average ET values were obtained for the irrigation strategies $C1_{60}$ and $C1_{80}$, 0.379 mm/h and 0.390 mm/h, with an average VWC value of 36.6% for both cases, see Fig. 4. The lowest average ET values were obtained for the irrigation strategies C0 and $C3_{20}$, 0.008 mm/h and 0.04 mm/h, with average VWC values of 4.0% and 10.0%, respectively. Thus, it can be said that the weekly average VWC value of the substrate had a significant impact on ET during the summer week.

For the winter week, the highest average ET values were achieved for the irrigation strategies $C1_{40}$ to $C5_{80}$, see Fig. 4. The case C0, which had no irrigation schedule, achieved the lowest value of ET, 0.008 mm/h, with an average VWC value of 15.7%. The average VWC value for C0 depended on the rain during this winter week. The results obtained for the winter week showed that average ET values did not have a significant variation when average VWC and irrigation strategy were modified.

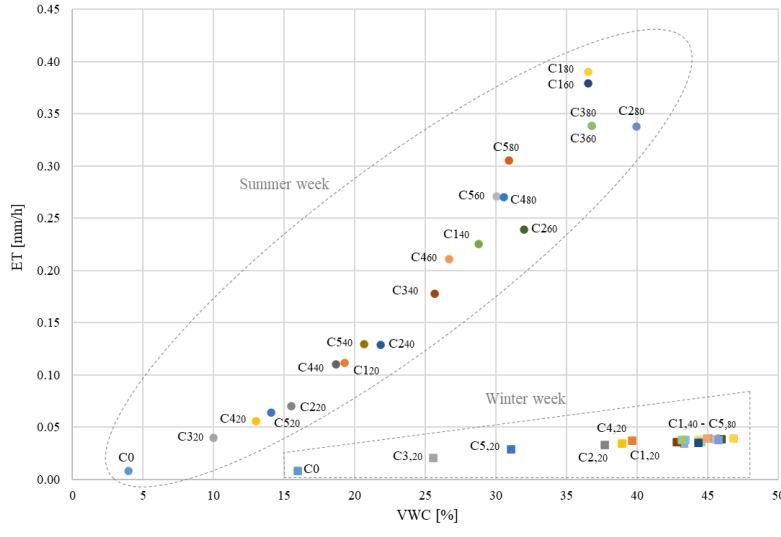

Fig. 4. Average weekly results of ET and VWC of the substrate.

Weekly energy analysis

A weekly study of the average heat fluxes, $\dot{Q}$, average evapotranspiration, ET, and irrigation strategies of the eco-roof was performed for the typical summer week selected, from 15/08/2015 to 21/08/2015. However, this analysis was not carried out for the winter week selected, because the ET values did not vary significantly with respect to the different irrigation strategies, as shown in section 3.2.2.

Effect of evapotranspiration on heat flux

The results of the relationship between average heat fluxes, $\dot{Q}$, and average evapotranspiration, ET, under the irrigation strategies are shown in Fig. 5. The $\dot{Q}$ values represented were the average positive heat flux values, energy flux gains. It can be observed that the average $\dot{Q}$ values were reduced when average ET values increased. This trend was opposite to the relationship between VWC on ET, as shown in Fig. 4. The lowest average $\dot{Q}$ values were achieved for $C1_{60}$ and $C1_{80}$, 6.5 W/m^2 and 6.4 W/m^2, coinciding with the highest ET values, 0.379 mm/h and 0.39

mm/h, respectively, see Fig. 5. The highest average $\dot{Q}$ values for the cases with an irrigation strategy, were achieved by $C3_{20}$ and $C4_{20}$, 29.7 W/m^2 and 29.3 W/m^2, respectively. For C0, an average $\dot{Q}$ value of 31.4 W/m^2 and an ET value close to zero were obtained, due to the absence of irrigation. The results showed that if a significant reduction of $\dot{Q}$ is required, high ET values are needed, i.e. irrigation strategies with a high quantity and frequency of water application should be used.

For the selected summer week, the $\dot{Q}$ value of the traditional gravel ballasted roof was 52.3 W/m^2, 40% more than the $\dot{Q}$ value of the eco-roof rate with no irrigation strategy, C0. The use of an irrigation strategy for the eco-roof allowed a significant reduction of the average $\dot{Q}$ value, up to 87.7% for the strategy $C1_{80}$ with respect to the traditional gravel ballasted roof. Therefore, an eco-roof provided with an optimized irrigation strategy could be used to to reduce the heat transfer through the roof assembly of a building.

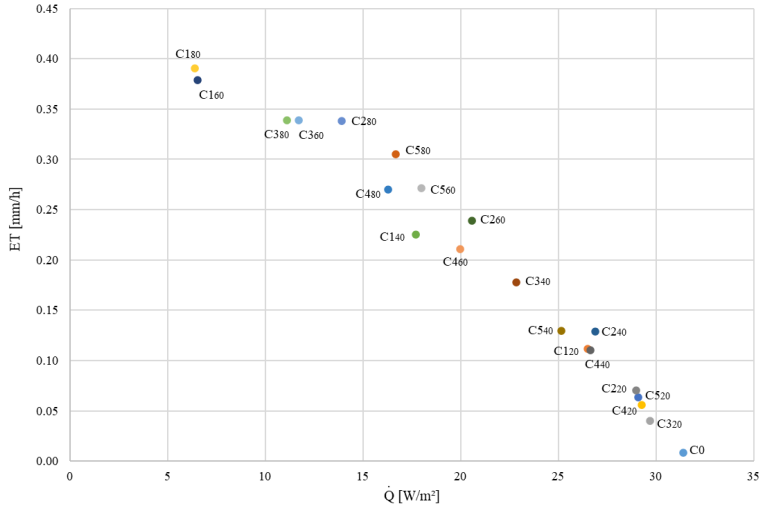

Fig. 5. Average weekly results of ET and $\dot{Q}$ for a typical summer week.

Effect of irrigation on weekly energy

The relationship between irrigation and Q for the different case studies is shown in Fig. 6. Comparing the irrigation strategies with the same quantity of water and different watering schedule, the results showed that for the case studies $C1_{20}$ to $C5_{20}$, the Q values obtained, from lowest to highest, were: $C1_{20}$, 1829.1 W·h/m^2;

$C2_{20}$, 2151.9 W·h/m^2; $C5_{20}$, 2153.9 W·h/m^2; $C4_{20}$, 2195.9 W·h/m^2, and $C3_{20}$, 2230.5 W·h/m^2, see Fig. 6. Therefore, for these case studies, the irrigation during the morning allowed the greatest reduction of Q to be obtained, as the highest values of ET and VWC were achieved during the morning, see Fig. 5 and Fig. 4. However, the lowest reduction of Q was obtained watering twice a day with the irrigation quantity divided between morning and evening, $C3_{20}$.

For the irrigation strategies $C1_{40}$ to $C5_{40}$, the Q values from lowest to highest were: $C1_{40}$, 1043.8 W·h/m^2; $C3_{40}$, 1440.0 W·h/m^2; $C5_{40}$, 1711.3 W·h/m^2; $C2_{40}$, 1828.2 W·h/m^2, and $C4_{40}$, 1838.1 W·h/m^2, see Fig. 6. Hence, the lowest value of Q was obtained by irrigating during the morning, while the highest was by irrigating at 1pm. These results agreed with the previous ET analysis, see Fig. 5.

Among the cases $C1_{60}$ to $C5_{60}$, the irrigation strategies with Q values from lowest to highest were: $C1_{60}$, 189.1 W·h/m^2; $C3_{60}$, 504.1 W·h/m^2; $C5_{60}$, 882.0 W·h/m^2; $C4_{60}$, 1198.0 W·h/m^2; $C2_{60}$, 1235.1 W·h/m^2, see Fig. 6. Therefore, the highest and lowest values of $\dot{Q}$ were achieved by watering during the morning, at 8:30 am, and during the night, at 1:00 pm, respectively.

Finally, for the cases $C1_{80}$ to $C5_{80}$, the irrigation strategies with Q values from lowest to highest were: $C1_{80}$, 168.5 W·h/m^2; $C3_{80}$, 454.7 W·h/m^2; $C2_{80}$, 695.1 W·h/m^2; $C5_{80}$, 750.9 W·h/m^2; $C4_{80}$, 878.8 W·h/m^2, see Fig. 6.

Comparing the irrigation strategies with the same watering schedule and different quantities of water, the results showed that Q value reduced as the quantity of water increased. For the cases C1, with irrigation at 8:30 am, $C1_{40}$ achieved a Q value 42.9% lower than $C1_{20}$, while $C1_{60}$ achieved a Q value 81.8% lower than $C1_{40}$. However, $C1_{80}$ presented a slight reduction in Q compared to $C1_{60}$, 10.8%. Therefore, the cases C1 followed an asymptotic trend.

Regarding cases C2, with irrigation at 8:30 pm. $C2_{40}$ achieved a Q value 15.0% lower than $C2_{20}$, while $C2_{60}$ achieved a Q value 32.4% lower than $C2_{40}$. Finally, $C2_{80}$ reduced the $\dot{Q}$ value 56.2% with respect to $C2_{60}$. It can be observed that the Q results for the cases C2 presented a decreasing linear trend.

For the cases C3, strategies with irrigation twice a day, $C3_{40}$ obtained a Q value 32.4% lower than $C3_{20}$, $C3_{60}$ obtained a Q value 65.0% lower than $C3_{40}$ and, $C3_{80}$ achieve a slight reduction in Q compared to $C3_{60}$, 9.8%. Therefore, the cases C3 also followed an asymptotic trend, as in cases C1.

For the cases C4, with the irrigation schedule at 1:00 pm, the Q value of $C4_{40}$ was 16.3% lower than $C4_{20}$, the Q value of $C4_{60}$ was 34.8% lower than $C4_{40}$, and finally, the Q value of $C4_{80}$ was 26.7% lower than $C4_{60}$.

Regarding cases C5, the strategies with irrigation on alternate days, it can be observed that $C5_{40}$ achieved 20.5% of Q values lower than $C5_{20}$, $C5_{60}$ achieved 48.4% of Q values lower than $C5_{40}$ and, finally, $C5_{80}$ obtained 14.8% of Q values lower than $C5_{60}$. Therefore, the results of the cases C5 presented a decreasing linear trend, with low reduction of Q values when the watering increased.

These results showed that the greatest reduction in Q was obtained for the strategies with irrigation once a day in the morning, at 8:30 am. In addition, the greater the irrigation of water, the greater the reduction of Q. In any case, it is important to stress that even with the same overall quantity of water, important differences in Q can be obtained, simply by changing the irrigation management. This implies that even under the same water use, it is important to optimize irrigation scheduling.

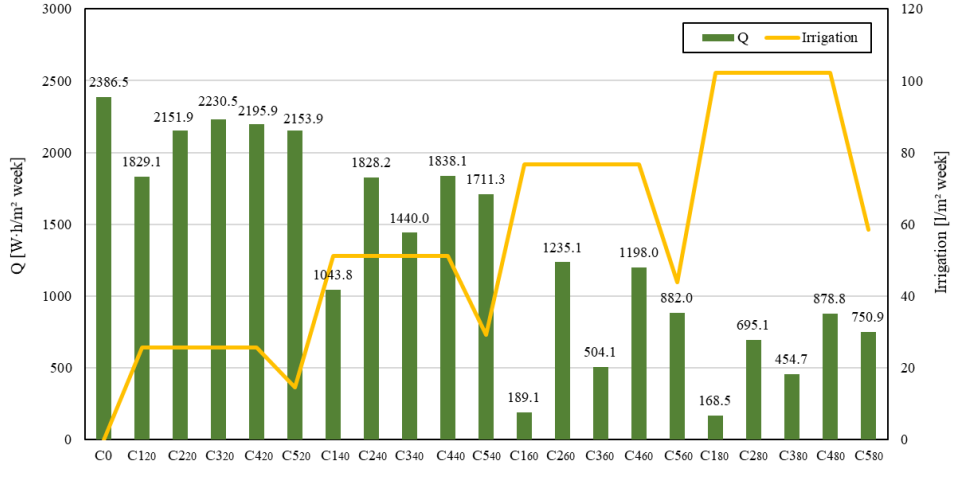

Fig. 6. Relationship between Q and irrigation for a typical summer week.

The reduction of Q due to the irrigation strategies, led to weekly reduction of energy demand, ED_w, in the studied building. The ED_w results of the eco-roof compared to the gravel ballasted roof for the selected summer week, are shown in Fig. 7. ED_w was calculated by Eq. (5). The results showed that the ED_w values were always higher than 40% for all the case studies, even for C0 that had no irrigation

schedule. Therefore, the eco-roof had a higher thermal insulation than the considered traditional gravel ballasted roof.

Comparing the irrigation strategies with the same watering schedule and different amount of water, it can be observed that watering in the morning, cases C1, always allowed higher ED_w values than those obtained at other schedules to be achieved. The highest ED_w value was achieved with $C1_{80}$, 87.8%. Nevertheless, there was no substantial improvement of the ED_w value between 60 min and 80 min of irrigation, a difference of 0.3%. Therefore, these results suggest that the irrigation strategy C1 allows the maximum ED_w values to be obtained for the week of August studied.

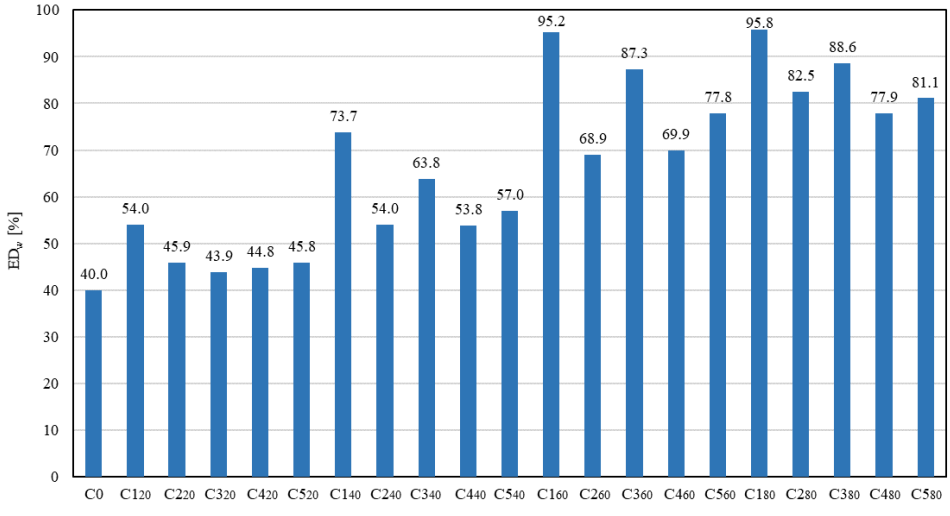

Fig. 7. Weekly results of the reduction of energy demand.

Annual energy analysis

An annual analysis of the reduction of energy demand, ED_y, and performance, P_{eco}, of the eco-roof for all the irrigation strategies was carried out. This analysis was performed from 01/01/2015 to 31/12/2015. The irrigation strategies were planned from 01/05/2015 to 31/10/2015.

The annual results of ED_y and the amount of irrigation and drained water are shown in Fig. 8. It can be observed that all the case studies achieved ED_y values higher than 43%. The strategy that achieved the highest ED_y value was $C1_{80}$, 78.7%, with 2660 l/m^2 of annual irrigation water, see Fig. 8. However, this strategy also

presented a significant annual drainage value, 191 l/m^2, so 7.2 % of water was not used to reduce the heat flux of the roof. The strategy $C1_{60}$ also achieved a high annual ED_y value, 76.6%, even with a lower amount of annual irrigation water, 1995 l/m^2, and lower annual drainage, 159 l/m^2, than those of $C1_{80}$. A significant annual ED_y value was obtained with the strategy $C1_{40}$, 62.8%. The amount of annual irrigation water used for $C1_{40}$ was 1330 l/m^2, 50% and 33.3% less than the amount of annual water used for $C1_{80}$ and $C1_{60}$, respectively. Furthermore, a low annual drainage value was found for $C1_{40}$, a 5% of irrigation water was drained. The case C0, that had no irrigation schedule, also achieved a significant annual ED value, 43.3%, due to the insulation effect of the substrate, see Fig. 8.

Therefore, it can be said that the installation of an eco-roof significantly improved the thermal performance of the building compared to a traditional gravel ballasted roof, achieving a high percentage of ED_y. In addition, adequate irrigation strategies allowed a further increase of this ED, up to 78.7% for $C1_{80}$.

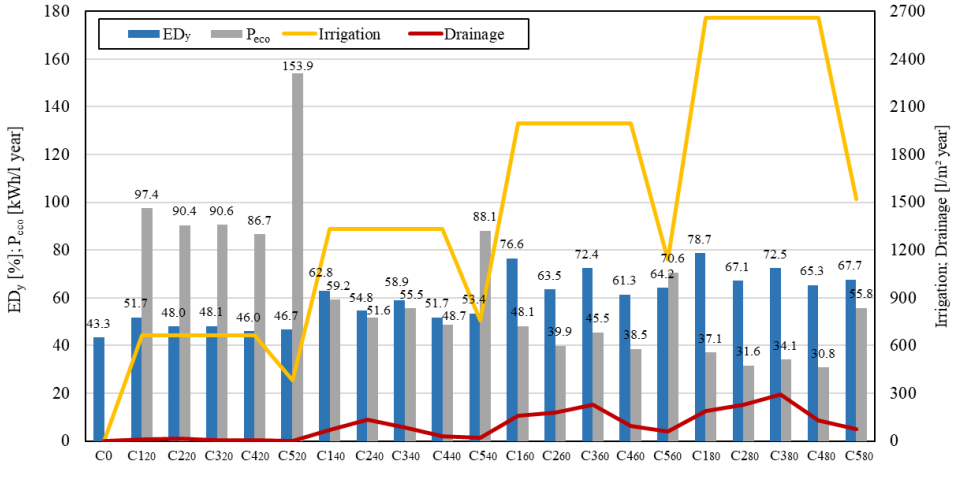

Fig. 8. Annual results of the reduction of energy demand, P_{eco}, irrigation and drainage.

The annual Peco results are also shown in Fig. 8. This parameter was used to evaluate the irrigation strategies that had the highest reduction of energy demand with respect to the lowest quantity of irrigation water, expressed by Eq. (6). It can be observed that the strategy with the highest P_{eco} value was $C5_{20}$, 153.9 [kWh/l year], mainly due to the low quantity of irrigation water, 380 l/m^2, see Fig. 8. $C5_{20}$ also presented the lowest annual drainage, only 1 l/m^2. Among the cases with the same irrigation schedule, the highest P_{eco} values were always found for C5, the

strategies with irrigation in alternate days. For the remaining cases with the same irrigation schedule, the highest P_{eco} values were obtained for C1, the cases with irrigation once a day at 9:00 am, as shown in Fig. 8, due to the high reduction of energy demand achieved with the eco-roof with respect to the traditional roof. The lowest P_{eco} values were found for C4, the cases with irrigation once a day at 1:00 pm.

Therefore, in the present work, an irrigation strategy on alternate days watering for 20 min in the morning, allowed an ED_y value up to 46.7 % with respect to the traditional gravel ballasted roof, and with a low waste of irrigation water to be achieved.

4. CONCLUSIONS

In this work, an analysis of the thermal performance of an eco-roof under 20 different irrigation strategies, compared to a traditional gravel ballasted roof, was carried out. Hence, a building model with two different roofs, an eco-roof and a traditional gravel ballasted roof, was calibrated with experimental data of heat flux. The study was performed during the year 2015 for the climatic conditions of Córdoba (Spain). An analysis based on evapotranspiration, ET, volumetric water content of the substrate, VWC, heat flux, $\dot{Q}$, and energy demand, ED, was performed.

The weekly results showed that the ET values increased when the values of outdoor air temperature, wind speed and solar radiation rose, and outdoor air relative humidity values decreased. The VWC value of the substrate also had a significant impact on ET during the summer, such that the higher the VWC, the higher the ET. The highest average ET values for the summer were obtained for the strategies with irrigation once a day at 8:30 am for 60 min and 80 min. The results obtained for the winter showed that average ET values did not have a significant variation when the VWC and irrigation strategy were modified.

ET had a great impact on the reduction of $\dot{Q}$ of the eco-roof, since the weekly $\dot{Q}$ values were reduced when weekly ET values increased. The lowest weekly $\dot{Q}$ values were achieved for the strategies with irrigation once a day at 8:30 am for 60 min and 80 min, coinciding with the highest weekly ET. The greatest reduction of weekly $\dot{Q}$ were always achieved by watering every day during the morning.

The annual results showed that the installation of the eco-roof significantly improved the thermal performance of the building compared to the traditional gravel ballasted roof, achieving a high percentage of ED, 43.3% for the case without irrigation. Moreover, the irrigation strategies further increased the ED values, up to 78.7% for the strategies with irrigation once a day at 8:30 am for 80 min. However, for this irrigation strategy, a percentage of water used for irrigation was drained, so this did not contribute to further reduce $\dot{Q}$ of the eco-roof. The strategy that had the highest reduction of energy demand with respect to the highest usage of irrigation water was the irrigation strategy on alternate days watering 20 min, achieving an ED value up to 46.7 %, with low waste of irrigation water.

These results strengthen the performance analysis of eco-roofs with a proper irrigation strategy, as well as their use as an interesting passive system for the rehabilitation of old buildings.

Acknowledgements

The climate data were obtained from the Agroclimatic network of Andalusia ("Red de Información Agroclimática de Andalucía") and were kindly provided by the Instituto de Investigación y Formación Agraria y Pesquera of the Consejería de Agricultura, Ganadería, Pesca y Desarrollo of the Junta de Andalucía.

The authors would like to express appreciation for the financial support of the European Regional Development Fund (ERDF) through the project GGI3003IDIB "Optimizing the potential of green roofs for building retrofit: interaction between recycled substrates, water properties and energy efficiency", by the Agency of Public Works of Andalucía, Junta de Andalucía, Spain.

REFERENCES

Akbari, H., Cartalis, C., & Muscio, A. (2015). Local climate change and urban heat island mitigation techniques – the state of the art. Journal of Civil Engineering and Management, 22(1), 1–16. https://doi.org/10.3846/13923730.2015.1111934

Azeñas, V., Cuxart, J., Picos, R., Medrano, H., Simó, G., López-Grifol, A., & Gulías, J. (2018). Thermal regulation capacity of a green roof system in the mediterranean region: The effects of vegetation and irrigation level. Energy and Buildings, 164, 226–238. https://doi.org/10.1016/j.enbuild.2018.01.010

Bandara, A. G. N., Balasooriya, B. M. A. N., Bandara, H. G. I. W., & Buddhasiri, K. S.

(2016). Smart Irrigation Controlling System for Green Roofs Based on Predicted Evapotranspiration. 1st International Conference - EECon 2016: 2016 Electrical Engineering Conference, 31–36.

Besir, A. B., & Cuce, E. (2018). Green roofs and facades: A comprehensive review. Renewable and Sustainable Energy Reviews, 82(September), 915–939. https://doi.org/10.1016/j.rser.2017.09.106

Bevilacqua, P., Mazzeo, D., Bruno, R., & Arcuri, N. (2016). Experimental investigation of the thermal performances of an extensive green roof in the Mediterranean area. Energy and Buildings, 122, 63–69. https://doi.org/10.1016/j.enbuild.2016.03.062

Cascone, S. (2019). Green roof design: State of the art on technology and materials. Sustainability, 11(11). https://doi.org/10.3390/su11113020

Cascone, S., Catania, F., Gagliano, A., & Sciuto, G. (2018). A comprehensive study on green roof performance for retrofitting existing buildings. Building and Environment, 136, 227–239. https://doi.org/10.1016/j.buildenv.2018.03.052

Cascone, S., Coma, J., Gagliano, A., & Pérez, G. (2019). The evapotranspiration process in green roofs: A review. Building and Environment, 147, 337–355. https://doi.org/10.1016/j.buildenv.2018.10.024

Coutts, A. M., Daly, E., Beringer, J., & Tapper, N. J. (2013). Assessing practical measures to reduce urban heat: Green and cool roofs. Building and Environment, 70, 266–276. https://doi.org/10.1016/j.buildenv.2013.08.021

Daly, D., Cooper, P., & Ma, Z. (2014). Implications of global warming for commercial building retrofitting in Australian cities. Building and Environment, 74, 86–95. https://doi.org/10.1016/j.buildenv.2014.01.008

DesignBuilder. (2014). https://doi.org/Available from: https://designbuilder.co.uk

Djedjig, R., Bozonnet, E., & Belarbi, R. (2015). Analysis of thermal effects of vegetated envelopes: Integration of a validated model in a building energy simulation program. Energy and Buildings, 86, 93–103. https://doi.org/10.1016/j.enbuild.2014.09.057

Dutil, Y., Rousse, D., & Quesada, G. (2011). Sustainable buildings: An ever evolving target. Sustainability, 3(2), 443–464. https://doi.org/10.3390/su3020443

EnergyPlus. (2014). US Department of Energy. https://doi.org/Available from: https://energyplus.net

European Parliament. European Directive 2010/31/EU on the Energy Performance of Buildings, Official Journal of the European Union § (2010). https://doi.org/doi:10.3000/17252555.L_2010.153.eng

European Union. (2012). Directive 2012/27/EU - “Energy Efficiency Directive.” Official Journal of the European Union.

FAO. (2006). Evapotranspiración del cultivo Guías para la determinación de los requerimientos de agua de los cultivos. Estudio Fao Riego Y Drenaje. https://doi.org/M-56

Frankenstein, S., & Koenig, G. (2004a). ERDC / CRREL TR-04-25 FASST Vegetation

Models Cold Regions Research and Engineering Laboratory, (December).
Frankenstein, S., & Koenig, G. G. (2004b). Fast All-season Soil STrength (FASST) Cold Regions Research, (September).
Gagliano, A., Poli, T., & Sciuto, G. (2019). Thermal performance assessment of extensive green roofs investigating realistic vegetation-substrate configurations. Building Simulation, 379–393.
Gomes, M. G., Silva, C. M., Valadas, A. S., & Silva, M. (2019). Impact of vegetation, substrate, and irrigation on the energy performance of green roofs in a Mediterranean climate. Water, 11(10). https://doi.org/10.3390/w11102016
Goussous, J., Siam, H., & Alzoubi, H. (2015). Prospects of green roof technology for energy and thermal benefits in buildings: Case of Jordan. Sustainable Cities and Society, 14(1), 425–440. https://doi.org/10.1016/j.scs.2014.05.012
He, Y., Yu, H., Ozaki, A., Dong, N., & Zheng, S. (2017). Influence of plant and soil layer on energy balance and thermal performance of green roof system. Energy and Buildings, 141.
Heusinger, J., Sailor, D. J., & Weber, S. (n.d.). Modeling the reduction of urban excess heat by green roofs with respect to different irrigation scenarios. Building and Environment, 131(October 2017), 174–183. https://doi.org/10.1016/j.buildenv.2018.01.003
Jim, C. Y., & Peng, L. L. H. (2012). Substrate moisture effect on water balance and thermal regime of a tropical extensive green roof. Ecological Engineering, 47, 9–23. https://doi.org/10.1016/j.ecoleng.2012.06.020
Kaiser, D., Köhler, M., Schmidt, M., & Wolff, F. (2019). Increasing Evapotranspiration on Extensive Green Roofs by Changing Substrate Depths, Construction, and Additional Irrigation. Buildings, 9(7), 173. https://doi.org/10.3390/buildings9070173
Kemp, S., Hadley, P., & Blanuša, T. (2019). The influence of plant type on green roof rainfall retention. Urban Ecosystems, 22(2), 355–366. https://doi.org/10.1007/s11252-018-0822-2
Kottek, M., Grieser, J., Beck, C., Rudolf, B., & Rubel, F. (2006). World Map of the Köppen-Geiger climate classification updated. Meteorologische Zeitschrift, 15(3), 259–263. https://doi.org/10.1127/0941-2948/2006/0130
Lee, L. S. H., & Jim, C. Y. (2018). Thermal-cooling performance of subtropical green roof with deep substrate and woodland vegetation. Ecological Engineering, (April).
Li, W. C., & Yeung, K. K. A. (2014). A comprehensive study of green roof performance from environmental perspective. International Journal of Sustainable Built Environment, 3(1), 127–134. https://doi.org/10.1016/j.ijsbe.2014.05.001
Lin, Y., & Lin, H. (2011). Thermal performance of different planting substrates and irrigation frequencies in extensive tropical rooftop greeneries. Building and Environment, 46(2), 345–355. https://doi.org/10.1016/j.buildenv.2010.07.027
Mahdiyar, A., Tabatabaee, S., Abdullah, A., & Marto, A. (2018). Identifying and assessing

the critical criteria affecting decision-making for green roof type selection. Sustainable Cities and Society, 39(March), 772–783. https://doi.org/10.1016/j.scs.2018.03.007

Mechelen, C. Van, Dutoit, T., & Hermy, M. (2015). Adapting green roof irrigation practices for a sustainable future : A review. Sustainable Cities and Society, 19, 74–90. https://doi.org/10.1016/j.scs.2015.07.007

Myers, G. E. (1980). Long-Time solutions to heat- conduction transients with time-dependent inputs. Journal of Heat Transfer, 102(1), 115–120. https://doi.org/10.1115/1.3244221

Naranjo, A., Mesa, J., & Maury, H. (2020). State-of-the-Art Green Roofs : Technical Performance. Coatings, 1–14. https://doi.org/10.3390/coatings10010069

Porcaro, M., Ruiz de Adana, M., Comino, F., Peña, A., Martín-Consuegra, E., & Vanwalleghem, T. (2019). Long term experimental analysis of thermal performance of extensive green roofs with different substrates in Mediterranean climate. Energy and Buildings, 197, 18–33. https://doi.org/10.1016/j.enbuild.2019.05.041

Qin, H., Peng, Y., Tang, Q., & Yu, S. (2016). A HYDRUS model for irrigation management of green roofs with a water storage layer. Ecological Engineering, 95, 399–408. https://doi.org/10.1016/j.ecoleng.2016.06.077

Ran, J., & Tang, M. (2018). Passive cooling of the green roofs combined with night-time ventilation and walls insulation in hot and humid regions. Sustainable Cities and Society, 38(August 2017), 466–475. https://doi.org/10.1016/j.scs.2018.01.027

Saadatian, O., Sopian, K., Salleh, E., Lim, C. H., Riffat, S., Saadatian, E., … Sulaiman, M. Y. (2013). A review of energy aspects of green roofs. Renewable and Sustainable Energy Reviews, 23, 155–168. https://doi.org/10.1016/j.rser.2013.02.022

Sailor, D. J. (2008). A green roof model for building energy simulation programs. Energy and Buildings, 40, 1466–1478. https://doi.org/10.1016/j.enbuild.2008.02.001

Santamouris, M. (n.d.). Cooling the cities - A review of reflective and green roof mitigation technologies to fight heat island and improve comfort in urban environments. Solar Energy, 103, 682–703. https://doi.org/10.1016/j.solener.2012.07.003

Seem, J. E. (1987). Modeling of Heat Transfer in Buildings ". Ph.D. Thesis , University of Wisconsin. Ph.D. Thesis , University of Wisconsin.

Shafique, M., Kim, R., & Rafiq, M. (2018). Green roof benefits, opportunities and challenges – A review. Renewable and Sustainable Energy Reviews, 90, 757–773. https://doi.org/10.1016/j.rser.2018.04.006

Speak, A. F., Rothwell, J. J., Lindley, S. J., & Smith, C. L. (2013). Reduction of the urban cooling effects of an intensive green roof due to vegetation damage. Urban Climate, 3, 40–55. https://doi.org/10.1016/j.uclim.2013.01.001

Susca, T. (2019). Green roofs to reduce building energy use? A review on key structural factors of green roofs and their effects on urban climate. Building and Environment, 162(June). https://doi.org/10.1016/j.buildenv.2019.106273

Tan, C. L., Tan, P. Y., Wong, N. H., Takasuna, H., Kudo, T., Takemasa, Y., … Chua, H. X. V. (2017). Impact of soil and water retention characteristics on green roof thermal performance. Energy and Buildings, 152, 830–842. https://doi.org/10.1016/j.enbuild.2017.01.011

Vaz Monteiro, M., Blanuša, T., Verhoef, A., Richardson, M., Hadley, P., & Cameron, R. W. F. (2017). Functional green roofs: Importance of plant choice in maximising summertime environmental cooling and substrate insulation potential. Energy and Buildings, 141, 56–68. https://doi.org/10.1016/j.enbuild.2017.02.011

Vijayaraghavan, K., Reddy, D. H. K., & Yun, Y. S. (2019). Improving the quality of runoff from green roofs through synergistic biosorption and phytoremediation techniques: A review. Sustainable Cities and Society, 46, 101381. https://doi.org/10.1016/j.scs.2018.12.009

Yang, W., Wang, Z., Cui, J., Zhu, Z., & Zhao, X. (2015). Comparative study of the thermal performance of the novel green(planting) roofs against other existing roofs. Sustainable Cities and Society, 16(C), 1–12. https://doi.org/10.1016/j.scs.2015.01.002

Zhang, G., He, B. J., & Dewancker, B. J. (2020). The maintenance of prefabricated green roofs for preserving cooling performance: A field measurement in the subtropical city of Hangzhou, China. Sustainable Cities and Society, 61(June), 102314. https://doi.org/10.1016/j.scs.2020.102314

Ziogou, I., Michopoulos, A., Voulgari, V., & Zachariadis, T. (2018). Implementation of green roof technology in residential buildings and neighborhoods of Cyprus. Sustainable Cities and Society, 40(March), 233–243. https://doi.org/10.1016/j.scs.2018.04.007

Appendix C

Capacidad de reducción de la temperatura del forjado de un edificio con una cubierta verde

The paper presented in this appendix is published in the *VII CONGRESO CIENTÍFICO DE INVESTIGADORES EN FORMACIÓN*, Cordoba, Spain, 2019: pp. 677-680.

Capacidad de reducción de la temperatura del forjado de un edificio con una cubierta verde

Manuela Porcaro, Manuel Ruiz de Adana

Universidad de Córdoba. Escuela Politécnica Superior de Córdoba. Departamento de Química Física y Termodinámica Aplicada. E-mail: manuela.porcaro12@gmail.com

Summary

Passive construction systems, such as the green roofs, contribute to achieve the goal of nearly zero energy buildings, nZEB. The main objective of this work was to determine experimentally the reduction of the temperature of the slab of a green roof compared with a traditional roof. Both roofs were installed in an office building of the University of Córdoba (Spain). This study was performed throughout a typical summer week for the climatic conditions of Córdoba.

The results showed significant reductions in the temperature of the slab of the green roof, with a maximum difference of 17.1 °C compared to the traditional roof, due to the capacity of the substrate to retain water. This study indicates that, a green roof allows to achieve important energy savings in buildings for hot climatic conditions of Southern Europe.

Resumen

Los sistemas de construcción pasivos, como las cubiertas verdes, contribuyen a alcanzar edificios de energía casi nula, nZEB. El principal objetivo de este trabajo fue determinar experimentalmente la reducción de temperatura del forjado de una cubierta verde frente al de una cubierta tradicional. Ambas cubiertas fueron instaladas en un edificio de oficinas en la Universidad de Córdoba (España). Este estudio fue realizado a lo largo de una semana típica de verano para las condiciones climáticas de Córdoba.

Los resultados mostraron reducciones significativas de la temperatura del forjado de la cubierta verde, con una diferencia máxima de 17,1 °C respecto a la cubierta tradicional, debido a la capacidad del substrato de retener agua. Este estudio indica que, una cubierta verde permite alcanzar importantes ahorros energéticos en los edificios para condiciones climáticas cálidas del sur de Europa.

Introducción

En Europa el 40% de energía se utiliza en el sector terciario y residencial. Las directivas europeas sobre el ahorro energetico refuerzan el objetivo de reducir los consumos energéticos en los edificios e introducen el concepto de edificios de energía casi nula (nZEB). Para alcanzar los objetivos marcados en los nZEB es necesario utilizar técnicas constructivas pasivas combinadas con instalaciones que utilizan energías renovables [1,2]. Unos de los sistemas pasivos utilizables es una cubierta verde extensiva, la cual tiene muchas ventajas en términos de retención de lluvia, reducción del efecto de isla de calor urbana, absorción de CO_2 y capacidad de aislamiento térmico [3,4]. En recientes estudios se ha evaluado el comportamiento de cubiertas verdes a través de parámetros dinámicos, como por ejemplo la capacidad de enfriamiento de las cubiertas verdes, la cual está directamente relacionada a la mitigación del efecto de isla de calor urbana [5,6]. Habitualmente las cubiertas verdes se instalan en lugares con climas fríos y lluviosos. Resultaría interesante estudiar el comportamiento de una cubierta verde instalada en climas del sur de Europa. El principal objetivo de este trabajo fue determinar experimentalmente la reducción de temperatura del forjado de una cubierta verde frente al de una cubierta tradicional, para condiciones climáticas de Córdoba.

Metodología

Una cubierta verde con substrato comercial se instaló en un edificio de oficinas en el campus universitario de Rabanales, Córdoba. La cubierta verde se compuso de diferentes capas, ordenadas de arriba abajo: vegetación mediterránea, medio de cultivo, lamina de filtro, capa de drenaje, barrera anti-raíz, membrana impermeable y capa de hormigón, ver Fig.1. Esta cubierta fue comparada con una cubierta tradicional, compuesta de: capa de grava, membrana impermeable y capa de hormigón. Las condiciones climáticas y las temperaturas de las dos cubiertas estudiadas fueron medidas a través de un sistema de monitorización. En la Tabla 1 se resumen las características de los sensores utilizados para las mediciones. La cubierta verde estudiada fue regada dos veces al día durante todo el periodo analizado.

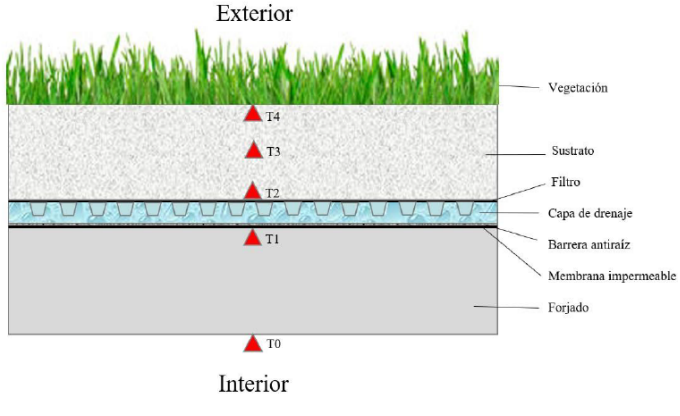

Figura 1. Esquema de las capas que componen la cubierta verde.

Tabla 1. Características de las sondas.

Equipo	Ajuste	Variables
Termistores	±0,6ºC	Temperatura
Reflectómetro de contenido de agua	±2,5%	Contenido de agua
Temperatura de resistencia de platino	0,2ºC	Temperatura del aire
Pluviómetro	98% a 20 mm/h	Precipitaciones

La diferencia de temperaturas entre el forjado de la cubierta tradicional y el forjado de la cubierta verde fue calculada con la Eq. 1.

$$\Delta T = T_{ct,max} - T_{cv,max} \quad (1)$$

Donde $T_{ct,max}$ es la máxima temperatura diaria del forjado de la cubierta tradicional y $T_{cv,max}$ es la máxima temperatura diaria del forjado de la cubierta verde. Ambas cubiertas fueron estudiadas experimentalmente durante una semana típica de verano, del 23 al 29 de julio 2016.

Resultados

Las temperaturas del forjado de la cubierta verde y del forjado de la cubierta tradicional durante la semana estudiada se muestran en la Figura 2. Las temperaturas del forjado de la cubierta verde oscilaron entre 28,0 ºC y 33,2 ºC y las de la cubierta tradicional entre 25,0 ºC y 50,1 ºC.

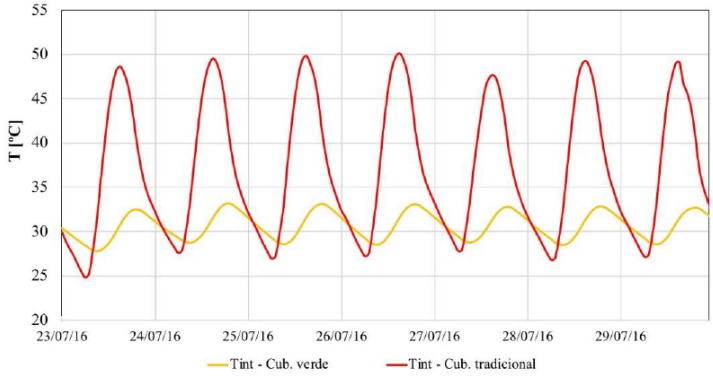

Figura 2. Temperaturas del forjado de la cubierta verde y cubierta tradicional.

Los resultados de la diferencia de temperatura que se alcanzaron en los forjados de las dos cubiertas se muestran el la Figura 3. Se puede observar que la máxima diferencia de temperaturas fue alcanzada para el día 26 de Julio, con un valor de 17,1 ºC. Sin embargo, la mínima diferencia de temperatura fue alcanzada para el día 27 de Julio, con un valor de 14,9 ºC. El valor medio semanal alcanzado fue de 16,3 ºC. Este comportamiento fue debido a la capacidad del substrato de retener agua, la cual permitió mantener constante la temperatura del forjado y disminuir su pico máximo.

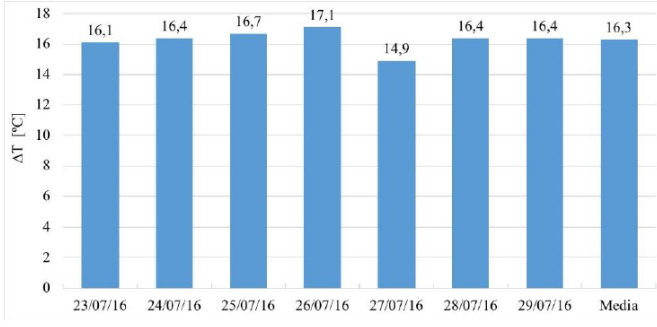

Figura 3. Diferencia de temperatura de los forjados entre la cubierta tradicional y la cubierta verde.

Conclusiones

Del estudio realizado para el objetivo planteado se han obtenido las siguientes conclusiones:

- Con la instalación de una cubierta verde se alcanzó una importante reducción de los picos de temperatura del forjado respecto a una cubierta tradicional, con una diferencia de temperatura máxima de 17,1°C. Este comportamiento fue debido principalmente a la capacidad de retención de agua del substrato.

- La capacidad de reducir la temperatura del forjado de la cubierta verde permite alcanzar significativos ahorros energéticos. Por lo tanto, el uso de un sistema constructivo pasivo como la cubierta verde podría ser uno de los pasos necesarios en la nueva construcción y rehabilitación de edificios para lograr el objetivo nZEB.

Bibliografia

[1] A. de Gracia, L. Navarro, J. Coma, S. Serrano, J. Romaní, G. Pérez, L.F. Cabeza, Experimental set-up for testing active and passive systems for energy savings in buildings – Lessons learnt, Renew. Sustain. Energy Rev. 82 (2018) 1014–1026.
[2] D.H.W. Li, L. Yang, J.C. Lam, Zero energy buildings and sustainable development implications - A review, Energy. 54 (2013) 1–10.
[3] M. Shafique, R. Kim, M. Rafiq, Green roof benefits, opportunities and challenges – A review, Renew. Sustain. Energy Rev. 90 (2018) 757–773.
[4] M. Karteris, I. Theodoridou, G. Mallinis, E. Tsiros, A. Karteris, Towards a green sustainable strategy for Mediterranean cities: Assessing the benefits of large-scale green roofs implementation in Thessaloniki, Northern Greece, using environmental modelling, GIS and very high spatial resolution remote sensing data, Renew. Sustain. Energy Rev. 58 (2016) 510–525.
[5] M. Xiao, Y. Lin, J. Han, G. Zhang, A review of green roof research and development in China, Renew. Sustain. Energy Rev. 40 (2014) 633–648.
[6] G. yu QIU, H. yong LI, Q. tao ZHANG, W. CHEN, X. jian LIANG, X. ze LI, Effects of Evapotranspiration on Mitigation of Urban Temperature by Vegetation and Urban Agriculture, J. Integr. Agric. 12 (2013) 1307–1315.

Appendix D

Cooling potential of green roofs under South European continental climate

The paper presented in this appendix is published in the "XI Congreso Nacional y II Internacional de Ingeniería Termodinámica", Albacete, Spain, 2018.

XI Congreso Nacional y II Internacional
de Ingeniería Termodinámica

11CNIT-XX-2018 FULLPAPER

Cooling potential of green roofs under South European continental climate

Manuela Porcaro[1], Manuel Ruiz de Adana[1], Francisco Comino[1], Adolfo Peña[2], Enriqueta Martín-Consuegra[3], Tom Vanwalleghem[4]

[1] Departamento de Química-Física y Termodinámica Aplicada, Escuela Politécnica Superior, Universidad de Córdoba, Campus de Rabanales, Antigua Carretera Nacional IV, km 396, 14071 Córdoba, Spain.
[2] Área de Ingeniería de Proyecto, Universidad de Córdoba, Campus de Rabanales, Antigua Carretera Nacional IV, km 396, 14071 Córdoba, Spain.
[3] Departamento de Biología Vegetal y Ecología, Div. Botánica, Facultad de Ciencias, Universidad de Córdoba, Campus de Rabanales, Antigua Carretera Nacional IV, km 396, 14071 Córdoba, Spain.
[4] Área de Ingeniería Hidráulica, Universidad de Córdoba, Campus de Rabanales, Antigua Carretera Nacional IV, km 396, 14071 Córdoba, Spain.
*Corresponding author e-mail address: z72popom@uco.es

ABSTRACT

In the scenario of nZEB (nearly zero energy buildings), passive construction techniques of low environmental impact should be used to reduce energy demand. Green roofs can be considered a good strategy to reduce energy demand with many advantages as it requires low maintenance, has good thermal insulation capacity, retain meteoric water and absorbs CO_2.

The main objective of this work was to determine the cooling potential of three green roofs with different substrates. The substrate composition of the three green roofs was different. The green roof 1 was composed of 100% of commercial growing medium; the green roof 2 of 75% of commercial growing medium and 25% of recycled construction materials, and finally, the green roof 3 was composed of 50% of commercial growing medium and 50% of recycled construction materials. Twelve different species were planted in the three green roofs.

The green roofs were installed in an office building of the University of Córdoba. The cooling potential of the three green roofs was obtained from experimentally measured values in each roof for summer climatic conditions of Córdoba, Spain.

The experimental results showed than the green roof 1 achieved the highest cooling potential, with a weekly average value of 16.3 ºC, mainly due to the composition of the substrate, which allowed a higher water retention and higher temperature reduction of the roof. The second roof with the highest cooling potential was the green roof 3, with a weekly average of 15.8 ºC, 3% less than the green roof 1. Finally, the green roof 2 had the lowest cooling potential compared to the rest of green roofs, 15% less than that green roof 1. Therefore, the higher the capacity to retain water in substrate, the higher cooling potential is.

These results suggest that green roofs allow a significant reduction of the slab temperature and the energy demand of a buildings for hot climatic conditions.

Keywords: green roof; cooling potential; recycled materials

1. Introduction

In the last forty years the use of fossil fuels to generate energy has increased exponentially and this has caused serious damage in terms of production of greenhouse gases. A high concentration of greenhouse gases allows solar radiation to pass through the atmosphere, causing an increase in the value of the earth's temperature, which has increased by 2°C since the pre-industrial era. This causes a slow but steady transformation of the earth with consequent extreme weather events.

In Europe, 40% of global final energy consumption is used in the residential and tertiary sector, mainly for buildings. According to the European directives [3,4], starting from 2020 all new buildings and all the existing buildings rehabilitated will have to be nearly zero energy buildings (nZEB) [5,8]. In order to achieve the goal of a nZEB, it is necessary to install active systems that employ renewable energies, use eco-friendly materials and reduce the energy demand of the building using passive constructive systems, such as green roofs.

Green roofs have a lot of environmental advantages, such as they absorb CO_2, minimise the heat island effects in cities, retain rain and ensure less energy losses in winter and less energy gains in summer [13]. There are three types of green roofs: intensive, semi-intensive and extensive, depending on the plant species used and the thickness of layers [6,14].

Some authors studied the performance of extensive green roofs with substrates composed of low cost materials derived from the construction sector [1,9,10], in order to reduce the economic costs of the green roofs. The effect of the amount of water on the substrate has also been previously analysed during warmer periods [2,12], obtaining a reduction of the slab temperature.

Dynamic parameters to study the performance of extensive green roofs have been analysed by other authors. One dynamic parameter is the cooling potential, which is directly related to the mitigation of the effects of urban heat islands [11,15].

The aim of this work was to determine the cooling potential of three green roofs with different substrates composed of different percentages of commercial growing medium and recycled construction materials. Other parameters to evaluate the behaviour of green roofs will also has been studied in other works. The results showed in this study has been carried out during a typical summer week in Córdoba, Spain.

2. Materials and methods

Three plots of extensive green roof, 14.78 m^2 each, were installed in an existing office building in the University of Córdoba, Spain. The terrace of the building with the three plots with green roof and a plot without green roof as reference was represented in Figure 1. The climatic conditions of Córdoba are defined as subtype Csa dry-summer subtropical, according to Köppen-Geiger climate classification [7], with mild winters and very warm summers.

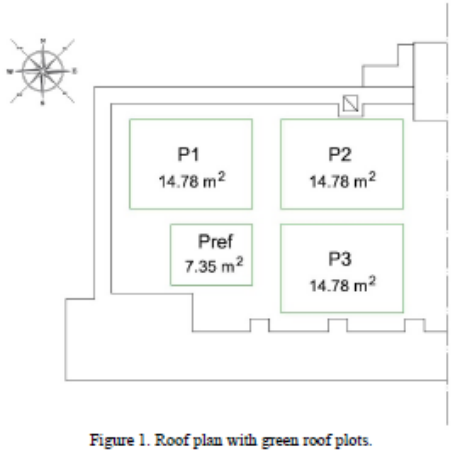

Figure 1. Roof plan with green roof plots.

The three plots with extensive green roof consisted of the following layers, ordered from top to bottom: Mediterranean vegetation, growing medium (0.1 m), filter sheet, a drainage and water storage layer, a root-barrier waterproof layer, water proof membrane and a roof assembly (0.3 m concrete), see Figure 2a. Each parcel had different substrates, with different percentages (by volume) of commercial growing medium and recycled construction materials, see Table 1. Moreover, twelve different species were planted in each parcel. The fractional vegetation coverage, σ_f, and the leaf area index, LAI, for each parcel are also shown in table 1.

The plots with green roof were provided of an irrigation system, which operated twice a day during the selected summer period, 10 minutes each time.

Table 1. Growing media composition of the three green roofs.

	P1	P2	P3
Commercial growing medium	100%	75%	50%
Recycled aggregates construction materials	0%	25%	50%
LAI	2	1.7	1.5
Fractional vegetation coverage, σ_f	0.59	0.56	0.53

The roof installation also included a plot with a traditional gravel ballasted roof, used as reference plot, Pref, that consisted of the following layers, ordered from top to bottom: layer of gravel ballasted (0.03 m), waterproof membrane and roof assembly (0.3 m concrete), see Figure 2b.

In the present work, the ambient air temperature, relative humidity, rainfall, atmospheric pressure, and solar radiation were measured throughout a typical summer week. These meteorological data were monitored by a weather station placed near the experimental installation. In the plots with green roof there were installed five probes of temperature, from $T_{0,Pi}$ to $T_{4,Pi}$, along the vertical profile, and one volumetric water content probe, W_{Pi}, see Figure 2a. In Pref, were also installed three temperature probes, from $T_{0,Pref}$ to $T_{3,Pref}$, along the vertical profile, see Figure 2b.

The technical characteristics of all the probes used in all the plots and used by the weather station are shown in Table 2.

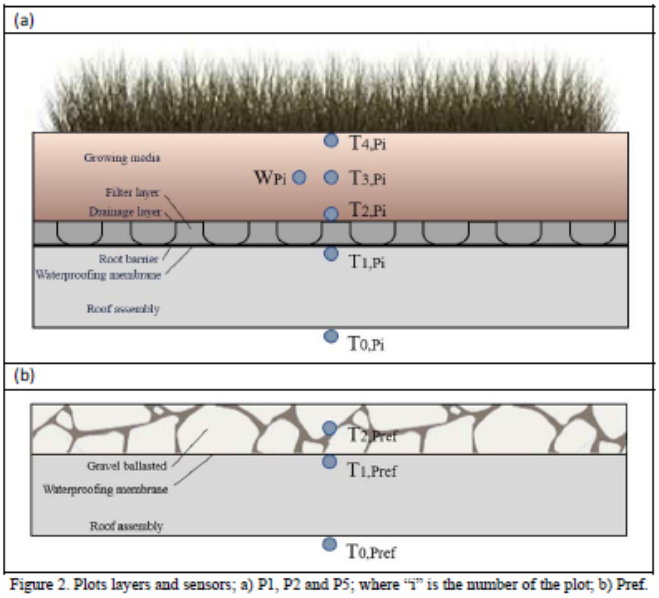

Figure 2. Plots layers and sensors; a) P1, P2 and P5; where "i" is the number of the plot; b) Pref.

Table 2. Variables measured in the experimental installation.

Equipment	Accuracy	Name
Thermistors	±0,6ºC (-50 to 70 ºC) ±0,25ºC (-10 to 70 ºC)	T
Water content reflectometer	±2.5% (0 to 50%)	W
Platinum resistance temperature	0.2ºC (-40 to 70ºC)	Ta
Capacitive relative humidity	2% (0 to 100%)	RH
Silicon photocell solar radiation	5% (350 nm to 1100 nm)	SR
Rain gauge	98% at 20 mm/h	RF

The dynamic parameter used for the analysis the performance of the three green roofs was the cooling potential, CP, calculated with Eq. (1).

$$CP = T_{1,Pref,max} - T_{1,Pi,max} \quad (1)$$

Where $T_{1,Pref,max}$ is the maximum slab temperature value for Pref and $T_{1,Pi,max}$ is the maximum slab temperature value for P1, P2 or P3.

The cooling potential was studied for the three plots with green roofs throughout a typical summer week, from 23/07/2016 to 29/07/2016, in Córdoba.

3. Results

3.1 Climatic conditions measured

The values of external air temperature, relative humidity and rainfall for the summer week studied, are shown in Figure 3. It can be observed that the external air temperature oscillated between 18.9 °C and 39.4 °C and the relative humidity oscillated between 14.5% and 73.7%. It can be also seen that there was absence of rainfall during all the selected summer week.

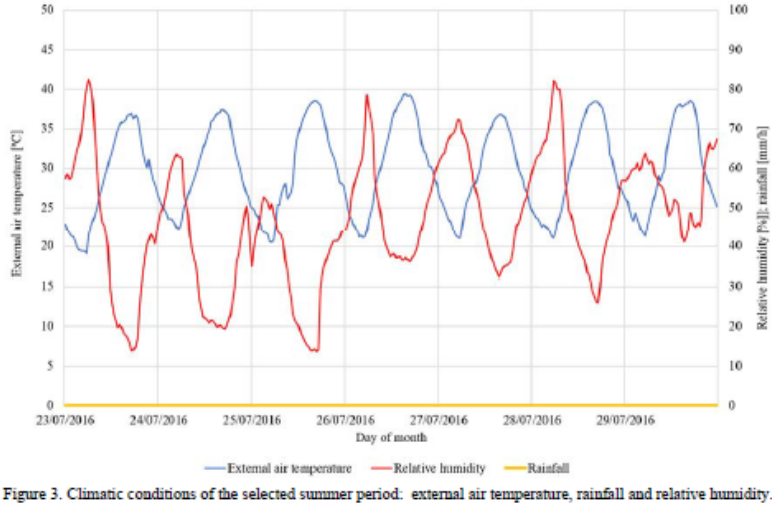

Figure 3. Climatic conditions of the selected summer period: external air temperature, rainfall and relative humidity.

3.2 Analysis of the temperature profile and water content in the plots

The slab temperature of all plots and the water content of the three parcels with green roofs are represented in Figure 4. The results showed that the slab temperature of P1, P2 and P3 was always lower than the slab temperature of Pref. In P1, the slab temperature oscillated between 27.7 °C and 33.2 °C. The oscillation for P2 was between 27.1 °C and 35.9 °C and, for P3 between 27.1 °C and 33.6 °C. However, Pref presented higher oscillations during all the summer week, between 24.8 °C and 50.1 °C.

In Figure 4, it can be also observed that the water content in all the parcels with green roofs were different, depending on the type of the substrate. The irrigation gave the same amount of water to all the parcels with green roofs. The substrate of P1, composed of 100% of commercial growing medium, retained more water than the other green roofs, between 18.3% and 26.4%. P2, with a substrate composed of 75% of commercial growing medium and 25% of recycled construction materials, retained between 9.7% and 12.8%, and finally, P3, with a substrate composed of 50%

of commercial growing medium and 50% of recycled construction materials, retained between 14.1% and 17.9%.

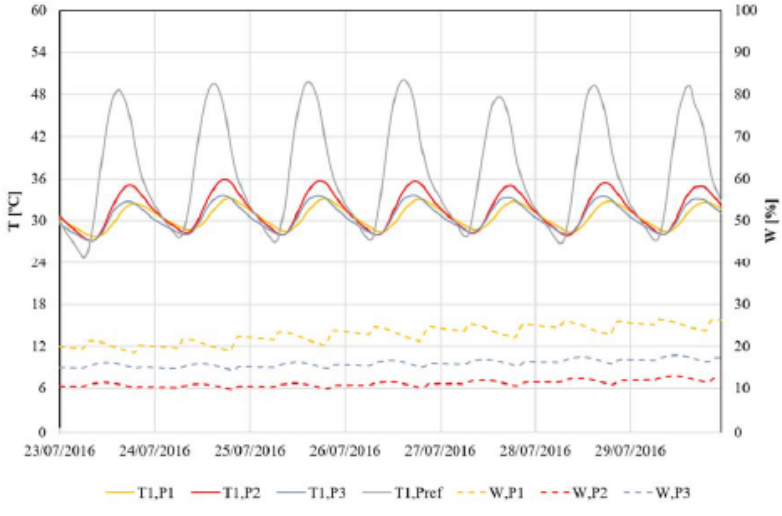

Figure 4. Values of slab temperature and water content measured in the plots.

3.3 Cooling potential

The cooling potential, CP, for the three green roofs was studied during the selected summer week, according to Eq. 1. The CP results are shown in Table 3. P1 was the plot with the highest CP values, with a weekly average value of 16.3 ºC and a maximum value of 17.0 ºC. This behaviour was mainly due to the capacity to retain water of the substrate of P1, see Figure 4. P3 presented a weekly average of CP of 15.8 ºC and a maximum value of 16.5 ºC. Finally, P2 was the plot with the lowest CP values, with a weekly average of 13.8 ºC, a 15% less than P1, and a maximum value of 14.5 ºC.

These results suggested that the higher the capacity to retain water in substrate, the higher CP is.

Table 3. Values of cooling potential for the three green roofs.

	23/07	24/07	25/07	26/07	27/07	28/07	29/07	Mean
P1	16.1	16.4	16.7	17.0	14.9	16.4	16.4	16.3
P2	13.6	13.6	14.1	14.5	12.7	13.8	14.2	13.8
P3	15.9	15.9	16.3	16.5	14.4	15.7	16.0	15.8

4. Conclusions

In this experimental work, the cooling potential of three plots with green roofs respect to a traditional gravel ballasted roof, was studied. The three plots had different substrates, composed

of different percentages of commercial growing medium and recycled construction materials. The study was carried out throughout a typical summer week in Córdoba (Spain), where the climate is dry-summer subtropical. The main conclusions obtained were:

- The three plots with green roofs obtained a great reduction of the slab temperature respect to the slab temperature of Pref. P1 obtained the best CP values, with a weekly average value of 16.3 °C, mainly due to the capacity of its substrate to retain water. Therefore, these results showed that the higher the capacity to retain water in substrate, the higher CP is.
- Green roof is a passive system that reduce the energy demand of the building and could be considered one of the possible measurements to achieve nearly zero energy buildings.

These results suggest that both the characteristics of the substrate used, and the amount of water retained, ensure a minimization of the oscillation of the indoor temperatures during the warmer months and consequently allow a reduction of the heat island effects in cities.

5. Acknowledgements

Weather data from the Agroclimatic Information Network of Andalusia which have been supplied by the Institute of Research and Agricultural and Fisheries Training of the CAPDR of the Andalucía Regional Administration, Junta de Andalucía.

The authors would like to express appreciation for the financial support of the European Regional Development Fund (ERDF) through the project GGI3003IDIB "*Optimizing the potential of green roofs for building retrofit: interaction between recycled substrates, water properties and energy efficiency*", by the Agency of Public Works of Andalucía, Junta de Andalucía, Spain.

REFERENCES

[1] BATES, A.J. et al. Effects of recycled aggregate growth substrate on green roof vegetation development: A six year experiment. In Landscape and Urban Planning. 2015. Vol. 135, pp. 22–31.

[2] CASTLETON, H.F. et al. Green roofs; Building energy savings and the potential for retrofit. In Energy and Buildings [online]. 2010. Vol. 42, no. 10. pp .1582–1591.

[3] EUROPEAN COMMISSION, Directive 2002/91/EC of the European Parliament and of the Council of 16 December 2002 on the energy performance of buildings, 2002.

[4] EUROPEAN PARLIAMENT, European Directive 2010/31/EU on the Energy Performance of Buildings, 2010.

[5] GRACIA, A. DE et al. Experimental set-up for testing active and passive systems for energy savings in buildings – Lessons learnt. In Renewable and Sustainable Energy Reviews. 2018. Vol. 82, no. September 2017, pp. 1014–1026.

[6] KARTERIS, M. et al. Towards a green sustainable strategy for Mediterranean cities: Assessing the benefits of large-scale green roofs implementation in Thessaloniki, Northern Greece, using environmental modelling, GIS and very high spatial resolution remote sensing data. In Renewable and Sustainable Energy Reviews. 2016. Vol. 58, pp. 510–525.

[7] KOTTEK, M. et al. World Map of the Köppen-Geiger climate classification updated. In Meteorologische Zeitschrift. 2006. Vol. 15, no. 3, pp. 259–263.

[8] LI, D.H.W. et al. Zero energy buildings and sustainable development implications - A review. In Energy. 2013. Vol. 54, pp. 1–10.

[9] MICKOVSKI, S.B. et al. Laboratory study on the potential use of recycled inert construction waste material in the substrate mix for extensive green roofs. In Ecological Engineering. 2013. Vol. 61, no. 1 PARTC, pp. 706–714.

[10] NAGASE, A. - DUNNETT, N. The relationship between percentage of organic matter in substrate and plant growth in extensive green roofs. In Landscape and Urban Planning. 2011. Vol. 103, no. 2, pp. 230–236.

[11] QIU, G. yu et al. Effects of Evapotranspiration on Mitigation of Urban Temperature by Vegetation and Urban Agriculture. In Journal of Integrative Agriculture. 2013. Vol. 12, no. 8, pp. 1307–1315.

[12] RAJI, B. et al. The impact of greening systems on building energy performance: A literature review. In Renewable and Sustainable Energy Reviews. 2015. Vol. 45, pp. 610–623.

[13] SAADATIAN, O. et al. A review of energy aspects of green roofs. In Renewable and Sustainable Energy Reviews. 2013. Vol. 23, pp. 155–168.

[14] SHAFIQUE, M. et al. Green roof benefits, opportunities and challenges – A review. In Renewable and Sustainable Energy Reviews. 2018. Vol. 90, pp. 757–773.

[15] XIAO, M. et al. A review of green roof research and development in China. In Renewable and Sustainable Energy Reviews. 2014. Vol. 40, pp. 633–648.

Appendix E

Energy saving potential of green roofs in South European climates

The paper presented in this appendix is published in the "*International Conference on GREEN CONSTRUCTION"*, Cordoba, Spain, 2019.

Energy saving potential of green roofs in South European climates

M. Porcaro[1)]*, M. Ruiz de Adana[1)], F. Comino[1)], A. Peña[2)], E. Quety[3)], T. Vanwalleghem[4)]
[1)]Department of Applied Thermodynamics, Universidad de Córdoba, Spain
[2)]Area of Project Engineering, Universidad de Córdoba, Spain
[3)]Department of Forest Engineering, Universidad de Córdoba, Spain
[4)]Area of Hydraulic Engineering, Universidad de Córdoba, Spain
*e-mail: z72popom@uco.es

Keywords: *extensive green roofs; recycles substrates; energy saving*

1. Introduction

Green roofs are passive construction systems that allow to reduce the thermal loads of a building and decrease the temperature fluctuations of the roof assembly (Li, 2013). Green roofs also help to mitigate the urban heat island effect through evapotranspiration process, absorb CO_2 and retain meteoric water (Shafique, 2018). This work focused on the study of extensive green roofs, which have a thickness of 60-200 mm and the plant species used require low maintenance (Besir, 2018).
The main objective of this study was to obtain experimentally the energy saving of three extensive green roofs with different substrates, compared to a traditional gravel ballasted roof, during the summer period, for the climatic conditions of Córdoba.

2. Materials and methods

The three plots with green roofs and a reference plot with gravel ballasted roof were installed in an office building located in the University of Córdoba. The substrates of the three green roofs were composed of commercial growing medium and recycled construction materials, each of them with a different percentage, see Figure 1. In each green roof were installed ten temperature probes along the vertical profile of the parcel, five in the east side and five in the west side. Two heat flux probes and two water content probes were also installed, one in the middle of each side, see Figure 1. In the reference plot were installed three temperature probes in the middle of the parcel, along the vertical profile, and two heat flux probes, see Figure 1.

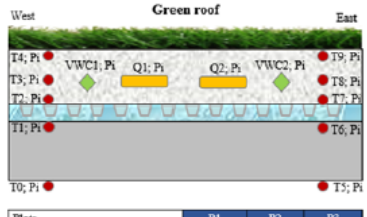

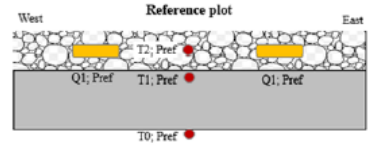

Plots	P1	P2	P3
Commercial growing medium (%)	100	75	50
Recycled aggregates (%)	0	25	50

Figure 1. Plots layers and sensors of the green roofs and the reference plot.

Experimental data of heat flux were collected during the summer period of 2016, from June to September. The energy saving of each plot was calculated with Eq. 1, where $\dot{q}$ is the heat flux [W/m^2] referred to the area of the parcel [m^2].

$$Energy\ saving\ [\%] = \frac{\dot{q}_{P_{ref}} - \dot{q}_{P_i}}{\dot{q}_{P_{ref}}} * 100 \qquad (1)$$

3. Results and conclusions

The results of energy saving of the three plots with green roofs, compared to the reference plot, are shown in Figure 2.

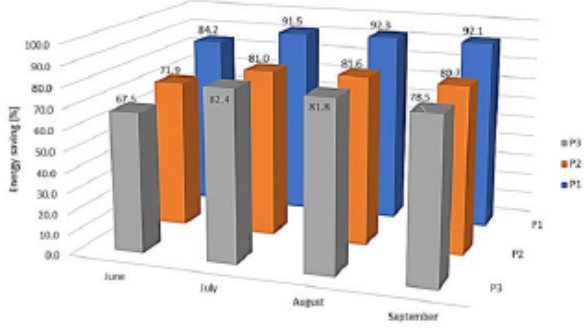

Figure 2. Energy saving of the three green roofs.

It can be observed than all plots with green roofs achieving energy saving greater than 67.5 %, respect to the reference plot. The plot that achieved the best results was P1, with a mean value of energy saving of 90.0%. The greater reduction was obtained in August, with a value of 92.3%. This behaviour is mainly due to the capacity of the substrate to retain water. The results suggested that all the green roofs allow a significant reduction of energy gains during the summer months. In conclusion, green roofs can be considered as an interesting passive construction system to achieve energy saving in buildings located in South European climates.

4. Acknowledgements

Weather data from the Agroclimatic Information Network of Andalusia which have been supplied by the Institute of Research and Agricultural and Fisheries Training of the CAPDR of the Andalucía Regional Administration, Junta de Andalucía. The authors would like to express appreciation for the financial support of the European Regional Development Fund (ERDF).

5. References

Besir, A.B., Cuce, E., 2018. Green roofs and facades: A comprehensive review. Renew. Sustain. Energy Rev. 82, 915–939.

Li, D.H.W., Yang, L., Lam, J.C., 2013. Zero energy buildings and sustainable development implications - A review. Energy 54, 1–10.

Shafique, M., Kim, R., Rafiq, M., 2018. Green roof benefits, opportunities and challenges – A review. Renew. Sustain. Energy Rev. 90, 757–773.